International Scientific-Technical and Production Journal

The Paton WELDING JOURNAL

August 2010 # 8

English translation of the monthly «Avtomaticheskaya Svarka» (Automatic Welding) journal published in Russian since 1948

Founders: *E.O. Paton Electric Welding Institute of the NAS of Ukraine International Association «Welding»* ***Publisher:*** *International Association «Welding»*

Address:
E.O. Paton Electric Welding Institute,
International Association «Welding»,
11, Bozhenko str., 03680, Kyiv, Ukraine
Tel.: (38044) 287 67 57
Fax: (38044) 528 04 86
E-mail: journal@paton.kiev.ua
http://www.nas.gov.ua/pwj

State Registration Certificate
KV 4790 of 09.01.2001

Subscriptions:
$324, 12 issues per year,
postage and packaging included.
Back issues available.

CONTENTS

According to estimations of specialists, a great number of structures, constructions and machine in operation in Ukraine have exhausted their designed service life. In this connection, of special current importance are the issues related to control of operating reliability and durability of critical facilities by determining their technical state, residual life and scientifically grounded safe operation life.

Below we give a selection of articles based on the results of studies completed in 2007–2009 under targeted integrated program RESOURCE of the National Academy of Sciences of Ukraine by involving scientists and specialists from 26 institutions of 8 departments of the Academy.

Editorial Board

SUBSTANTIATION OF THE SYSTEM OF DEOXIDATION AND MICROALLOYING OF DEPOSITED METAL WITH ELECTRODES FOR WELDING AND REPAIR OF BRIDGE AND TRANSPORT STRUCTURES

I.K. POKHODNYA, A.E. MARCHENKO, I.R. YAVDOSHCHIN, N.V. SKORINA and **O.I. FOLBORT**
E.O. Paton Electric Welding Institute, NASU, Kiev, Ukraine

The paper provides substantiation of the system of deoxidation and microalloying of weld metal produced with electrodes that are designed for welding and repair of bridge and transport structures. The main characteristics of the electrodes developed by using this system are described.

Keywords: *arc welding, structural low-alloy steels, covered electrodes, welding and repair of structures, microalloying system*

The Second Pan-European Transport Conference held in 1994 passed the program of development of the continental transport network, according to which nine main transcontinental cargo transportation directions, called «Crete Corridors», were to be built. Four of them are to pass through the territory of Ukraine. Taking a central place in Europe in this way, i.e. having the highest transit traffic factor among the neighbouring European countries, Ukraine should become a peculiar bridge between Europe and Asia to substantially reduce traffic expenses and delivery time in the system of international goods exchange. The program was approved for building and functioning of the national network of international transport corridors in Ukraine [1].

To implement this program, it will be necessary to upgrade railways, so that they meet modern requirements for speed, length and weight of the passed-through trains, build new highways of the international level, construct many bridges, tunnels and crossroads, as well as 26 unique transport-storehouse terminals.

Transport problems have to be solved also because of the European Football Championship to be held in Ukraine in 2012. City and belt highways are reconstructed in Kiev and other cities of Ukraine. Bridges across the Dnieper River, over- and underpasses, as well as junctions at most intensive traffic crossroads are built. This will require involvement of metalwork and transport engineering factories, as well as building and assembly organisations that intensively employ welding technologies. For factory conditions, these are mostly mechanised welding processes. However, part of the operations, which are associated, as a rule, with welding of the most critical structures and repair of defects are traditionally performed under factory conditions by using covered electrodes. In field, the major part of spatial welds, which for technical reasons cannot be made by the mechanised welding methods, are usually produced by manual covered-electrode arc welding.

Operation of bridge and transport structures, which were built earlier, is accompanied by current repairs and overhauls to maintain them in an appropriate condition. After liquidation of the united national economy system of the USSR, condition of basic assets of the key industries and inter-industry manufacturing infrastructure in Ukraine and other CIS countries is constantly deteriorating.

To prevent probable man-caused crises, the supervision authorities and Public Committee «2005» formed at the initiative of the Ukrainian Government have been performing for a number of years a careful monitoring of safety of structures, constructions and related machines. The above monitoring covers railway and motor transport bridges, offshore and pipeline transport facilities, transport infrastructure in the form of inter- and multi-modal, as well as terminal systems, which under no circumstances must be weak points of the «Crete Corridors», etc. All of the above facilities are built, maintained in a working condition and repaired by using welding technologies.

Steel for bridge and transport structures. Evolution of chemical composition and properties of rolled stock of structural steels is shown in Figure 1 [2, 3]. Low-alloy silicon-manganese steels of the 09G2S (class S345) and 12G2S (class S375) grades according to GOST 19281–89, low-alloy (with chromium and nickel) steels of the 10KhSND and 12KhSND grades (class S390) according to GOST 6713–91, medium-alloy (with molybdenum) steels of the 14G2AF (class S390), 16G2AF (class S440) and 12GN2MFAYu (class S590) grades according to GOST 19281–89 are used to construct and repair the bridge and transport structures.

At present the metallurgical industry produces grades 09G2S and 12G2S from steels, the requirements to which are specified by inter-state standards. Production of steels classed as S390, S440 and S590 has been practically ceased, as GOST 19281–89 permitted a high content of harmful impurities in them, which made them susceptible to brittle fracture.

Steels 15KhSND and 10KhSND turned out to be too expensive. In addition, as found out, they no longer corresponded to modern requirements for purity, performance and weldability imposed by bridge constructors. In this connection, consumption of these steels had been dramatically reduced by the beginning of the 1990s. Now Ukraine produces only a limited volume of rolled products from them. The Russian Federation continues using them in bridge construction. Structures fabricated earlier from the said steels are still in operation, and this fact should be taken into account when choosing welding consumables to repair them.

Factories of the South of Ukraine managed production of other grades of this class of steels using their own specifications. The Mariupol Institute of Structural Materials «Prometey» developed niobium-containing steels of the 06GB and 06G2B grades, which meet requirements to strength classes S355–S490. They are produced according to TU U 14-16-150–99 and supplied in the form of 8 to 50 mm thick plates. Different modes of heat treatment of the rolled stock provide four level of its strength ($\sigma_t \geq 450$, 490, 540 and 590 MPa, and $\sigma_y \geq 355$, 440 and 490 MPa, respectively) at almost identical values of ductility and impact toughness. The required Z-properties and continuity at a level of class 0 are guaranteed.

Steel of the 09G2SYuch grade is supplied according to TU U 322-16-127–97 in 8 to 40 mm plates. Its mechanical properties are provided within the following ranges, depending upon the plate thickness and heat treatment method: $\sigma_y = 325$–450 MPa, $\sigma_t = 480$–570 MPa, $\delta_5 = 19$ %, $KCU \geq 29$ J/cm^2 and $KCV \geq 29$ J/cm^2 at a temperature of −40 to −70 °C.

The said steel grades have different weldability. Steel 06G2B has the lowest value of carbon equivalent calculated by the IIW formula, and steels 09G2SYuch

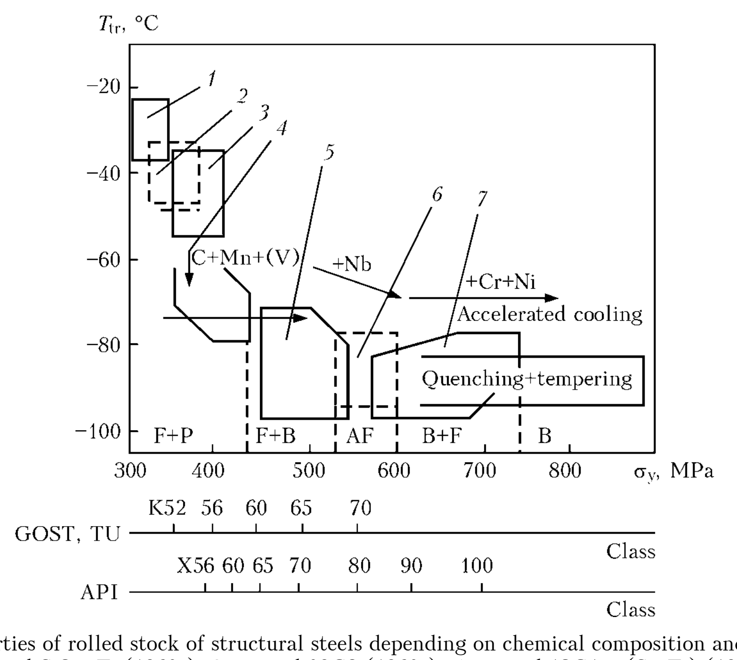

Figure 1. Evolution of properties of rolled stock of structural steels depending on chemical composition and manufacturing technology: *1* — steel St3 (1950s); *2* — steel St3 + Ti (1960s); *3* — steel 09G2 (1960s); *4* — steel 13G1 + (Si, Ti) (1965–1970); *5* — steel 10G2 + (V, Nb, Ti) (1970s); *6* — steel 09G2 + (Nb, Ti, B) (1980s); *7* — steel 09G2 + (Cr, Ni, V, Nb); F — ferrite; B — bainite; AF — acicular ferrite; P — pearlite

and 10KhSND have the highest value. Indeed, the latter used to fabricate welded structures involves technological problems, which are noted by the authors of study [4]. When welding steel 06G2B, one might expect the weldability problems related to niobium contained in it. The above considerations are proved by the results of investigation of weldability of steels 10KhSND and 09G2SYuch, compared with molybdenum-containing steel 06G2B [5]. It was established that steel 06G2B is characterised by the highest resistance to delayed fracture. In the rest two steel grades the required value of resistance to delayed fracture is provided only at a concentration of hydrogen in the deposited metal that is not in excess of 7 ml/100 g. Steel 10KhSND reacts more intensively to increase in the concentration of hydrogen. Based on the investigation results, steel of the 06G2B grade is recommended for application in bridge construction [6].

Manufacture of transport structures is traditionally oriented to application of rolled stock of low-alloy steels 09G2S with thickness of no more than 20 mm.

Welding electrodes. Bridge and transport welded structures operate under very unfavourable service (impact, dynamic and vibration loads, atmospheric corrosion) and climatic conditions (negative temperatures in winter go down to −40 °C in Ukraine, and even lower outside Ukraine). Emergency failure of these structures may lead to substantial technical, economic and environmental losses. Therefore, the quality of welds and reliability of welded joints should meet sufficiently high requirements.

According to the regulatory documents, electrodes of the low-hydrogen class, types E42A and E50A (GOST 9467–75), are recommended for construction and repair of bridge and transport structures. To avoid technological defects, welding should be performed with electrodes having high welding-operational properties.

Table 1. Consumables for manual arc welding of bridge structures [7]

Steel grade (strength class)	Type and grade of electrodes for manual arc welding
T-, fillet and overlap joints	
15KhSND 15KhSNDA 09G2SD 12G2SBD (345)	E46A – UONI-13/45 E50A – UONI-13/55 E50A – MTG-02
10KhSND 10KhSNDA (390)	E46A – UONI-13/45 E50A – UONI-13/55 E50A – MTG-02
Butt joints	
15KhSND 15KhSNDA 09G2SD (345)	E50A UONI-13/55 MTG-01K MTG-02 MTG-03

Russian regulatory documents provide for the use of electrodes UONI-13/45 and UONI-13/55, as well as electrodes of the MTG grade, which were initially developed for construction of pipelines. They are manufactured under licenses of European companies by the Sychevsky Electrode Factory (RF). Types and grades of electrodes are given in Table 1.

In the national practice, electrodes UONI-13/45 and UONI-13/55, which were developed 70 years ago and no longer meet the up-to-date requirements, are mainly used for welding of bridge and transport structures from carbon and low-alloy steels. The key drawbacks of the UONI-13 type electrodes are as follows:

- inconsistency of mechanical properties of the weld metal, primarily impact toughness at low temperatures. The cold-shortness threshold of the weld metal obtained by using these electrodes is −30 to −40 °C;
- low welding-operational properties (welds are formed with reinforcement, poor slag crust detachability, increased spattering, possibility of performing welding only at direct current);
- low manufacturability showing up in susceptibility of the covering mixture to solidification and non-uniform outflow from the head of the electrode-covering press in deposition of covering on the rod;
- increased hygroscopicity of the covering.

The task posed for development of new electrodes for welding bridge and transport structures was to eliminate drawbacks peculiar to electrodes of the UONI-13 type. One of the main tasks was to ensure high impact toughness of the weld metal at negative temperatures, down to −60 °C.

Selection and experimental substantiation of weld metal deoxidation system. Gas- and slag-forming system $CaCO_3$–CaF_2–SiO_2–TiO_2 is used in the majority of grades of low-hydrogen electrodes. Welding-operating properties of electrodes and efficiency of molten metal shielding are regulated with this system by the $CaCO_3/CaF_2$ ratio and covering thickness.

Domestic developments of low-hydrogen electrodes of the E42A and E50A types according to GOST 9467–75 are traditionally oriented to a complex system of deoxidation of weld metal with manganese, silicon, titanium and aluminium, which is contained in the form of a concurrent element in ferrotitanium (up to 8 %). In the opinion of developers of the electrodes, titanium and partially aluminium, characterised by high affinity for oxygen, combined with manganese and silicon should provide high mechanical properties because of deep deoxidation of the weld metal, as well as its favourable structure-phase composition, which is formed under conditions of welding thermal cycle.

It is a known fact that structure of the weld metal in low-alloy welds includes ferrite of a different morphology (xenomorphic in the form of interlayers along the prior austenite grain boundaries, polygonal, lamellar, acicular and lath) with regions of the second phase, which consists of carbides, martensite, bainite, retained austenite or their mixture [8–10].

Boundaries of disoriented individual lamellae and laths of ferrite are low-angle. Structural elements of acicular ferrite, fine and uniformly distributed within each grain, form high-angle boundaries, which are more favourable in terms of brittle fracture resistance [10–12]. In fracture, a crack in such a structure has to change its propagation direction more frequently, this leading to a considerable increase in fracture resistance. For this reason, the weld metal with acicular ferrite dominating in its structure is characterised by higher values of impact toughness, including at low temperature.

High cold resistance of the weld metal can be achieved if the second phase, which forms simultaneously with acicular ferrite, is of a ductile nature, rather than of the brittle one.

The effect of alloying elements on structure and properties of the weld metal can be explained as follows. Manganese provides the high values of strength and impact toughness of the welds. The 1.4–1.6 wt.% manganese content is considered optimal [13–15]. In this case, the highest yield of acicular ferrite is achieved in structure of the weld metal.

Increasing the silicon content from 0.2 to 0.9 wt.% leads to growth of the volume content of acicular ferrite in the deposited metal. But this increases the amount and deteriorates the morphology of the second phase, i.e. cementite films and bainite and pearlite islands are replaced by martensite and austenite [16], which leads to decrease in the level of impact toughness. The optimal values of impact toughness of metal deoxidised with silicon and manganese are provided at a manganese content of 1.4–1.6 wt.% and silicon content of 0.2–0.4 wt.%.

The effect of titanium on structure and mechanical properties of the weld metal is considered in studies [17–19] etc. Their authors note a positive effect of titanium on impact toughness of metal of the welds made with low-hydrogen electrodes. However, the optimal content of titanium in the weld metal, reported by different authors, varies over wide ranges, depending upon the presence and proportion of other alloying elements. It is unclear why titanium fails to always provide the expected high toughness of the welds made with electrodes UONI-13, and does not provide it, as a rule, if welding is performed using electrodes with a covering, which greatly differs in proportion of main slag-forming materials from electrodes of the UONI-13 type.

Most of the above-quoted results of metal science research were obtained under conditions of metallurgical welding systems reliably «closed» from ambient air. Ideal deoxidisers (titanium instead of ferrotitanium, metal manganese instead of ferromanganese), which do not occur in real industrial conditions, were used in the electrode covering applied for research. It is hard to understand from the publications how high the degree of robustness of the found balance of microalloying elements is with respect to variation in material composition of the covering, including its ability to efficiently shield the molten metal from the ambient air.

The authors conducted experimental studies of the system of deoxidation and microalloying of the weld metal based on manganese, silicon and titanium in coverings of low-hydrogen electrodes for welding of bridge and transport structures. For this, experimental electrodes based on marble, fluorspar and rutile (or quartz sand) were manufactured and tested. Total contents of main gas- and slag-forming ($CaCO_3$ and CaF_2), as well as metal components of the coverings (ferroalloys with iron powder), and their proportions are given in Table 2.

Commercial ferroalloys were used as deoxidisers: electric-furnace low-carbon ferromanganese (88 wt.% Mn), ferrosilicium (granulated with 15 wt.% Si, or lumpy with 45 wt.% Si) and ferrotitanium (35 wt.% Ti, 5 wt.% Si, and 8 wt.% Al). The total content of ferroalloys and iron powder in a covering varied from 22 to 44 wt.%.

The contents of ferroalloys, ritule or quartz sand in coverings of electrodes of series 2M, 3M, 2T and 3T were regulated so that the planned increase of the titanium content of the deposited metal did not change, if possible, the content of manganese and silicon within each series of the electrodes. At the same time, the assigned content of ferromanganese in cov-

Table 2. Base of coverings, dimensional and technological parameters of experimental electrodes

Electrode series	Content in covering, wt.%				Parameters of electrodes			
	$CaCO_3$	CaF_2	$CaCO_3/CaF_2$	Metal components	D/d	$K_{c.w}$, %	$K_{s.sh}$, %	$\tau_{s.c}$, ms
2M	51.0	18.0	3/1	22–24	1.50	35	25	7.5
3M	51.0	18.0	3/1	24–28	1.50	–	–	–
2T	26.0	26.0	1/1	35–46	1.55–1.60	45	22	14.5
3T	26.0	26.0	1/1	39–46	1.55–1.60	–	–	–
R	26.5	22.5	1.2/1.0	44–46	1.65	55	25	10.5

Note. $K_{c.w}$ – covering weight factor; $K_{s.sh}$ – slag shielding factor; $\tau_{s.c}$ – short circuit duration.

Table 3. Chemical composition of metal deposited with experimental electrodes

Electrode series	C	Mn	Si	O	N	Ti
2M	0.05–0.07	0.67–0.84	0.20–0.32	370–530	110–160	0–330
3M	0.07–0.09	1.38–1.73	0.37–0.52	280–500	110–150	0–420
2T	0.04–0.06	0.87–1.32	0.28–0.41	270–390	130–360	10–640
3T	0.06–0.07	1.17–1.34	0.33–0.42	260–320	130–240	20–700
R	0.04–0.06	0.75–1.75	0.25–0.90	240–360	70–130	80–520
Note. Contents of C, Mn and Si is given in wt.%, and contents of other elements is given in ppm.						

erings of electrodes of series 3M and 3T was deliberately made higher than in series 2M and 2T.

The content of ferroalloys in coverings of electrodes of series R was calculated by the method of active experimental design using the D-optimal plan.

The iron powder in all series of experimental electrodes was used as a balance compensator. Diameter of the electrodes was 4 mm. Other dimensional and technological parameters of the electrodes are given in Table 2, and chemical composition of the deposited metal is given in Table 3.

As follows from Tables 2 and 3, coverings of series M reproduce the gas- and slag-forming base, as well as dimensional and technological parameters of coverings of electrodes UONI-13. The $CaCO_3/CaF_2$ ratio in them is 3/1. Hence, they feature a high oxidation potential, sufficiently effective shielding of molten metal from air, and spray transfer of electrode metal. Coverings of electrodes of series T model similar parameters of electrodes ANO-7, «Garant», as well as many grades of electrodes of ESAB, «Thyssen» etc. The $CaCO_3/CaF_2$ ratio in their covering is 1/1. Hence, its oxidation potential is much lower, and the ability of metal shielding from air is also lower, in view of its nitrogen content. The electrode metal transfer is globular. In covering of electrodes of series R the $CaCO_3/CaF_2$ ratio is 1.2/1.0. Compared to electrodes of series T, their metallurgical and technological characteristics are much better, and shielding function of the covering is at a high level because of its large thickness.

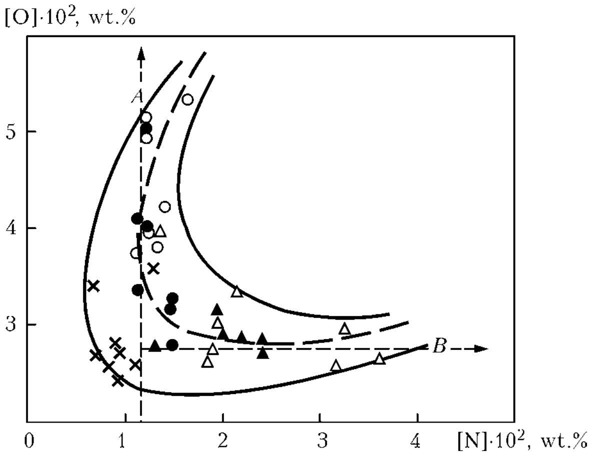

Figure 2. Comparison of oxygen and nitrogen contents of metal deposited with experimental electrodes having coverings of series 2M (○), 3M (●), 2T (Δ), 3T (▲ and R (×)

The content of titanium in the deposited metal was varied from 0 to 700 ppm, that of oxygen — from 240 to 530, and nitrogen — from 70 to 360 ppm (see Table 3), i.e. oxygen and nitrogen, along with manganese, silicon and titanium, should be regarded as elements that actively affect mechanical properties, including ductility of the weld metal.

The values of strength (σ_y and σ_t) and ductility (δ and KCV_T) of multilayer weld metal were investigated on 18 mm thick low-carbon steel. Below we analyse only the KCV_{+20} values obtained by testing specimens with a notch passing through all the layers of the weld.

Limits of variations in the contents of oxygen and nitrogen are shown in Figure 2. It can be seen from the Figure that the weight content of nitrogen is of the same order of magnitude as the equilibrium concentration of nitrogen in iron containing titanium and oxygen. However, as proved by our analysis, in contrast to the equilibrium concentration, it grows with increase in the titanium content of the weld, rather than decreases. This is an indirect confirmation that the source of nitrogen is air, from which it is absorbed by titanium. The weight content of oxygen is an order of magnitude higher than the equilibrium concentration of oxygen in iron deoxidised with titanium, which is characteristic of metal deposited by fusion arc welding. In this case, non-metallic inclusions, which form at a stage of solidification of the weld pool and have no time to go to the slag, are the main source of oxygen. The points located along vertical A in Figure 2 reflect results obtained mainly with electrodes of series M ($[O]_{var}$ at $[N]$ = const), and those along horizontal B — results obtained mainly with electrodes of series T ($[N]_{var}$ at $[O]$ = const). The data given confirm a differing oxidation and shielding ability of coverings of the compared experimental series of electrodes. Electrodes of series R provide a low content of both oxygen and nitrogen in the deposited metal, i.e. they are characterised by a low oxidation ability of their covering (like electrodes of series T) and its sufficiently effective ability to shield from air (like electrodes of series M).

Metal deposited with the experimental electrodes can be classed in chemical composition with the Fe–Mn–Si–Ti–O–N system. In this case, titanium acts as deoxidiser, like silicon and manganese, and, at the same time, as a nitride-forming element. Depending upon the conditions of shielding the electrode metal from air, part of titanium can be combined to form nitrides, and other part — to form oxides.

Consequences of the above double role of titanium revealed by analysing results on KCV_{+20} were determined by using the following experimental results processing approaches.

The system of deoxidation of welds with silicon and manganese is based on the following chemical reaction:

$$[Si] + 2(MnO) = 2[Mn] + (SiO_2). \qquad (1)$$

The equilibrium content of oxygen in the deposited metal can be calculated from equation [20, 21]:

$$[O] = K_{Si-Mn} ([Mn]\cdot[Si])^{-0.25}. \qquad (2)$$

The temperature dependence of the equilibrium constant of chemical reaction (1) has the following form:

$$\lg K_{Si-Mn} = -\frac{15518}{T} + 6.01. \qquad (3)$$

Deoxidation parameter $([Mn]\cdot[Si])^{-0.25}$ is complex, as it reflects the effect of the total content of manganese and silicon, as well as their ratio on residual oxygen in the deposited metal, which has the form of non-metallic inclusions formed at a stage of cooling and solidification of the weld pool. A low value of negative exponent in the deoxidation parameter means that control of oxygen in the metal by changing manganese and silicon in it is very limited, compared, for example, to the operating welding parameters, and is indicative of the presence of other deoxidisers, etc. Nevertheless, it permits evaluating the oxygen content component that is caused by complex deoxidation of the weld metal with silicon and manganese. By giving our results on KCV_{+20} depending on the deoxidation parameter, we thus relate them to the content of oxygen that remained in the weld as a result reaction (1), and consider the entire revealed situation to be a consequence of the effect of other factors (e.g. titanium and oxygen that do not participate in reaction (1), and nitrogen).

The Fe–Ti–O–N system, which we arrive at as a result of excluding oxygen that remains in the deposited metal after it has been deoxidised with silicon and manganese, can be described by three equations:

$$Ti_xO_y(s) = x[Ti] + y[O]; \qquad (4)$$

$$TiN(s) = [Ti] + [N]; \qquad (5)$$

$$xTiN(s) + y[O] = Ti_xO_y(s) + x[N], \qquad (6)$$

where (s) is the solid state of an ingredient [22, 23]. Note that equation (6) was derived by subtracting (5) from (4).

To describe conditions of formation (decomposition) of nitride in iron alloys containing, as in our case, less than 0.05 % Ti, the use is made of equations (4) and (6), which characterise affinity of titanium and its nitride for oxygen. Equation (6) in its explicit form reflects relationship between the equilibrium concentrations of nitrogen and oxygen in iron in the presence of titanium. In view of a very low concentration of the above components, thermodynamic calculations of constants are made by using their concentration instead of activity, and, based on the form of oxide Ti_2O_3 revealed in the experiments, it is suggested that temperature dependence of the constants should be evaluated from the following equations [22, 23]:

$$\lg K_4 = -\frac{55200}{T} + 16.4; \qquad (7)$$

$$\lg K_5 = -\frac{19000}{T} + 6.48; \qquad (8)$$

$$\lg K_6 = \lg [N]^x/[O]^y = \frac{14200}{T} - 3.44. \qquad (9)$$

Equation (6) shows that TiN in the melts reliably shielded from air, like titanium in reaction (4), may act as deoxidiser of molten steel. The $[N]^x/[O]^y$ ratio is, in fact, an equilibrium constant of reaction (6) that depends upon the total concentration of nitrogen and oxygen, as well as stoichiometric coefficients, which, in turn, are determined by the composition of the forming titanium oxides (TiO_2, Ti_2O_3 or TiO) depending on the deoxidation conditions and on the contribution to this process made by manganese, along with titanium, as well as by silicon and aluminium contained in ferrotitanium.

Finally, we used the coefficient of imbalance of nitrogen caused by titanium, B_N, for consideration of the Fe–Ti–O–N system. Its values are calculated from the actual composition of the deposited metal as a content of nitrogen that is not fixed into titanium nitrides, using the following formula [24, 25]:

$$B_N = 14/48[Ti] - [N]. \qquad (10)$$

Aluminium was not taken into account in this case, as it is a weaker nitride-former, compared to titanium, and better shields it from oxidation than from interaction with nitrogen.

As follows from Figure 3, *a*, the impact toughness values depending on the deoxidation parameter can be distributed into three groups. For groups of series *V*1 and *V*2, which include results of testing the electrodes of series 3M, 2T and 3T (in Figure 2, they are located mostly along vertical *A* and horizontal *B*, respectively), impact toughness of the weld metal changes for some reasons that are not related to the deoxidation parameter ($([Mn]\cdot[Si])^{-0.25}$) and, hence,

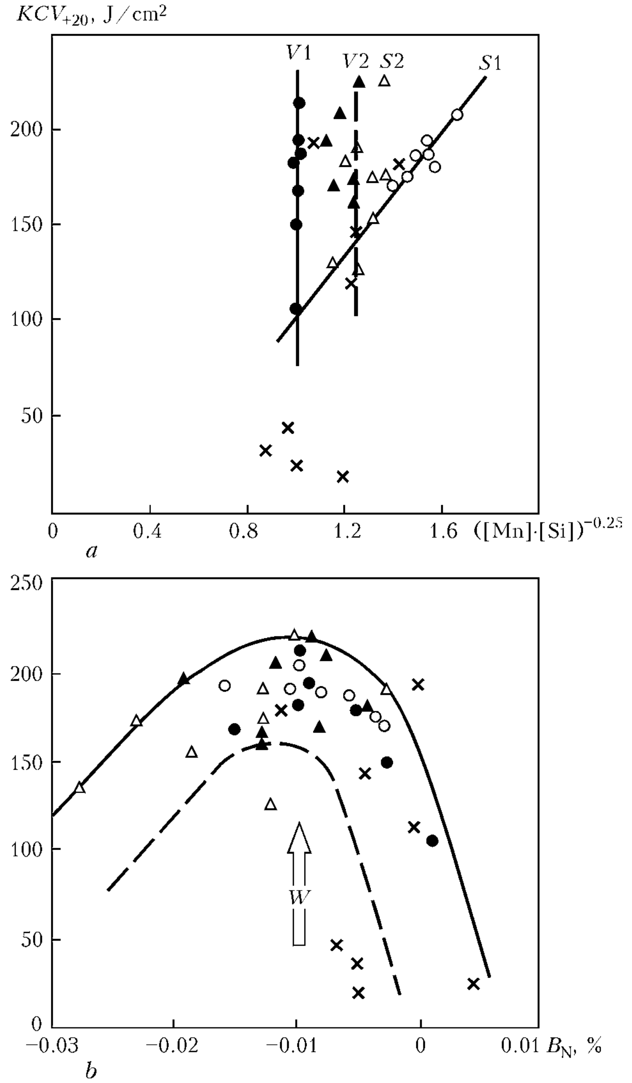

Figure 3. KCV_{+20} versus parameter of complex deoxidation of deposited metal with manganese and silicon, $([Mn]\cdot[Si])^{-0.25}$ (*a*), and versus coefficient of imbalance of titanium and nitrogen contents of deposited metal, B_N (*b*): ○ — electrodes of series 2M; ● — 3M; Δ — 2T; ▲ — 3T; × — R

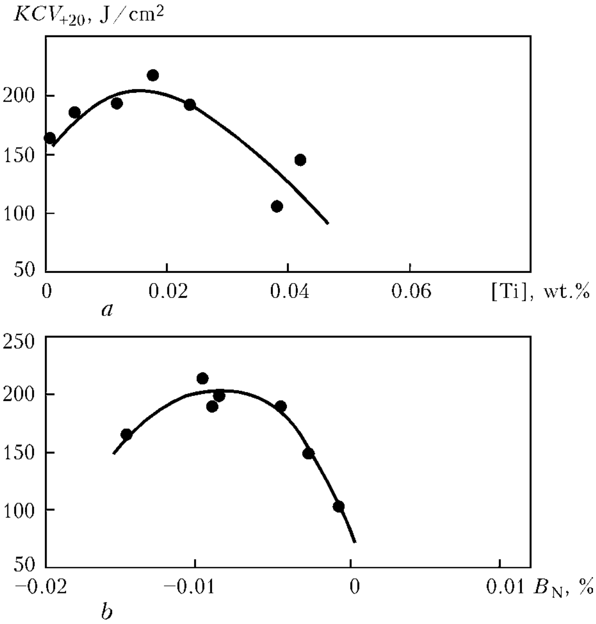

Figure 4. KCV_{+20} versus titanium content (*a*) and B_N (*b*) in metal of the welds made with electrodes of experimental series *V*1

to oxygen of manganese silicates, the content of which for each of these groups is constant, as it was planned by the experimental design. The said reasons of changes in impact toughness are analysed below. For group *S*1, which includes mostly the results of testing the electrodes of series 2M and 2T, impact toughness of the weld grows with increase in the deoxidation parameter and, hence, with increase in the weight content of oxygen fixed into manganese silicates. The reasons of this dependence are not considered in this publication.

The values of impact toughness of the weld versus the coefficient of imbalance of nitrogen caused by titanium, which are shown in Figure 3, form an extreme region with maximum at $B_N \approx -0.01$ %. To the left of maximum of KCV_{+20}, its decrease should be considered a consequence of increase in the weight content of nitrogen not fixed into titanium nitrides in the weld metal, while that to the right — a consequence of increase in the weight content of redundant titanium not fixed into nitrides. A change in impact toughness of the weld in a range of maximum amounts to a factor of one and a half. The causes of this are not related to the Ti–N balance described by equation (10). They will also be considered below.

Seemingly, the results of experiments on series *V*1 can be explained by fully excluding from consideration the effect of nitrogen on impact toughness because of its low content. Deoxidation of the weld metal with titanium occurs by reaction (4), i.e. it is enough to allow for the effect on KCV_{+20} by changes in the concentration of titanium and oxygen remained in the weld metal in quasi-equilibrium with silicon and manganese. As follows from literature data, non-metallic inclusions must form at an optimal proportion of titanium and oxygen. These inclusions facilitate initiation and provide the highest yield of acicular ferrite, which is a structural component responsible for high impact toughness of the low-alloy weld. It follows from Figure 4, *a* that the maximal value of KCV_{+20} takes place at 0.018–0.020 wt.% Ti, which is in good agreement with the data published by other authors. This optimum is implemented in all modern developments of electrodes close to electrodes UONI-13/55 in their covering composition. It is likely that the effect of this favourable factor is suppressed to the right of maximal KCV_{+20}, in addition, by a too high level of strengthening of the metal by titanium.

At the same time, imbalance coefficient B_N can also be used as an argument for representing results on experimental series *V*1 (Figure 4, *b*), as at such a low concentration of nitrogen B_N is equivalent to the content of titanium not fixed into nitrides in the deposited metal.

The results on experimental series *V*2, which is represented by electrodes of series 2T and 3T, are more difficult to interpret by this scheme, as titanium acts here mainly as a nitride-former. It can be seen from Figure 5 that the extreme character of variations in impact toughness takes place when it is considered depending on B_N. In this case, a substantial change in KCV_{+20} at $B_N \approx$ const is observed in maximum, like in Figure 3, *b*, and the cause of it remains unclear so far.

Assume that in experimental series *V*2 the process of deoxidation of the weld metal occurs by reaction (6). Show results on KCV_{+20} scattered in maximum in Figure 5 depending on the [N]/[O] ratio, which is a particular case of equilibrium constant of chemical reaction (6), where stoichiometric coefficients are assumed to be equal to $x = y = 1$, as the real form of deoxidation products is unknown to us. As follows from Figure 6, *a*, dependence $KCV_{+20} = f([N]/[O])$ is described by an inclined line showing that in the case of insufficient shielding of the molten metal from ambient air, which takes place when using electrodes of series 2T and 3T, involvement of titanium into the nitride formation reaction leads to substantial deterioration of impact toughness of the weld metal. The highest value of KCV_{+20} is observed when such a reaction is eliminated.

Figure 6, *b* shows the same interpretation of the results on experimental series *W* scattered in maximum of $KCV_{+20} = f(B_N)$ in Figure 3, *b* at $B_N \approx -0.01$. It can be seen that the values of KCV_{+20} are distributed in two levels, each corresponding to its peculiar contents of oxygen and nitrogen. Although we compare electrodes that are different in their metallurgical nature, the lines are parallel to each other and have a slope identical to that of the curve in Figure 5, when the concentration of oxygen in the deposited metal was kept constant. The data presented show that variation in KCV_{+20} in maximum in Figure 3, like in Figure 5, is also caused by growth of the [N]/[O] ratio.

Both titanium oxides and nitrides forming at a stage of solidification of the weld pool are considered in a number of references to be the centres of nucleation of acicular ferrite in γ–α transformation taking place in cooling of the weld metal. The results presented showed that titanium nitrides could hardly act as such nucleators of acicular ferrite. As evidenced by the results of a number of studies, titanium nitrides forming at the last stages of solidification, in particular as well as sulphides, precipitate on the surface of titanium oxide inclusions and suppress their ability to act as centres of nucleation of acicular ferrite. This point of view seems fairly plausible, although requiring a more painstaking substantiation.

Therefore, our results suggest that the favourable role of titanium in increasing impact toughness of the weld metal produced by using low-hydrogen electrodes can be enhanced by improving the efficiency of shielding the molten metal from air through increasing thickness of the electrode covering.

Under the efficient shielding conditions, the said role of titanium can be increased by using it in a

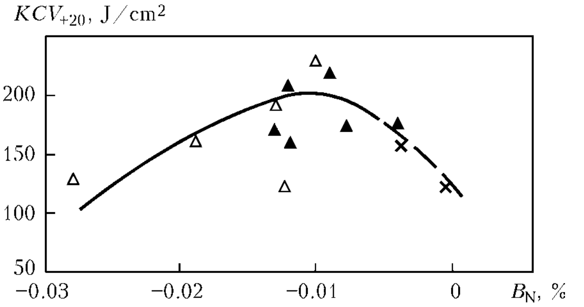

Figure 5. KCV_{+20} versus B_N in metal of the weld made with electrodes of experimental series *V*2

combination with boron. When present in metal in a concentration that is an order of magnitude lower than that of titanium, boron concentrates along the austenite grain boundaries and, in opinion of some specialists, blocks the mechanism of nucleation of grain-boundary ferrite, thus creating conditions for increasing formation of acicular ferrite on titanium oxide inclusions inside grains. As shown by our investigations, this leads to a substantial increase in impact toughness not only at room temperature, but also at negative temperatures down to −60 °C [26].

Main characteristics of the developed electrodes. The slag-forming system of covering, consisting of marble, fluorite, rutile and feldspar ($CaCO_3:CaF_2 \approx \approx 1:1$), was used to achieve good welding-operating

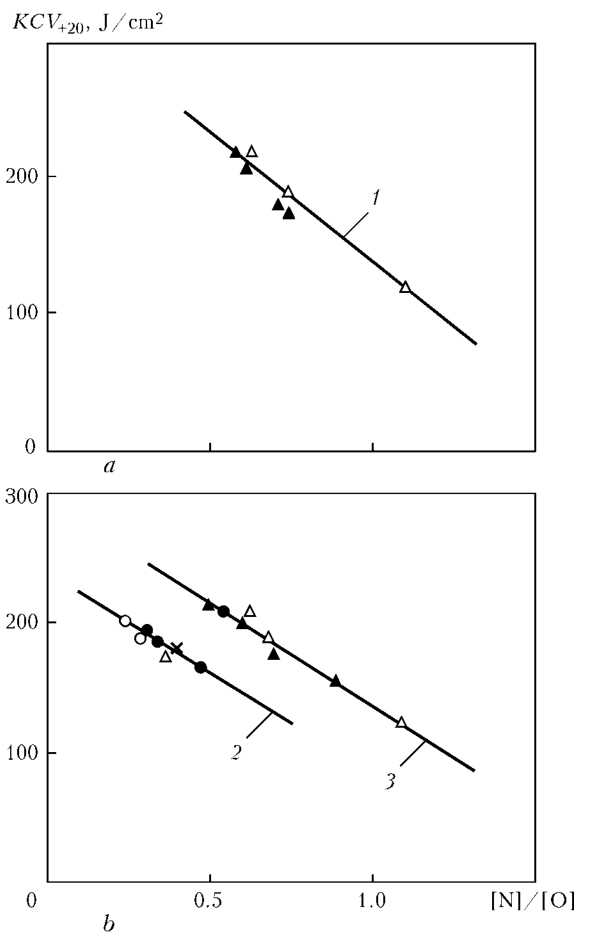

Figure 6. Curve $KCV_{+20} = f([N]/[O])$ plotted in experimental series *V*2 (*a*) and *W* (*b*): *1* — $B_N = 0.0105$ %; *2* — $[N]_{mean} = 0.013$ %, $[O] = 0.04$ %; *3* — $[N]_{mean} = 0.02$ %, $[O]_{mean} = 0.03$ %

Table 4. Mechanical properties of weld and deposited metals produced by using developed electrodes

Electrode diameter, mm	Steel		σ_y, MPa	σ_t, MPa	δ_5, %	KCV, J/cm^2, at temperature, °C			
	Grade	δ, mm				20	−20	−40	−60
3.0	St3*	20	584	641	23	160	95	53	35
4.0	St3*	20	510	579	28	180	175	170	55
5.0	St3*	20	494	581	26	168	150	112	42
4.0	09G2S	14	477	593	28	200	133	70	35
4.0	09G2	14	513	606	27	187	133	113	98

*Deposited metal (variant *A* acc. to GOST 9466–75), the rest of the specimens — weld metal (variant *B* acc. to GOST 9466–75).

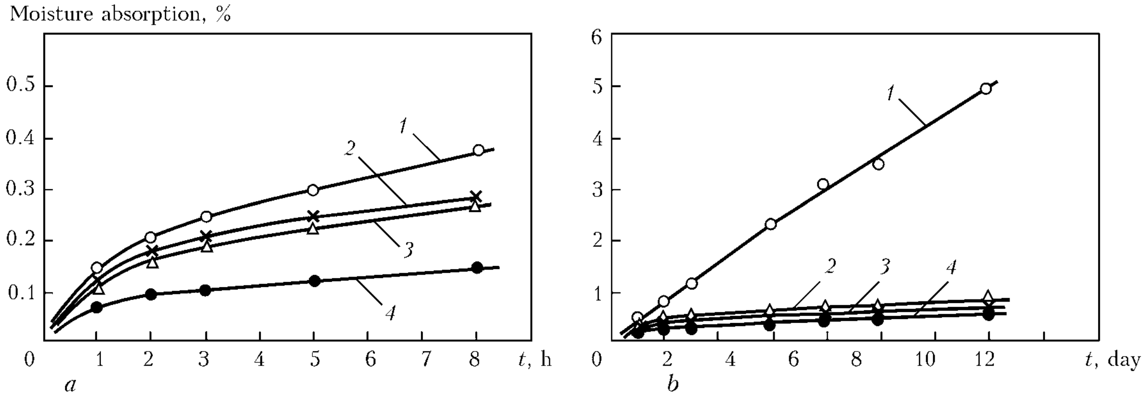

Figure 7. Kinetics of sorption of atmospheric moisture by covering of experimental electrodes observed for time t in hours (a) and in days (b) without (*1*) and with (*2–4*) different technological anti-hygrosorption additions

properties of electrodes. This system provides good formation of the weld metal, high detachability of the slag crust and negligible metal spattering.

The Ti + B microalloying system (Ti = 250–350 ppm, and B = 40–60 ppm) was selected, the optimal content of Mn being 1.2–1.6 wt.%, and that of Si = 0.2–0.4 wt.%. This provides the weld metal with a sufficiently high cold resistance. A relatively high basicity of the gas-slag system of the covering, and the use of complex deoxidation and alloying of the electrode metal (Mn–Si–Ti) decrease transfer of harmful sulphur and phosphorus impurities from the covering to the weld metal.

The decreased content of marble in the covering (51 wt.% $CaCO_3$ in UONI-13, and 28 wt.% $CaCO_3$ in a new electrode) provided improvement of operating properties of the covering mixtures due to suppression of the process of interaction of marble with liquid glass and solidification of the covering mixture in the press head.

Mechanical properties of the deposited and weld metals produced by using the developed electrodes are given in Table 4.

Figure 7 compares the hygrosorption resistance of the electrode covering with and without technological anti-hygrosorption additions. It can be seen that resistance of the coverings to absorption of the atmospheric moisture under the effect of the technological additions grows to a level that meets requirements to electrodes having an index of high hygrosorption resistance of their coverings (HMR).

CONCLUSIONS

1. In welding with covered electrodes, the welding zone is not shielded from the ambient air as reliably as in the case of using other welding consumables. Under such conditions, titanium exhibits not only deoxidising properties (like manganese and silicon), but also nitride-forming ones. This double role of titanium does not allow using it to the full extent as a microalloying element to efficiently regulate impact toughness of the weld metal.

2. Based on analysis of literature sources and results of own investigations, conditions are suggested for using the systems of Mn–Si–Ti alloying and microalloying of the weld metal produced with low-hydrogen electrodes having a different gas-slag base of the covering, which promote increase in impact toughness of the weld metal. It was established that this can be achieved by improving the efficiency of shielding of the welding zone from interaction with air through increasing the $CaCO_3/CaF_2$ ratio in the covering and its thickness. This leads to reduction of the probability of formation of titanium nitrides with nitrogen that gets into the welding zone from the ambient air.

3. The concentration of Mn–Si–Ti in metal deposited with low-hydrogen electrodes having a different

$CaCO_3/CaF_2$ ratio in the covering was selected, providing good welding-operating properties of the electrodes and high impact toughness of the weld metal.

4. Under conditions of efficient shielding of molten metal from air, impact toughness of the weld metal can be additionally increased not only at room temperature, but also at negative temperatures down to −60 °C by combining titanium as a microalloying element with boron.

5. Hygroscopicity of the electrode coverings with technological anti-hygrosorption additions was studied. As established, they substantially increase resistance of the electrode coverings to absorption of the atmospheric moisture.

6. The investigation results were used for the development of low-hydrogen electrodes intended to replace electrodes UONI-13/15 for welding of carbon and low-alloy steels and repair of bridge and transport structures.

1. (1998) *On approval of the Program for establishing and functioning of the national network of international transport passageways in Ukraine:* Resolution of the Cabinet of Ministers of Ukraine of 20 March 1998.
2. Lyakishev, N.P. (1998) Structural and some functional materials. Present and future. In: *Current materials science of the 21st century*. Kiev: Naukova Dumka.
3. Lyakishev, N.P. (2000) Natural gas–metal–pipes. *Problemy Sovremen. Materialovedeniya*, **2**, 89–94.
4. Zhiznyakov, S.N., Konopatov, V.S., Lyalin, K.V. (1988) Causes of formations of defects in welded joints on metal structures of oxygen-converter workshop at the Magnitogorsk Metallurgical Plant. In: *Erecting and special building works.* Fabrication of metallic and erection-building structures Series, **11**, 1–5.
5. Mikhoduj, L.I., Kirian, V.I., Poznyakov, V.D. et al. (2003) Sparselly-alloyed high-strength steels for welded structures. *The Paton Welding J.*, **5**, 34–37.
6. Kovtunenko, V.A., Gerasimenko, A.M., Godulyak, A.A. (2006) Selection of steel for critical building welded structures. *Ibid.*, **11**, 27–31.
7. *STO-GK Transstroj-005–2007*: Steel structures of bridges. Technology of erection welding. Moscow.
8. Grabin, V.F., Denisenko, A.V. (1978) *Physical metallurgy of welding of low- and middle-alloy steels*. Kiev: Naukova Dumka.
9. Cochane, R.C. (1982) Weld metal microstructures: a state-of-the-art rev. *IIW Doc. IX-1248–82*.
10. Levin, E., Hill, D.C. (1977) Structure-property relationships in low C weld metal. *Met. Transact. A*, 8(**9**), 1453–1463.
11. Choi, C.L., Hill, D.C. (1978) A study of microstructural progression in as-deposited weld metal. *Welding J.*, **8**, 232–236.
12. Ricks, R.A., Howell, P.A., Darrite, G.S. (1982) The nature an acicular ferrite in HSLA weld metals. *J. Mater. Sci.*, **17**, 732–740.
13. Evans, G.M. (1980) Effect of manganese on the microstructure and properties of all-weld metal deposits. *Welding J.*, 59(**3**), 67–75.
14. Evans, G.M. (1981) Factors affecting the microstructure and properties of C–Mn all weld metal deposits. *IIW Doc. II-957–81*.
15. Abson, D.J., Evans, G.M. (1989) A study of the manganese-oxygen system in low hydrogen MMA all-weld metal deposits. *IIW Doc. IIA-770–89*.
16. Evans, G.M. (1986) The effect of silicon on the microstructure and the properties of C–Mn all-weld metal deposits. *Oerlikon Schgweissmitteilungen*, 44(**110**), 19–33.
17. Evans, G.M. (1991) The effect of titanium on the microstructure and properties of C–Mn all-weld metal deposits. *IIW Doc. II-A-827–91*.
18. Sakaki, H. (1960) Effect of alloying elements on notch toughness of basic weld metals. Rep. on effect of aluminium and titanium. *J. JWS*, 29(**7**), 539–544.
19. Nakano, S., Shiga, A., Tsuboi, J. (1975) Optimising the titanium effect on weld metal toughness. *IIW Doc. XII-B-182–75*.
20. Wolsh, R.A., Ramachandran, S. (1963) Equilibrium in the Fe–Mn–Si–O system. *Transact. of Metallurg. Soc. of AJME*, 227(**3**), 560–562.
21. Grong, O., Siewerts, T.A., Martins, G.P. et al. (1986) A model for the silicon-manganese deoxidation of steel weld metals. *Metallurg. Transact. A*, 17(**10**), 1797–1807.
22. Gurevich, Yu.G. (1972) Solubility of titanium, oxygen and nitrogen in molten iron. *Izvestiya Vuzov. Chyorn. Metallurgiya*, **5**, 42–45.
23. Gurevich, Yu.G. (1960) Interaction of titanium with nitrogen and carbon in molten steel. *Ibid.*, **6**, 59–67.
24. Rittinger, J., Fehervari, A. (1976) Mikrootvozo elemek hatasa szerkezeti acelok szivossagara. *GEP XXVIII Evfolyam*, **7**, 267–272.
25. Fehervari, A., Rittinger, J. Comments on Intern. Inst. of Welding. *IIW Doc. XII-B-98–71, XII-B-109–72*.
26. Yavdoshchin, I.R., Pokhodnya, I.K., Folbort, O.I. (2007) Increase in cold resistance of welds by optimization of alloying and microalloying systems in covered-electrode welding of increased- and high-strength steels. In: *Proc. of 4th Int. Conf. on Welding Consumables in the CIS Countries «Welding Consumables. Development. Technology. Production. Quality. Competitiveness»* (Krasnodar, 18–21 June 2007). Krasnodar, 218–223.

NEW TECHNOLOGY FOR REPAIR OF GUIDE SURFACES OF AXLE BOX OPENING OF SIDE FRAME OF THE 18-100 MODEL FREIGHT CAR TRUCK

G.V. KUZMENKO[1], **V.G. KUZMENKO**[1], **V.I. GALINICH**[1], **V.I. LIPISY**[2] and **V.V. NESTYKAJLO**[2]
[1]E.O. Paton Electric Welding Institute, NASU, Kiev, Ukraine
[2]Rolling Stock Design and Technology Bureau of «Ukrzaliznytsya», Kiev, Ukraine

The electric arc hardfacing technology based on application of embedded electrodes with wire feed channels is described. The technology provides the specified thickness of the deposited layer. The quality of formation corresponds to the quality of the cast metal surface and requires no machining. Welding consumables (flat electrode and flux-cored wire) as well as special equipment were developed.

Keywords: *electric arc hardfacing, embedded electrode, railway cars, hardfacing equipment, hardfacing consumables, repair of parts, side frame of truck*

The progress in modern engineering is characterized by constant overloading of service conditions of machines and equipment. For such conditions, most parts in machine building are recommended to manufacture with wear-, corrosion- or heat-resistant coatings on their working surfaces. The quality of metal surfaces of parts and units subjected to the heaviest wear can be improved by different methods. Hardfacing is the simplest, most affordable and least expensive method among them. It provides metal saving, improves performance of equipment and machines, reduces their downtimes due to repair, and leads to increase of the efficiency of public works.

Railway transport comprises a large number of parts which intensively wear out during operation. These parts include a wheel–rail pair, surfaces of the devices for coupling of cars, parts and units of car trucks, etc. One of such parts is a side frame of truck of the 18-100 model freight car, which is most common in the territory of the CIS and Baltic countries (Figure 1). The surfaces of axle box opening of this part suffer from an intensive impact-abrasive loading in the process of operation. The side frame is a large-size (measuring 2413 × 654 × 620 mm, and approximately 420 kg in weight) cast structure made from low-alloy steel 20GL or 20GFL. It is the main element of the freight car truck, which transfers load on the axle through axle boxes.

The guide surfaces of the side frame axle box opening (four surfaces 45 × (120–150) mm in size per opening, or eight surfaces of a total area of about 500 cm^2 per frame) are subject to repair, according to the existing norms, to ensure the required width of the axle box opening, in case of their wear to not more than 8 mm per side. These surfaces are clad by the existing technology using mechanized or manual arc hardfacing methods, which fail to provide the required quality of repair and productivity of work. As a result, a large amount of the side frames soon need to be repaired again. In this connection, it is a pressing problem to develop such a technology for repair of guide surfaces of the side frame, which would provide their quality repair and high wear resistance at high deposition efficiency.

It is known that the deposition efficiency can be increased by increasing the welding current. In automatic single-wire hardfacing, the value of the welding current is limited by section of the electrode and reliability of its contact with the current contact jaw. The use of two or more wires reduces this limitation, since the electrode section and contact area with the current contact jaw increase, thus allowing reduction of the welding current. Therefore, automatic multi-

Figure 1. Side frame of four-wheel truck of 18-100 model freight car

electrode hardfacing is more efficient than the single-electrode one. Increase in the number of electrodes also leads to qualitative changes in the process of their melting, which transforms from the continuous into pulse one. This provides decrease in total heat input and deformation, substantial reduction of the base metal penetration depth (by 10–15 %), 25 % decrease in consumption of the electric power per kilogram of the deposited metal, and improvement of quality and performance of the deposited layer [1]. At the same time, multi-electrode hardfacing under forced conditions has an important drawback — satisfactory formation of the deposited metal is possible only in flat position.

The fundamentally new electric arc welding and hardfacing process developed by the E.O. Paton Electric Welding Institute of the NAS of Ukraine in the last several years [2, 3] was used for the development of the technology for repair of side frame guide surfaces. It consists in utilization of the large-section flat electrode with an insulating coating, which is preliminarily introduced into a gap between the parts to be welded (embedded electrode technology). Steel core of the electrode has longitudinal channels, through which solid or flux-cored wires in amounts that depend on width of the electrode are fed in the process of its melting. In hardfacing, one of the parts is replaced by a forming device. Thus, this is a principle of forced formation of the deposited metal, which allows applying this process in positions other than the flat one without significant limitation of hardfacing conditions. Flow diagram of hardfacing with embedded electrode is shown in Figure 2. Its advantage in comparison with the other existing ones is the possibility of performing the process with the electric arc that burns in parallel to the surface treated. This makes it possible to avoid the direct effect of the arc on surface of the base metal and considerably decrease the degree of penetration of the latter. In addition, electric arc hardfacing with embedded electrode allows deposition of fairly large surfaces per pass. The scheme of positioning of the flat electrode in parallel to the deposited surface and utilization of the principle of forced formation permit thickness of the deposited layer to be preset quite accurately within the certain ranges (from 5 to 20 mm) by using corresponding sizes of the embedded electrode and forming device, as well as by regulating the gap between the latter and base metal surface.

The following sequence of operations was used for the development of the technology for repair of side frame guide surfaces:

• if necessary, manual or mechanized hardfacing of the guide surfaces to provide their required width size (nominal — 160^{+1}_{-2} mm);

• machining of worn-out guide surfaces to provide 346 mm width of the axle box opening;

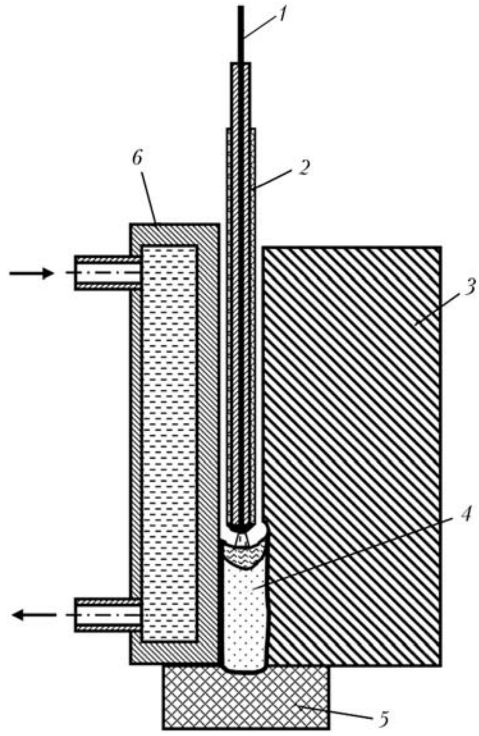

Figure 2. Flow diagram of the process of electric arc hardfacing with embedded electrode: *1* — welding wire; *2* — embedded electrode; *3* — part being clad; *4* — deposited metal layer; *5* — backing; *6* — water-cooled mould

• automatic hardfacing of the guide surfaces to provide 335 mm nominal width of the axle box opening.

With this technology there is no need to apply machining after hardfacing, which leads to increase in hardness of the deposited metal and may significantly extend the overhaul life and limit repair costs.

The specialists of Rolling Stock Design and Technology Bureau of «Ukrzaliznytsya» and E.O. Paton Electric Welding Institute developed the experimental setup (Figure 3) for optimization of the hardfacing equipment and technology, which consists of:

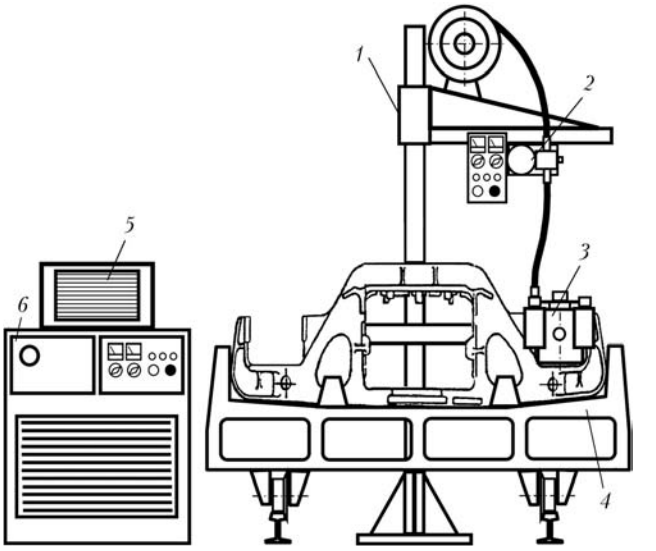

Figure 3. Scheme of experimental setup for hardfacing of side frame guide surfaces of truck of freight car (see designations in the text)

Figure 4. Experimental-industrial setup for hardfacing of guide surfaces of axle box opening of side frame of truck of the 18-100 model freight car

• building berth for positioning and fixing of the side frame during hardfacing in «opening up» position;

• block of chill moulds *3*, providing quality formation of the guide surfaces (the chill moulds are equipped with special devices for fixation of the embedded electrodes and supply of the welding current to them. They are mounted on each block in front of the corresponding surface being deposited, and are electrically insulated from the chill mould);

• automatic welding device *2*, which is intended to feed welding wires to the deposition zone via longitudinal channels in an embedded electrode, and consists of a welding wire feeder to feed three 1.6 mm diameter wires at a feed speed of 30 to 200 m/h, power and control units, fasteners for welding wires reels, flexible channels for feeding the wires, and power and control cables;

• welding current source *6* — thyristor rectifier VDU-1202;

• independent unit for chill moulds cooling *5*.

The automatic welding device is mounted on rotary column *1*, this providing hardfacing of all side frame guide surfaces in turn.

The setup indexed as KT-107 (Figure 4) was manufactured and tested at experimental production of the Rolling Stock Design and Technology Bureau of «Ukrzaliznytsya». Besides, the special machine tool for milling of the guide and bearing surfaces of the side frame before hardfacing was also manufactured there.

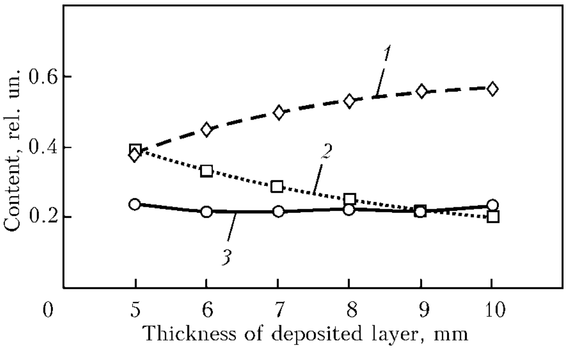

Figure 5. Content of wire (*1*), electrode (*2*) and base metal (*3*) in deposited metal depending on thickness of the deposited layer

The contents of base, electrode and wire metals in the deposited metal for different thicknesses of the deposited layer and optimal process conditions (600 A, 25 V) were calculated from the experimental data, based on the fact that thickness of the deposited layer may change in a wide range (from 5 to 10 mm) depending on the degree of wear of the guide surfaces. As can be seen from Figure 5, whereas the content of the base metal remains almost constant and equal to about 0.21–0.23 with a change in thickness of the deposited layer, similar indicators for the electrode and wire vary within sufficiently wide ranges, i.e. from 0.20 to 0.39 and from 0.38 to 0.57, respectively. Thus, the electrode and wire metals should be close in composition, so that a change in thickness of the deposited layer does not lead to any substantial variations in its chemical composition and hardness. Therefore, alloying of the deposited metal should be carried out simultaneously through the embedded electrode and welding wire and in equal proportions to increase its hardness.

Special flat metal-cored embedded electrode ANPM-40 with a section of 3 × 40 mm and 250 mm length, having a 1 mm thick insulating coating on each side (Figure 6), was developed for hardfacing of the side frame guide surfaces. Thus, the total electrode thickness is 5 mm, which provides the deposition thickness over the entire required range from 5 to 8 mm. The electrode core is made from low-carbon cold-rolled steel of the 08kp (unkilled) grade, while the necessary alloying of the deposited metal is per-

Chemical composition of the materials and their hardness

Object of investigation	Content of element. wt.%						Hardness *HB*
	C	Si	Mn	V	S	P	
Embedded electrode ANPM-40	0.12	0.23	0.78	–	0.018	0.023	–
Wire PP ANPM-4	0.11	0.31	1.43	–	0.014	0.016	–
Metal of side frame (steel 20GL)	0.21	0.27	1.37	–	0.032	0.028	125–131
Metal of side frame No.2 (steel 20 GFL)	0.23	0.33	1.39	0.011	0.035	0.032	154–165
Deposited metal No.1	0.14	0.26	1.26	–	0.021	0.023	135–143
Deposited metal No.2	0.13	0.25	1.32	–	0.019	0.020	139–147

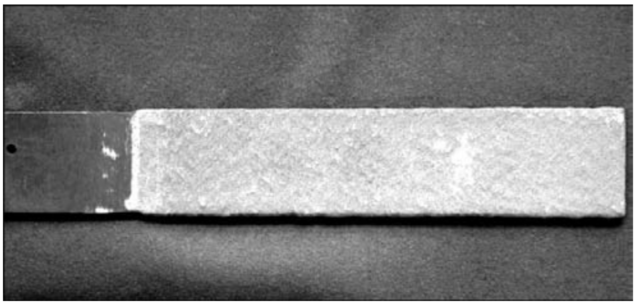

Figure 6. Embedded electrode ANPM-40 for hardfacing of side frame guide surfaces

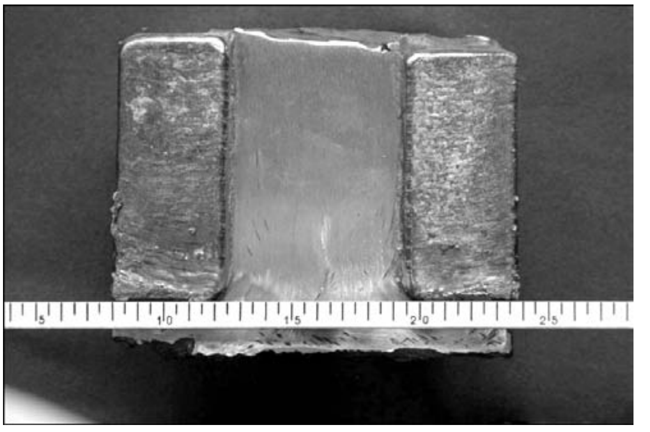

Figure 7. Fragment of side frame with two deposited guide surfaces

formed through its coating, the weight factor of which is approximately 35 %. The 1.6 mm diameter flux-cored wire of the PP ANPM-4 grade was also developed to compensate for shortage of the deposited metal and provide its additional alloying.

Samples of the side frames were deposited with the KT-107 setup by using electrodes ANPM-40 and wire PP ANPM-4. At I_w = 650 A and U = 26 V, the time of deposition of each surface is about 1.5 min, which, including the preparation time, allows achieving the efficiency of up to 8 side frames per shift.

Examination of the deposited metal showed that it had no pores, cracks and slag inclusions. Chemical compositions of the base metal of the side frames, embedded electrode, wire, metal of experimental depositions and their hardness are given in the Table. As can be seen from the Table, hardness of the deposited metal is at a level of the corresponding value of the side frame base metal. To increase wear resistance of the side frames, the samples were also deposited by using welding consumables that provide increased hardness of the deposited metal. For that, ferroalloys (ferrochromium, ferromolybdenum, ferrovanadium etc.) were additionally introduced into a composition of the embedded electrode coating and into the charge of the flux-cored wire, which provided hardness of the deposited metal at a level of *HB* 250–300.

Quality of the deposited metal surface corresponded to that of the cast metal and required no subsequent machining. A fragment of the side frame with two deposited surfaces is shown in Figure 7.

CONCLUSIONS

1. The fundamentally new technology for electric arc hardfacing of worn-out surfaces was developed by the E.O. Paton Electric Welding Institute of the NAS of Ukraine. The technology is based on the use of a flat electrode coated by an insulating layer with channels to feed wire, which is preliminarily introduced into the gap of a specific size between the surface to be deposited and a special copper water-cooled forming device (chill mould).

2. Experimental-industrial setup KT-107 was developed and manufactured together with Rolling Stock Design and Technology Bureau of «Ukrzaliznytsya» for hardfacing of side frame guide surfaces of truck of the 18-100 model freight car. The setup is composed of a special welding equipment and building berth for positioning of frames during hardfacing. In addition, the E.O. Paton Electric Welding Institute developed specialized welding consumables, in particular, flat electrode ANPM-40 and flux-cored wire PP ANPM-4.

3. Experimental-industrial repair of worn-out side frames by the new hardfacing technology with embedded electrode was carried out by using a setup located in the territory of Rolling Stock Design and Technology Bureau of «Ukrzaliznytsya». The time necessary for hardfacing of one frame (8 surfaces 45 × × 50 mm in size) is such that it makes it possible to repair up to eight frames per shift.

4. The new hardfacing technology provides preset thickness of a layer of the deposited metal, the quality of its surface corresponding to that of the cast metal, thus requiring no additional machining. Moreover, increased hardness of the deposited metal (*HB* 250–300) can be provided by its additional alloying through the coating of the embedded electrode and charge of the flux-cored wire, which can significantly increase wear resistance of the side frame guide surfaces.

5. The technology and equipment developed for repair of the guide surfaces of axle box opening of truck of the 18-100 model freight car can be recommended for implementation at «Ukrzaliznytsya» car-repair enterprises.

1. Melikov, V.V. (1988) *Multi-electrode hardfacing*. Moscow: Mashinostroenie.
2. Kuzmenko, V.G., Kuzmenko, G.V. *Method of consumable electrode arc welding and electrode for its realization*. Pat. 2219021 RF. Int. Cl. B32K 9.14, 35/36. Publ. 20.12.2003.
3. Kuzmenko, V.G., Kuzmenko, G.V. *Method of consumable electrode arc welding and electrode for its realization*. Pat. 68361 Ukraine. Int. Cl. B23K 9/2. Publ. 16.08.2004.

PROPERTIES OF WELDED JOINTS OF RAIL STEEL IN ELECTRIC ARC WELDING

V.D. POZNYAKOV, V.M. KIRIAKOV, A.A. GAJVORONSKY, A.V. KLAPATYUK and **O.S. SHISHKEVICH**
E.O. Paton Electric Welding Institute, NASU, Kiev, Ukraine

The results of investigations of effect of thermodeformational cycles of welding on structural changes, strength and ductility properties of HAZ metal of welded joints of rail steel with carbon content of 0.72 % are given. Influence of preheating temperature and value of welding heat input on delayed fracture resistance of HAZ metal and cold crack formation in the joints was studied.

Keywords: *arc welding, railway rails, welded joints, heat-affected zone, delayed fracture, cold cracks*

At manufacturing of railway rails the high-carbon silicon-manganese steel with carbon content of 0.71–0.82 % and manganese of 0.75–1.05 % is used. The adding of manganese in such amount into rail steel in comparison with carbon steel sharply decreases critical rate of hardening and increases considerably the depth of its heat treatment. Therefore, the welding of such type of steels is connected with considerable difficulties which lie in development of measures on prevention of occurrence of crystalline (hot) and delayed (cold) cracks in weld metal and near-weld HAZ metal [1, 2].

Initiation of hot cracks in weld metal takes place as a result of increase of carbon content at its stirring with a base metal in the process of arc welding. To increase resistance of weld metal against hot cracks is possible due to application of electrode materials with decreased carbon content, welding at conditions providing minimal penetration of base metal and also increasing a coefficient of deposition [1]. At mechanized methods of welding the best results are achieved using wires of small diameter at straight polarity and decreased heat inputs.

The largest difficulties during welding of high-carbon steels appear due to formation of cold cracks in joints. Their formation is predetermined by tendency of high-carbon steels to hardening and correspondingly determined by peculiarities of structural transformations in HAZ metal under the influence of thermodeformational cycle of welding. It is especially difficult to prevent the cold cracks formation when a joint could not be subjected to special heat treatment directly after welding.

As to the main value of steel weldability and resistance of welded joints against cold cracks formation the high-carbon rail steel is very close to high-strength medium-alloy steels, the carbon content of which is 0.3–0.4 %. The value of carbon equivalent for these steels is approximately the same (C_{eq} = 0.8–1.0 %) [2]. Therefore, to prevent the cold cracks formation in welded joints of rail steel the similar technological solutions as in welding of medium-alloyed steels can be applied.

During investigations of weldability of medium-alloyed steels the most efficient methods of preventing the cold cracks formation in HAZ metal of joints are established [2, 3]. They include control of thermal cycle of welding and temporary welding stresses, application of welding wires with a low melting temperature, decrease of content of diffusive hydrogen in weld metal, application of additional technological procedures like preliminary surfacing of groove edges of a joint, special technology of welding and other.

The most simple and convenient method is control of thermal cycle using preliminary and concurrent heating of the joint along with the optimal selection of welding conditions. In many cases the welding of medium-alloyed carbon steels at such approach allows almost complete eliminating the danger of cold cracks formation in the joint. The perfect thermal welding cycle is considered to be that one which excludes overheating of metal in the near-weld HAZ area as a result of its rapid heating and cooling at temperatures above the temperature A_{c_1}. The delayed cooling below A_{c_1} temperature facilitates the development of pearlite and intermediate transformations of overcooled austenite. Here the amount of hardening structures is considerably decreased and resistance of HAZ metal against fracture is increased.

As to investigations of weldability of rail steel, then these data are limited. They concern mainly the problems of increase of quality of rails during their manufacture and also welded joints, performed using the resistance method of welding [4–6].

The purpose of this work was to study the influence of thermodeformational cycle of welding (TDCW) on the formation of structure, change of strength and ductile properties of metal, resistance of HAZ metal to delayed fracture and resistance of welded joints of high-carbon rail steel to cold cracking.

At the first stage of investigations the simulation method of TDCW was used on the basis of installation

Table 1. Cooling rate in HAZ metal in mechanized welding of rail steel joints

Q_w, kJ/cm	T_{preh}, °C	$w_{6/5}$*, °C/s
8.6	20	20–25
27.5	20	11–13
8.6	100	13–15
8.6	150	10–12
8.6	200	4.5–6.0
8.6	250	3.0–4.2

*The cooling rate after the first pass is given.

MSR-75 using electronic programming devices [7]. Structural transformations in the metal under the influence of TDCW were studied using thermal differential analysis. The specimens of 120 × 12 × 12 mm size of rail steel with carbon content of 0.72 % were used which were heated using electric current (maximal temperature of heating was 1320 °C, rate of heating was 220–250 °C/s, cooling rate in the range of temperatures 600–500 °C was 3–22 °C/s). The investigated range of cooling rates is mostly characteristic of butt joints of rail steel of 300 × 150 × 15 mm size, performed using mechanized welding in shielding gas and wire Sv-08G2S of 1.2 mm diameter (Table 1).

Figure 1 shows the diagram of transformation of overcooled austenite of rail steel, and Figure 2 shows the typical areas of microstructure of simulated HAZ metal. It is seen that transformation of overcooled austenite at cooling rates 10–22 °C/s occurs mostly in martensite area (Figure 2, *a, b*). The temperature of beginning of martensite transformation is 220 °C.

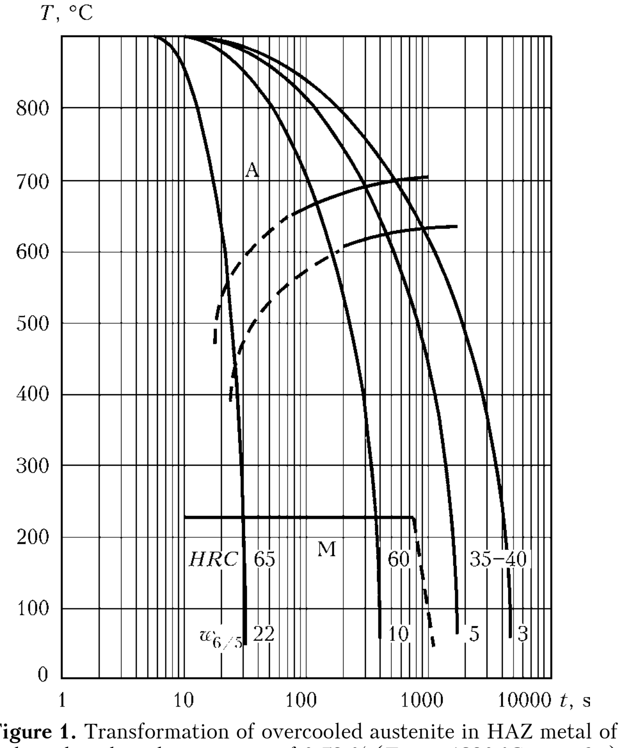

Figure 1. Transformation of overcooled austenite in HAZ metal of rail steel with carbon content of 0.72 % (T_{max} = 1320 °C, t_h = 6 s)

The hardness of hardened metal is *HRC* 60–65. The decrease in cooling rate in this range does not lead to considerable changes in the structure. The further delay in cooling ($w_{6/5} \le 10$ °C/s) facilitates decrease in hardness of metal, which is connected with kinetics of austenite decay. At the cooling rate of 3–5 °C/s the hardened structures are absent, the transformation in HAZ metal occurs mostly in pearlite area, and hardness of metal decreases to *HRC* 35–40 (Figure 2, *c*).

Thus, in HAZ metal of rail steel with carbon content of 0.72 % the formation of hardened structures occurs at the cooling rates above 5 °C/s. To avoid conditions of hardening of HAZ metal in welding is possible by applying the preheating of joints of up to 200 °C (see Table 1). Considering that carbon content in rail steel can be higher (up to 0.82 %) and martensite transformation can take place at lower cooling rates ($w_{6/5} \le 5$ °C/s), the temperature of preheating T_{preh} in welding of rails should be not less than 250–300 °C.

The strength and ductile properties of HAZ metal of rail steel were evaluated by standard methods. For this purpose special specimens were manufactured

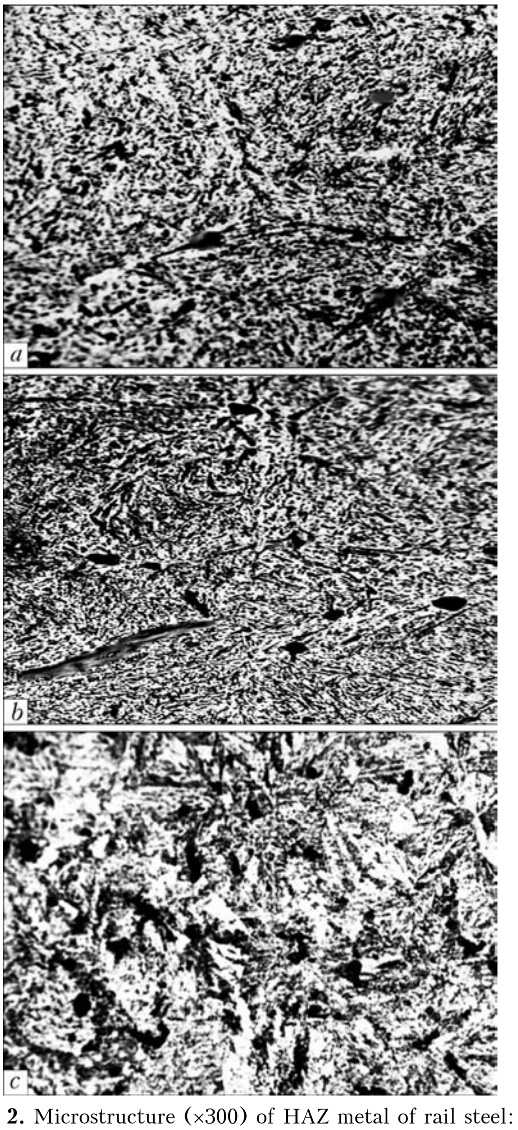

Figure 2. Microstructure (×300) of HAZ metal of rail steel: *a* — $w_{6/5}$ = 22; *b* — 10; *c* — 3 °C/s

Table 2. Mechanical properties of HAZ metal of rail steel with carbon content of 0.72 %

$w_{6/5}$, °C/s	σ_y, MPa	σ_t, MPa	δ_5, %	ψ, %	KCU_{+20}, J/cm^2
5	830	1120	7.7	21.4	6.7
10	880	1250	5.0	12.6	6.2
22	920	1280	4.7	12.6	5.8

from simulated pieces for static tensile tests of metal according to GOST 1497–84 and impact bend tests according to GOST 9454–78. The generalized results of tests are given in Table 2.

As is seen, at high cooling rates when transformation of overcooled austenite occurs mainly in the martensite region, the structure of hardened metal with increased properties of strength and low ductility is formed in HAZ metal of joints. Such metal has low deformability and relatively increased tendency towards delayed fracture. To improve the ductile properties of HAZ metal is possible due to delayed cooling of welded joints. With decrease of cooling rate to $w_{6/5} \leq 5$ °C/s the values of ductility of metal are 1.5–2 times increased.

It is obvious that due to a low ductility of HAZ metal of rail steel the relaxation of stresses in the joint will be complicated. Therefore, in welding of rails without application of preheating it is practically impossible to avoid cold cracks formation in joints. At low cooling rates ($w_{6/5} \leq 5$ °C/s) the transformation of austenite occurs with formation of more ductilec structures, but also with extremely high level of strength. Such metal is more capable to microplastic deformations, and resistance to delayed fracture of joints should be comparatively higher.

The quantitative estimation of resistance of single-pass welded joints of rail steel to delayed fracture was performed using Implant method [2]. In the course of experiments the cylinder specimens-inserts of 6.0 mm diameter without screw thread were used. Figures 3 and 4 present results of investigations of resistance of single-layer welded joints of rail steel to delayed fracture.

It is seen from the given data that during conventional welding conditions using wire Sv-08G2S at heat input Q_w = 8.6 kJ/cm without application of preheating (T_{preh} = 20 °C) HAZ metal of joints has very low level of resistance to delayed fracture. The critical stresses of fracture σ_{cr} = 60 MPa, which amounts only to $0.07\sigma_y$. The preheating up to 250 °C facilitates the increase of resistance of HAZ metal to delayed fracture of more than 7 times ($\sigma_{cr} = 0.55\sigma_y$). At preheating of up to 300 °C the delayed fracture of Implant specimens was not observed.

The increase in heat input of welding up to 27.5 kJ/cm (T_{preh} = 20 °C) also facilitates the increase in resistance of joints to delayed fracture. The level of σ_{cr} is 280 MPa. The welding at the given heat input positively influences the change of HAZ metal structure which is comparable with welding at heat input of 8.6 kJ/cm using preheating up to 150 °C. Using both variants of welding the cooling rate in joints (see Table 1) and formed structure of metal of near-weld HAZ area are almost the same. Therefore, single-layer welded joints are fractured approximately at the same level of loading.

The application of preheating in welding delays cooling. In HAZ metal of joints of rail steel the more ductile structures are formed. As is known, it facilitates development of local microplastic deformations in hardened HAZ metal, which results in more intensive proceeding of relaxation processes and increase of resistance of welded joints to delayed fracture [8, 9].

In welding using wire Sv-08Kh20N9G7T (A + F) at heat input of 8.6 kJ/cm without preheating (T_{preh} = = 20 °C) critical stresses of fracture amount only to 100 MPa. This is a bit higher than at similar conditions of welding using ferrite-pearlite wire Sv-08G2S (F +

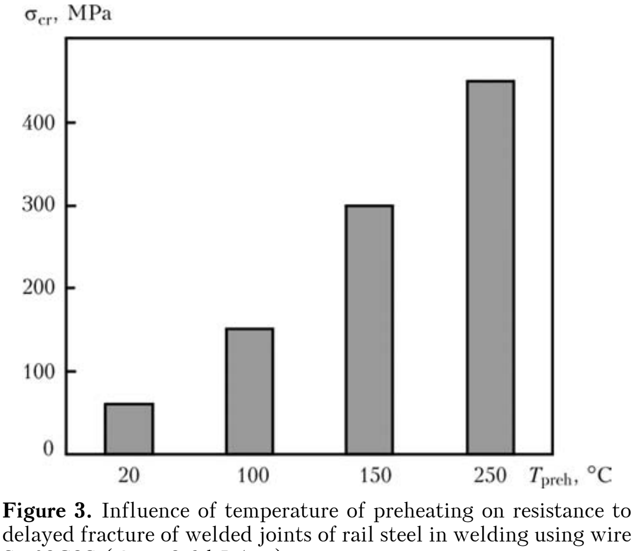

Figure 3. Influence of temperature of preheating on resistance to delayed fracture of welded joints of rail steel in welding using wire Sv-08G2S (Q_w = 8.6 kJ/cm)

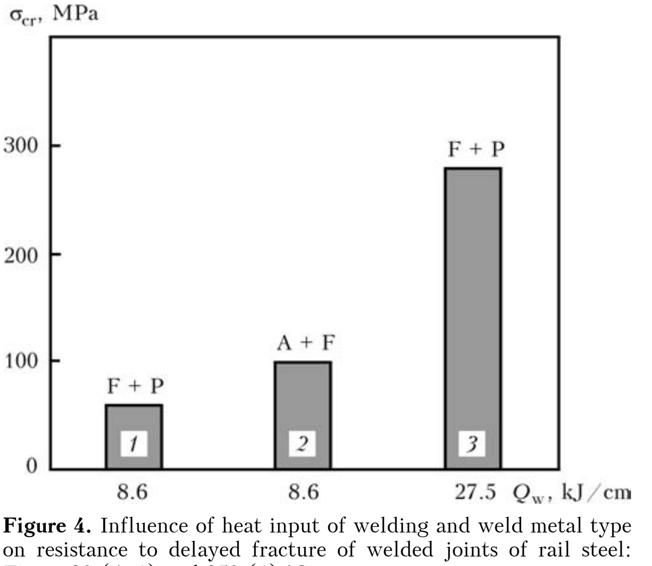

Figure 4. Influence of heat input of welding and weld metal type on resistance to delayed fracture of welded joints of rail steel: T_{preh} = 20 (*1, 2*) and 250 (*3*) °C

Table 3. Characteristics of cold cracks in the joints of rail steel in welding of technological samples «rigid boxing»

No.	Welding conditions	Longitudinal crack	Transverse crack
1	Q_w = 8.6 kJ/cm T_{preh} = 20 °C	Crack along the fusion line, 100 % in the height of a joint During welding a crack escaped to the surface of a joint after overlapping of each layer	Crack crosses the weld into HAZ and further to the base metal for the depth up to 10 mm During welding a crack escaped to the surface of a weld after overlapping of each layer
2	Q_w = 27.5 kJ/cm T_{preh} = 20 °C	Crack along the fusion line, 50 % in the height of a joint During welding there was no crack on a surface of a joint	Crack propagation into the weld for the depth of up to 30 % Crack on the surface of a weld escaped after welding of the second layer
3	Q_w = 8.6 kJ/cm T_{preh} = 250 °C	No cracks	No cracks

+ P), however, considerably lower than the level of σ_{cr}, which is provided by application of preheating of metal up to the temperature of 250 °C.

It is known that in welding of high-strength alloyed steels with carbon content of up to 0.4 % the austenite-ferrite weld metal positively influences the formation of HAZ metal structure. Using given materials it is possible to considerably increase resistance of joints to delayed fracture [2, 3]. However, using such welds in welding of high-carbon rail steel due to formation of low-ductile structures in HAZ metal at high cooling rates no considerable increase of resistance of joints to delayed fracture occurs.

The further investigations were directed to study of influence of technological factors on the peculiarities of cold cracks formation in multi-layer welded joints of rail steel.

The resistance of joints of high-strength rail steel against cold cracks formation was investigated in welding of technological samples «rigid boxing». The technological samples represent butt joints which are prewelded-in to massive base along the contour. To evaluate the resistance of joints against formation of longitudinal cold cracks, the butt joints of the size 300 × 100 × 45 mm were used, and for transverse cracks the butt joints of 300 × 300 × 15 mm size were used. Concentrators of stresses in samples are corre-

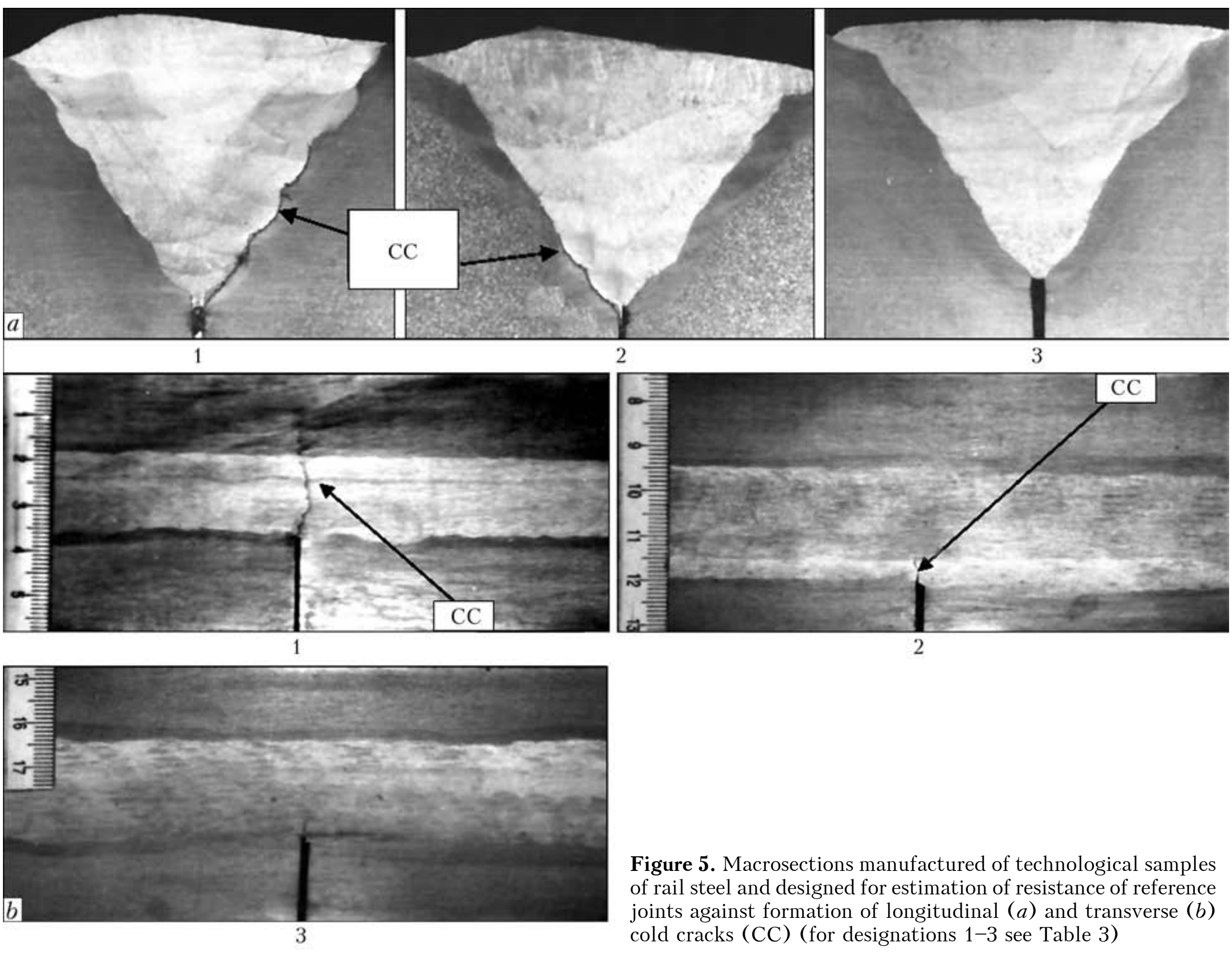

Figure 5. Macrosections manufactured of technological samples of rail steel and designed for estimation of resistance of reference joints against formation of longitudinal (*a*) and transverse (*b*) cold cracks (CC) (for designations 1–3 see Table 3)

spondent design lacks of penetration in longitudinal or transverse directions. The multilayer welding of such samples was performed using wire of the type Sv-08G2S of 1.2 mm diameter in shielding gas. To fix the moment of formation and process of cold cracks propagation in welding of reference butt weld of technological samples the method of acoustic emission was applied. After completion of welding the samples were subjected to holding at room temperature up to 3 days. Further the reference butt weld was separated from the base and sections were cut of it for visual inspection for the presence of cold cracks in the joint.

Table 3 presents the generalized results of investigations in welding of technological samples, and Figure 5 shows macrosections of the reference joints. As is seen, the welded joints of rail steel at conventional conditions of mechanized welding without application of preheating have low resistance against formation of both the longitudinal, as well as transverse cold cracks. To increase resistance of welded joints of rail steel against cold cracks formation is possible by applying preheating and increasing heat input of welding.

The results of carried out investigations on the influence of TDCW on the structure and properties of welded joints are basic for development of reliable technology of electric arc welding of railway rails. The main technological requirement in electric arc welding of high-strength rail steel is the application of preheating of joints up to the temperatures of not lower than 250 °C.

CONCLUSIONS

1. The complex of investigations was carried out for establishment of influence of TDCW on formation of structure and mechanical properties of rail steel with carbon content of 0.72 %. It was found that at the cooling rates $w_{6/5} > 5$ °C/s the martensite structure is formed in metal. The hardened metal with such structure has increased values of strength ($\sigma_t \geq$ ≥ 1250 MPa) and low ductility ($\delta_5 = 5.0$ %, $\psi =$ $= 12.6$ %). To increase ductile properties of metal (1.7 times) is possible at delayed cooling ($w_{6/5} \leq 5$ °C/s). The resistance of metal to delayed fracture is considerably increased (σ_{cr} are increased from 60 to 450 MPa).

2. In electric arc welding of rail steel the HAZ metal is most dangerous from the point of view of cold cracks initiation. Without application of preheating up to the temperature of 250 °C it is impossible to prevent cold cracks formation in the joints. The increase in heat input of welding facilitates only delay of processes of cold cracks propagation in welded joints, but it does not prevent their initiation.

1. (1974) *Technology of fusion electric welding of metals and alloys*. Ed. by B.E. Paton. Moscow: Mashinostroenie.
2. Makarov, E.L. (1981) *Cold cracks in welding of alloy steels*. Moscow: Mashinostroenie.
3. Makara, A.M., Mosendz, N.A. (1971) *Welding of high-strength steels*. Kiev: Tekhnika.
4. Sergienko, Yu.V., Sagirov, I.V. (2000) Prediction of formation of hardening structures in welding of rail steels. In: *Proc. of Sci. Seminar on Current Achievements in Welding, Hardfacing and Related Technologies* (Mariupol, November 2000). Mariupol: PriazovGU, 9–12.
5. Grigorovich, K.V., Trushnikova, A.S., Arsenkin, A.M. et al. (2006) Study of structure and metallurgical quality of rail steels from various manufacturers. *Metally*, **5**, 1–16.
6. Genkin, I.Z. (2004) Welding and heat treatment of rail joints. *Svarochn. Proizvodstvo*, **9**, 31–36.
7. Sarzhevsky, V.A., Sazonov, V.Ya. (1981) Unit for simulation of thermal cycles on the base of machine MSR-75. *Avtomatich. Svarka*, **5**, 69–70.
8. Alekseeva, L.E., Sarrak, V.I., Suvorova, S.O. et al. (1975) About two ways of relaxation of residual microstresses in martensite of steel. *Metallofizika*, Issue 61, 79–84.
9. Sarrak, V.I., Filippov, G.A. (1976) Delayed fracture of steel after quenching. *Fiziko-Khimich. Mekhanika Materialov*, **12**, 44–54.

DEVELOPMENT OF THE TECHNOLOGY FOR REPAIR MICROPLASMA POWDER CLADDING OF FLANGE PLATFORM FACES OF AIRCRAFT ENGINE HIGH-PRESSURE TURBINE BLADES

K.A. YUSHCHENKO[1], **V.S. SAVCHENKO**[1], **A.V. YAROVITSYN**[1], **A.A. NAKONECHNY**[1], **G.F. NASTENKO**[1], **V.E. ZAMKOVOJ**[2], **O.S. BELOZERTSEV**[2] and **N.V. ANDREJCHENKO**[2]

[1]E.O. Paton Electric Welding Institute, NASU, Kiev, Ukraine

[2]Zaporozhie Machine-Building Design Bureau «Progress» named after Academician A.G. Ivchenko, Zaporozhie, Ukraine

Described is the technology developed by the E.O. Paton Electric Welding Institute for repair microplasma powder cladding of flange platform faces of high-pressure turbine blades made from alloy JS32-VI for engine D18T by using an additive powder with a composition similar to that of the base metal. It was shown that the one-layer deposited metal preserves the preferred inheritance of structure of the base metal. It was established that specimens simulating the repair cladding conditions, when tested to long-time strength at a temperature of 1000 °C, exhibited a strength level of about 50 % of that of the base metal along the fusion line.

Keywords: *microplasma powder cladding, high-pressure turbine blades, heat-resistant nickel alloy, flange platform faces, inheritance of structure, long-time strength*

Currently, the growing volumes of orders for air shipments of non-standard outsized freights have resulted in a shortage of fleet of transport ramp airplanes with the aircraft engines that are certified abroad. Now it is a pressing problem to extend life of the AN-124 aircraft «Ruslan» equipped with the last-generation engine D18T [1] from 24,000 to 40,000 flight hours, which will increase the service life of aircraft to 30–32 years [2]. This, in particular, will require extension of life of the high-pressure turbine (HPT) blades, which have been in operation for quite a long time.

In addition to service wear of faces and webs of the flange platforms, also thermal-fatigue cracks are detected in the blades of alloy JS32-VI that go to repair. Because of increase in service damages on the flow-through surfaces of the HPT blades of engine D18T (ZMBDB «Progress»), it was decided to improve the earlier applied technology for their repair by the argon-arc cladding method [3, 4].

The following technological tasks were posed for repair of the flow-through surfaces of the HPT blades of alloy JS32-VI:

- restoration of flange platform faces to a height of 2.5 mm and, at the presence of thermal-fatigue cracks, to a height of 4–5 mm after machining of damaged regions of the blades;
- thickening of the flange platform within the repair cladding zone to 1.5 mm that is specified by the blade drawing;
- limitation of the postweld heat treatment temperature to 1050 °C in order to preserve functional properties of thermal-barrier diffusion coating SDP-2 on the blade zones that are not subjected to repair.

The problem of repair of heavily damaged flange platform faces of the HPT blades of heat-resistant nickel alloy JS32-VI (chemical composition, wt.%: 0.15 C, 5 Cr, 9.3 Co, 2–10 W, 0.5–5.0 Mo, 4.5–8.0 Al, 1.5–5.0 Nb, 4 Re, 4 Ta, 0.01–0.03 B) with directed solidification and γ'-phase content of 62 % [5] was successfully solved by means of microplasma powder cladding using an additive powder with a composition similar to that of the base metal.

The powder of alloy JS32-VI was produced by the method of dry atomisation of ingots in argon atmosphere. The powder with particles 63–160 μm in size (according to GOST 6613–86), which constituted about 30–40 % of the initial mass of an atomised ingot, was used for repair microplasma cladding of the flange platform faces. Investigations in the following areas were carried out for repair microplasma powder cladding of heat-resistant dispersion-hardening alloy JS32-VI:

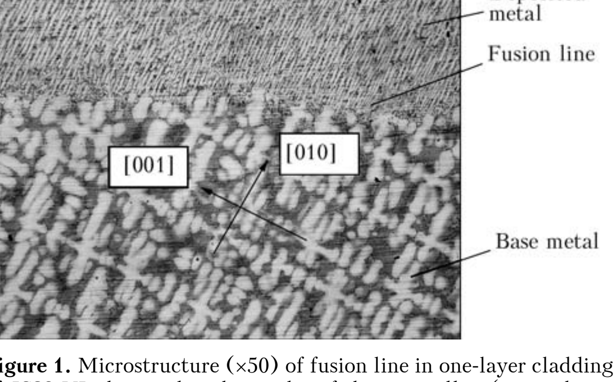

Figure 1. Microstructure (×50) of fusion line in one-layer cladding of JS32-VI plate end with powder of the same alloy (ion etching; arrows indicate directions of crystallographic orientation in base metal)

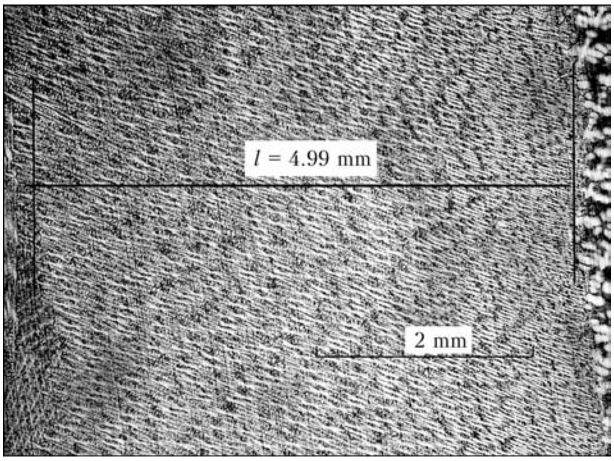

Figure 2. Microstructure (×25) of one-layer powder cladding of JS32-VI plate end (ion etching; l — height of a layer of oriented structure in deposited metal)

• examination of microstructure of welded joints on a narrow substrate to ensure their operational strength in cladding and subsequent heat treatment;

• providing of formation of the deposited metal on the flange platform faces;

• evaluation of the level of mechanical properties of the welded joints of alloy JS32-VI produced by repair microplasma powder cladding.

Peculiarity of microstructure of one-layer microplasma powder cladding of alloy JS32-VI is a highly dispersed dendritic structure, the oriented growth of which is caused by a directed removal of heat deep into the base metal (Figure 1). The layer with the oriented structure may be about 5 mm high (Figure 2). Preferred inheritance of the oriented structure disappears in subsurface layers in one-layer cladding (Figure 2), and also in the second cladding layer (Figure 3).

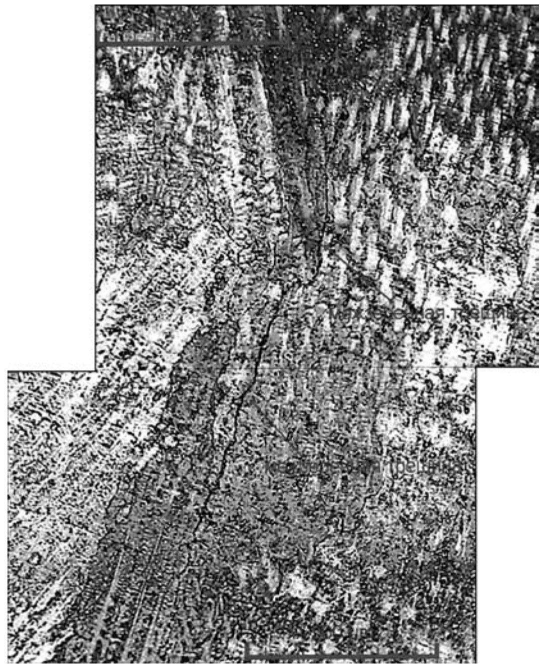

Figure 4. Microstructure (×113) containing intergranular crack in deposited metal of alloy JS32-VI in a region of fusion line between the first and second layers of deposited metal

As found out in optimisation of the cladding technology, transition from one- to two-layer cladding leads to a substantial increase in the probability of underbead cracking (Figure 4) during the postweld heat treatment process. Therefore, to provide an acceptable level of operational strength of the repair welds on the flange platform faces, it was decided to

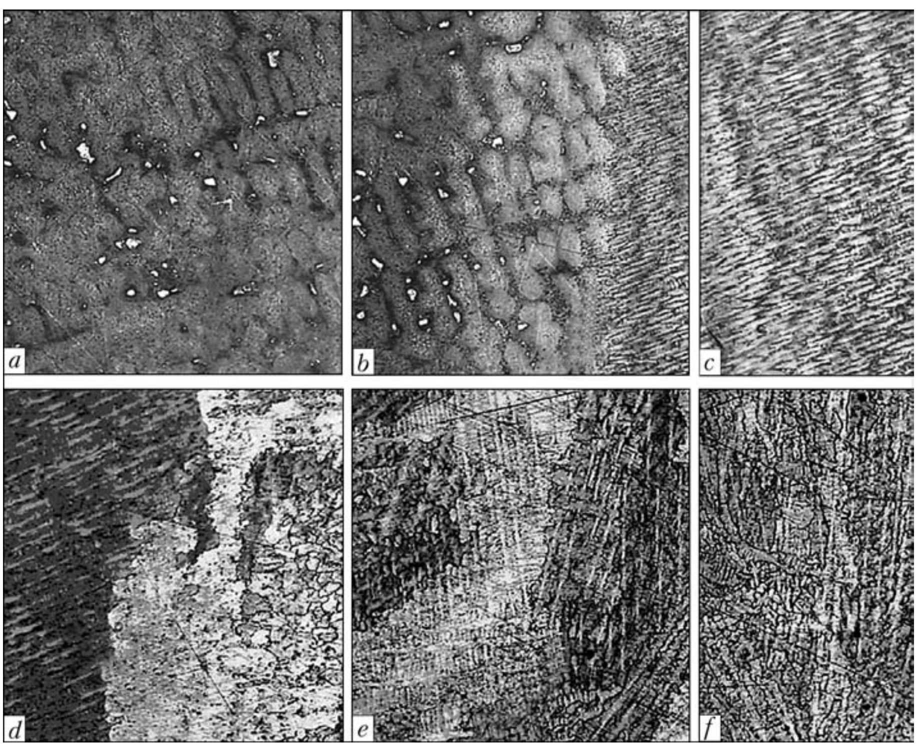

Figure 3. Microstructures (×75) of two-layer cladding of flange platform face of JS32-VI blade with powder JS32-VI (chemical etching in Marble's reagent): *a* — base metal; *b* — fusion region; *c*–*f* — deposited metal of the first and second layer, respectively

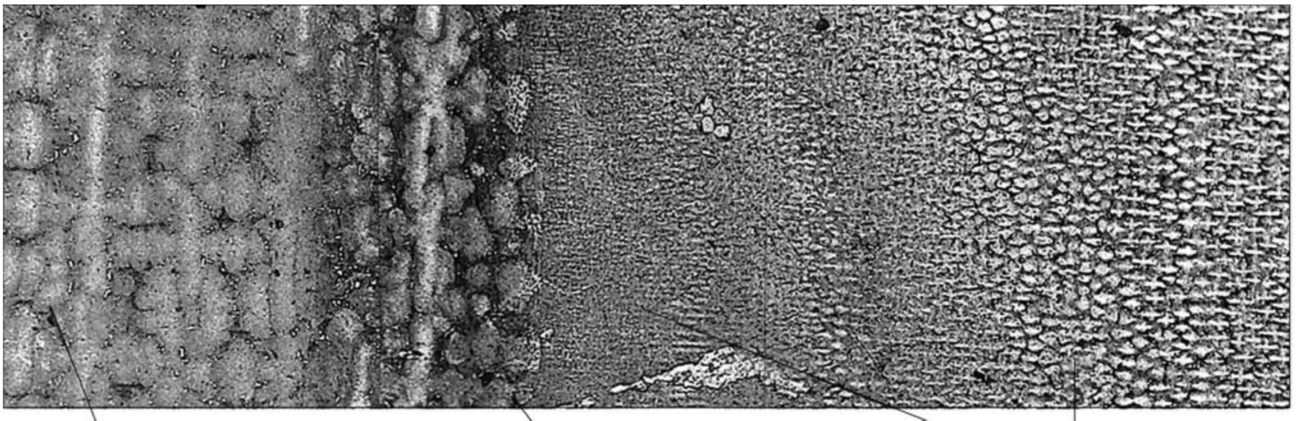

Figure 5. Microstructure (×75) of one-layer cladding on flange platform face (chemical etching in Marble's reagent)

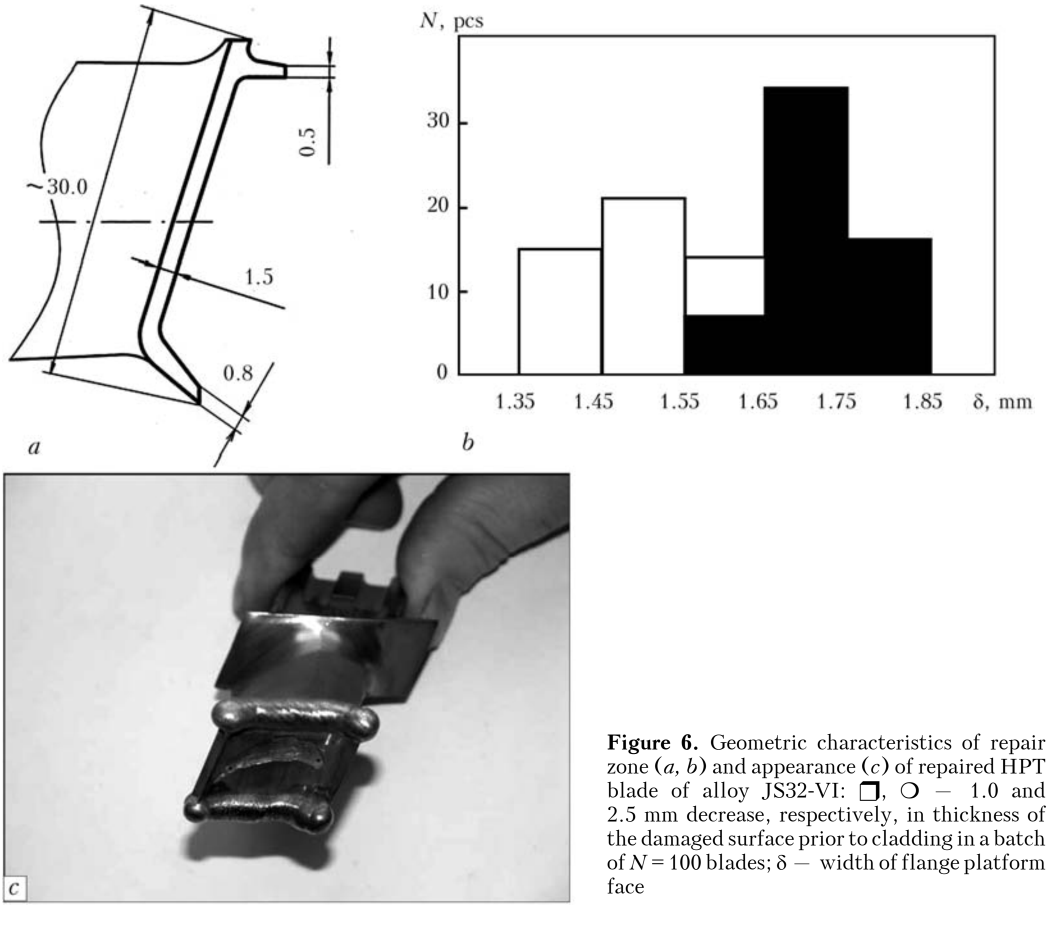

Figure 6. Geometric characteristics of repair zone (*a, b*) and appearance (*c*) of repaired HPT blade of alloy JS32-VI: ❒, ❍ — 1.0 and 2.5 mm decrease, respectively, in thickness of the damaged surface prior to cladding in a batch of $N = 100$ blades; δ — width of flange platform face

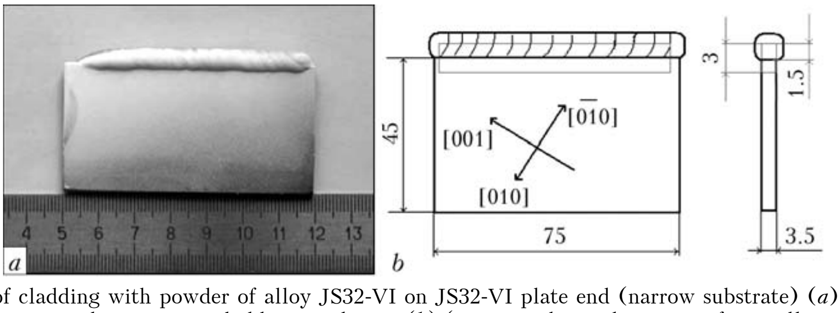

Figure 7. Appearance of cladding with powder of alloy JS32-VI on JS32-VI plate end (narrow substrate) (*a*), and scheme of cutting of mechanical test specimen simulating repair cladding conditions (*b*) (arrows indicate directions of crystallographic orientation in base metal)

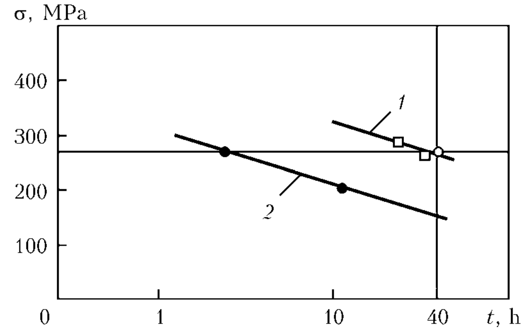

Figure 8. Long-time strength σ at T = 1000 °C of base metal (*1*) and specimen (*2*) simulating one-layer cladding on flange platform: ❒, ❍ — experimental and literature data, respectively

limit cladding to one layer of the deposited metal (Figure 5).

In terms of the cladding procedure, the flow-through surface of flange platforms of the HPT blades (Figure 6) is characterised by a complex shape, different thickness of the flange platform elements ranging from 0.50 to 1.85 mm, and presence of three adiabatic cladding start–end boundaries. To provide the required height of the deposited layer, keep the weld pool on a narrow substrate and improve formation of the deposited metal, microplasma powder cladding was performed in a copper fixture at a current of 8–20 A by using the Ar + 10 % H_2 mixture as a shielding gas.

Cladding with the JS32-VI powder on a narrow substrate, 3.5 mm wide (Figure 7, *a*) was carried out to evaluate long-time strength of the specimens simulating real conditions of repair microplasma cladding of the HPT blades. A plate of alloy JS32-VI, measuring 75 × 40 mm, was subjected to standard heat treatment. Prior to cladding it was additionally heat treated under conditions simulating preparation of blades for repair welding (holding for 2 h 30 min at $T = (1050 \pm 10)$ °C). After cladding the plate was heat treated under the same conditions. The absence of defects (cracks, lacks of fusion) at each stage was determined by the dye penetrant inspection method. The scheme of cutting of a specimen in the form of 50 % base metal and 50 % deposited metal of alloy JS32-VI is shown in Figure 7, *b*. Thickness of the gauge length of a metal specimen was about 3 mm. According to the data of study [6], it included the zone of $\gamma + \gamma' \rightarrow \gamma \rightarrow \gamma + \gamma'$ phase transformation affected by the cladding thermal cycle, which is one of the most dangerous points of fracture in mechanical tests of heat-resistant nickel alloys.

Long-time strength tests of the specimens simulating the repair cladding conditions at 1000 °C for 40 h were conducted by using the MP-3G testing machine. Section of the gauge length of a specimen was approximately 3.0 × 3.5 mm. Results of the tests are shown in Figure 8. It was established that for a specimen of 50 % base metal and 50 % deposited metal JS32-VI, which was tested along the fusion line at 1000 °C for 40 h, was 135 MPa and the level of strength of the specimen relative to that of the base metal was 50 %.

The E.O. Paton Electric Welding Institute performed repair of an experimental-industrial batch of the HPT blades of alloy JS32-VI, consisting of 512 blades (4 sets for engine D18T), by microplasma powder cladding. The blades repaired by microplasma powder cladding were transferred to ZMBDB «Progress» for machining and capillary inspection LYuM1-OV. According to statistical investigations conducted by ZMBDB «Progress» on the basis of the data of capillary inspection LYuM1-OV, the total amount of reject in repair of flange platform faces of the HPT blades by microplasma cladding with the JS32-VI powder was not in excess of 3–5 %.

The technology developed by the E.O. Paton Electric Welding Institute for repair microplasma powder cladding of JS32-VI blades for engine D18T and 2 sets of specialised equipment were commercially applied at ZMBDB «Progress» (Zaporozhie).

1. Pejchev, G.I., Zamkovoj, V.E., Akhrameev, N.V. (2000) ZMBDB «Progress»: new materials and advanced technologies in aircraft engine construction. *Tekhnol. Sistemy*, **2**, 5–15.
2. News of 14 November 2006. *www.avia.ru*.
3. Peremilovsky, I.A., Petrik, I.A. (2002) Strengthening of flange platforms of turbine blades with heat-resistant alloys. *Gazoturbin. Tekhnologii*, **3**, 90–92.
4. Pejchev, G.I., Shurin, A.K., Zamkovoj, V.E. et al. (2000) Development and application of high-temperature wear-resistant alloy for strengthening of flange platforms of gas-turbine engine blades. *Tekhnol. Sistemy*, **3**, 40–42.
5. Melekhov, R.K., Pokhmursky, V.I. (2003) *Structural materials for power generation equipment. Properties, degradation*. Kyiv: Naukova Dumka.
6. Yushchenko, K.A., Savchenko, V.S., Chervyakov, N.O. et al. (2004) Character of formation of hot cracks in welding cast heat-resistant nickel alloys. *The Paton Welding J.*, **8**, 34–38.

FLASH-BUTT WELDING OF REINFORCEMENT BARS OF A400S–A600S CLASSES IN CONSTRUCTION OF STRUCTURES OF MONOLITHIC REINFORCED CONCRETE

P.N. CHVERTKO
E.O. Paton Electric Welding Institute, NASU, Kiev, Ukraine

The application of flash-butt welding of reinforcement bars in civil engineering under site and semi-stationary conditions in construction of monolithic reinforced concrete structures is considered. This method is characterized by a high stability of characteristics of quality of concrete reinforcement being welded and absence of auxiliary consumables. The main technological parameters of the process were determined, basic technologies were developed, providing the increase in service life of reinforced concrete structures, improvement of their reliability and guarantee of high service life.

Keywords: *flash-butt welding, reinforcement bars, welded joints, site conditions, monolithic reinforced concrete*

In construction and repair of reinforced concrete constructions and structures the different methods of arc welding of concrete reinforcement are used. The manual and semi-automatic electric arc welding, bath-arc welding and others have found the widest spreading. It should be noted that at plants and industrial groups of as-assembled reinforced concrete a flash-butt welding with a continuous flashing is widely used, except the above-mentioned methods. Now, it is one of main methods of producing the butt joints of concrete reinforcement under the shop conditions.

The flash-butt welding is characterized by a high stable quality of welded joints, almost equal in strength to the parent metal that makes it possible to increase greatly the reliability and service life of reinforced concrete structures and to provide the high productivity. The process of welding is performed in the automatic conditions, combines the assembly and welding operations in a single cycle, does not require application of auxiliary consumables (electrodes, welding wire, fluxes, gases, etc.). Moreover, special requirements to the welder's qualification are not specified. At the present time, this method is not used in site, first of all, due to the absence of special technologies and equipment.

The existing experience in the development of technologies and specialized equipment of the flash-butt welding in the field conditions of railway rails and pipes allows applying this method for joining the reinforcement bars of concrete under site and semi-stationary conditions. For this purpose, it is necessary to define the technological features of the process and requirements to the specialized equipment, which depend mainly on the conditions of its service. The equipment should be mobile, compact, have available a minimum possible electric power and maximum protection from the environment effect.

As a rule, the concrete reinforcement bars of up to 22 mm are joined by the flash-butt welding with a continuous flashing, and the large-diameter bars are joined by using a flashing with a preliminary resistance preheating. The latter is characterized by a wide instable HAZ. The flash-butt welding with a pulsed flashing allows joining all the assortment of reinforced bars and has advantages over the above-mentioned methods.

In construction of monolithic reinforced concrete structures the reinforcement of A400S–A600S classes of steels St3Gps (semi-killed), 25G2S and 35GS in hot-rolled or heat-hardened state are most widely used in accordance with recommendations [1]. Technological investigations and development of a basic technology were made using this concrete reinforcement. Mechanical characteristics of these steels in hot-rolled state are given in Table 1, and chemical composition is given in Table 2.

The carried out technological investigations of welding the hot-rolled reinforcement bars made it possible to establish the values of main parameters of welding conditions: adjusting length L_{adj}, tolerances for flashing L_{flash} and upsetting L_{upset}, open-circuit secondary voltage $U_{2o.-c}$, rates of flashing v_{flash} and upsetting v_{upset}, time of welding t_w and time of upsetting under current $t_{upset I}$ (Table 3). The values of tolerances, necessary for attaining the required heating of the zone of plastic deformation of metal in upsetting with account for beveling the parts being

Table 1. Mechanical characteristics of bar reinforcing steels

Steel grade	$\sigma_{0.2}$, MPa	σ_t, MPa	δ, %
35GS	370–500	610–670	18–30
25G2S	380–400	590–620	23–31
St3Gps	235	370–490	25

Table 2. Chemical composition of bar reinforcing steels, wt.%

Steel grade	C	Mn	Si	Cr	Ni	S	P	Cu
25G2S	0.20–0.29	1.20–1.60	0.60–0.90	<0.30	<0.30	<0.045	<0.040	<0.30
35GS	0.30–0.37	0.80–1.20	0.60–0.90	<0.30	<0.30	<0.045	<0.040	<0.30
St3Gps	0.14–0.22	0.80–1.10	<0.15	<0.30	<0.30	<0.050	<0.040	<0.30

Table 3. Parameters of conditions of welding the hot-rolled concrete reinforcement of A240S–A500S classes

D, mm	$U_{2o.-c}$, V	L_{flash}, mm	L_{upset}, mm	t_w, s
12–18	5.5–6.0	10–12	3	8–10
20–28	5.5–6.0	11–15	4–5	15–20
32–40	6.0–6.5	13–17	5–6	Up to 30

Table 4. Results of mechanical tests of welded joints of hot-rolled concrete reinforcement of A400S class of stell 35GS

D, mm	σ_y, MPa	σ_t, MPa
16	432.7–472.4 457.9	721.2–731.1 726.1
18	361.4–402.6 387.9	628.8–660.2 647.6
20	394.7–451.2 418.0	652.5–719.4 699.4
22	356.6–394.4 372.2	639.3–684.0 657.7
25	399.2–482.8 432.9	652.5–754.4 678.7
28	455.1–513.0 490.0	674.8–754.4 724.8
32	456.2–565.8 505.9	684.4–719.4 697.1
36	469.4–517.3 498.1	646.2–757.6 708.8

welded, were determined experimentally. It was found that the rate of flashing at the beginning of the process is 0.4–0.5 mm/s, and it is increased up to 2.0–2.5 mm/s directly before upsetting. The open-circuit secondary voltage, which provides a stable proceeding of heating process in flashing, should be minimum [2].

Mechanical testing of full-scale specimens of joints of a hot-rolled reinforcement bars of steel 35GS, welded by a continuous flashing at optimum conditions, were performed in accordance with requirements [3]. Their results are given in Table 4. Fracture of all specimens occurred in the parent metal at a large distance from the welded joint and HAZ (Figure 1).

Similar results were obtained also on steels St3Gps and 25G2S in a hot-rolled state. Macrosection of the joint and distribution of microhardness are shown in Figure 2, microstructure of zone of joint and parent metal is given in Figure 3.

Preliminary thermal hardening of reinforcing steel increases greatly the requirements to the selection of its heating condition in welding, guaranteeing the formation of welded joint equal in strength to the parent metal.

In welding of heat-hardened reinforcement bars using a continuous flashing at soft conditions or flashing with a preliminary resistance preheating the reduction of tensile strength to the level of tensile strength of steel, which was not subjected to preliminary heat treatment, is observed in HAZ metal. As main varied parameters of the welding condition, the values L_{adj}, L_{flash} and $t_{upset\,I}$ were selected.

It was determined during investigations and development of the technology of welding of heat-hardened reinforcement bars of steel 25G2S that the optimum value of an adjustable length is within the same limits as in welding of a hot-rolled reinforcement bars $(1.7–2.0)D$. The value of tolerance for flashing is also little differed and it can be taken equal to appropriate tolerance, defined for the hot-rolled reinforcement bars.

The increased sensitivity to heating of heat-hardened reinforcement bars specifies the additional requirements to thermal cycles of heating in welding. As the main condition parameters of welding the hot-rolled and heat-hardened concrete reinforcement have almost similar values, the time of upsetting under current, i.e. the value of weakening, which depends

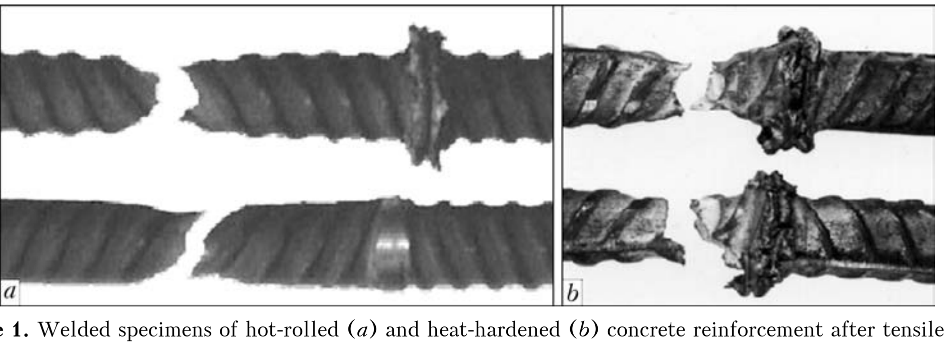

Figure 1. Welded specimens of hot-rolled (*a*) and heat-hardened (*b*) concrete reinforcement after tensile tests

Table 5. Welding condition parameters and results of mechanical tests of concrete reinforcement of A600S class of steel 25G2S

L_{adj}, mm	L_{flash}, mm	$t_{upset I}$, s	σ_t, MPa	$\sigma_{w.j}/\sigma_{p.m}$, %	Place of fracture
25	11	0.10	$\frac{830–850}{847}$	$\frac{96.1–98.2}{97.3}$	HAZ
11	4	0.10	$\frac{800–825}{816}$	$\frac{93.7–96.6}{95.5}$	In butt
7	4	0.10	$\frac{870–875}{873}$	$\frac{93.7–102.0}{97.9}$	Same
12	8	0.04	$\frac{825–845}{831}$	$\frac{95.5–97.0}{96.3}$	In butt 2 specimens
15	10	0.04	$\frac{835–845}{836}$	$\frac{96.1–97.0}{96.4}$	Same
17	12	0.04	$\frac{820–850}{838}$	$\frac{95.0–98.2}{96.7}$	In parent metal 2 specimens

greatly on additional heating in upsetting, has the highest effect on mechanical characteristics of the joint.

During investigations the time of upsetting under current varied from 0.10 up to 0.04 s. The obtained results are given in Table 5.

During the mechanical tests the first five welded specimens had a ductile fracture in HAZ with a weakening of not more than 2–4 % (see Figure 1, *b*).

In welding at conditions with smaller tolerances for flashing the brittle fracture is occurred, caused by an intensive heat dissipation into welding machine electrodes being cooled. The increase in zone of heating during flashing with a simultaneous reduction of time of upsetting under current allowed producing welded joints, being almost equal in strength to the parent metal. The weakening did not exceed 2 %. Moreover, the fracture of most specimens (about 90 %) occurred in parent metal beyond HAZ. Macrosection of such joint and distribution of hardness in it are given in Figure 4.

To prevent the occurrence of different defects of welding, it is necessary to keep strictly the recommended conditions, especially in work with heat-hardened concrete reinforcement. It was shown above that at insufficient heating of parts being welded the ductile characteristics of the concrete reinforcement are reduced greatly. During mechanical tests the brittle fracture is occurred directly in butt or HAZ. The joint overheating leads to decrease in strength characteristics of HAZ. At further increase of heating cycle up to 30–40 s the typical fracture is occurred with the presence of hot cracks in the joint plane (Figure 5, *a*), tensile strength here is not exceeding 100–140 MPa.

Besides, the fracture of specimens in burnt spots was observed in some cases (Figure 5, *b*). As a rule, the formation of these defects occurs at insufficient force of clamping of parts being welded or heavy contamination of current-carrying jaws. In place when the part is not tightly adjacent to the electrode the

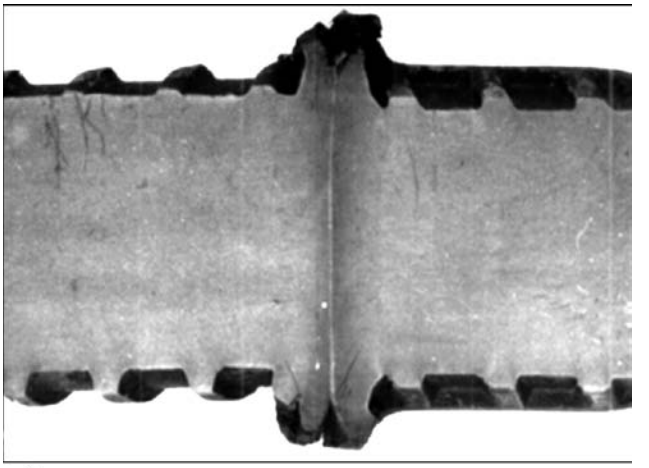

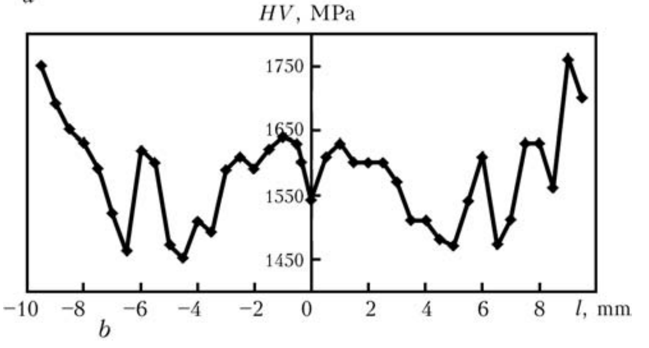

Figure 2. Macrosection (*a*) and distribution of microhardness (*b*) in the zone of welded joint of reinforcement bar of steel St3Gps

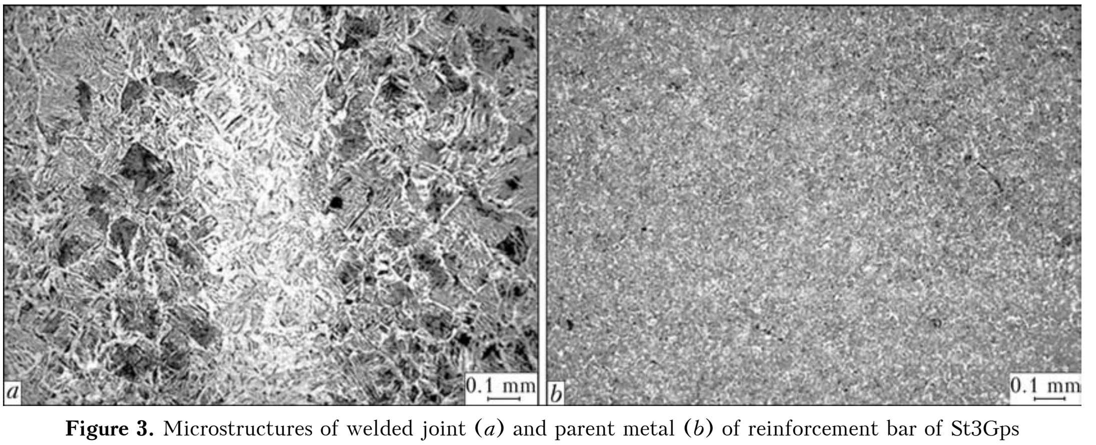

Figure 3. Microstructures of welded joint (*a*) and parent metal (*b*) of reinforcement bar of St3Gps

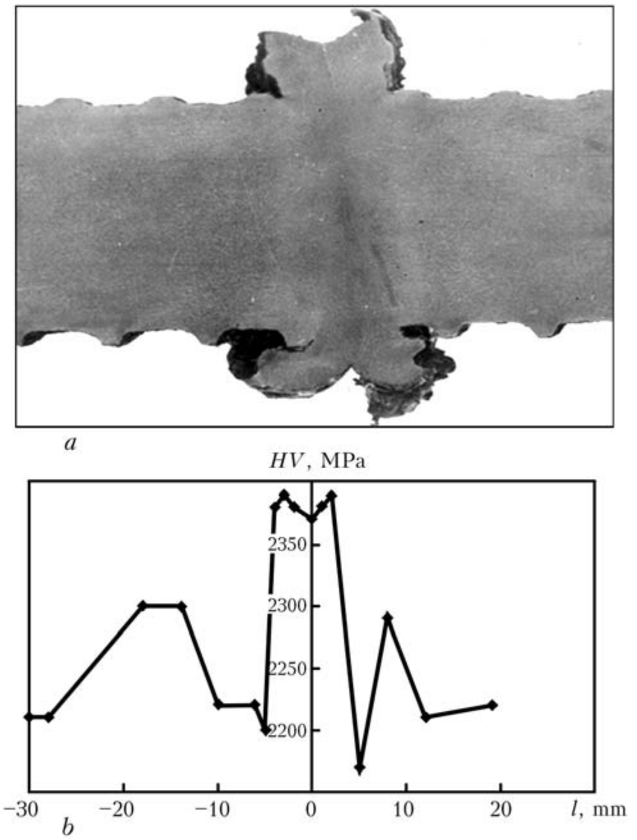

Figure 4. Macrosection (*a*) and distribution of hardness (*b*) in the zone of welded joint of reinforcement bar of steel 25G2S

transient electric resistance is increased to the value exceeding the resistance of spark gap and the process of a local flashing along the part–electrode contact surface begins. As was noted above, the burnt spots, forming in the form of craters, decrease greatly the mechanical properties of welded joints. The formation of burnt spots is also caused by an increased electrical resistance between the profiled lateral surface of the concrete reinforcement and electrode. Therefore, the force of clamping is selected at least 2 times higher than the upsetting force.

The decrease in probability of formation and amount of burnt spots is attained by a proper selection of specific clamping force, regular cleaning of current-carrying electrodes every 5–10 welding operations and maximum possible reduction of the secondary voltage $U_{2o.-c}$.

Application of technologies of joining of hot-rolled and heat-hardened concrete reinforcement will make it possible to produce butt joints equal in strength to the parent metal under the site and semi-stationary conditions, to increase the service life of reinforced concrete structures, to increase their reliability and to guarantee the high service life.

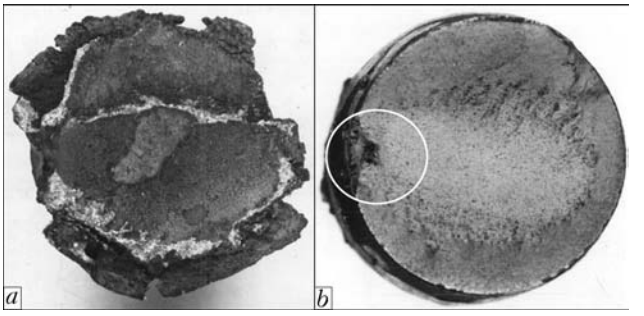

Figure 5. Fracture of reinforcement bar after tensile tests: *a* — overheating in welding; *b* — presence of a burnt spot

CONCLUSIONS

1. Application of flash-butt welding is challenging for butt welding of concrete reinforcement of high-strength steels. It is performed in automatic condition and does not require the application of auxiliary consumables. Moreover, the qualification of welders does not influence the quality of welded joints. The efficiency of the process is rather high, the time of welding of one joint does not exceed 1 min.

2. In the presence of a large amount of welded joints (for example, from hundreds of thousands up to millions of welded joints are performed on one bridge passage) the application of the flash-butt joints under site and semi-stationary conditions provide the high economic efficiency, increases the productivity of construction and reduces greatly the amount of rejected joints.

3. Distribution of temperature in a near-contact zone in welding with a continuous flashing at rigid conditions and especially using a pulsed flashing creates the most favorable conditions for plastic deformation during upsetting.

4. The application of method of flash-butt welding with a pulsed flashing provides a stable quality of welded joints of high-strength and heat-hardened reinforcing steels. In this case, the value of weakening does not exceed 2–4 %.

5. Increase in current density at pulsed flashing as compared with that of continuous flashing causes the hazard of formation of burnt spots that influences negatively the quality of welded joints.

1. *DSTU 3760:2006*: Reinforced bar for concrete structures. General requirements. General specification. Kyiv: Derzhspozhyvstandart.
2. Kuchuk-Yatsenko, S.I. (1992) *Flash-butt welding*. Kiev: Naukova Dumka.
3. *GOST 10922–90*: Reinforced and embedded welded pieces of concrete structures. General specification. Moscow: Standart.

IMPROVEMENT OF SERVICE LIFE OF RESISTANCE WELDING MACHINE ELECTRODES IN WELDING GALVANIZED STEEL

V.A. ANOSHIN[1], **V.M. ILYUSHENKO**[1], **R.V. MINAKOVA**[2] and **N.I. GRECHANYUK**[2]
[1]E.O. Paton Electric Welding Institute, NASU, Kiev, Ukraine
[2]N.I. Frantsevich Institute of Problems of Materials Science, NASU, Kiev, Ukraine

Existing methods for manufacture of high-temperature copper alloys were analyzed, and service durability of different electrode materials in spot welding of galvanized steel was evaluated. The effect of composition of electrode materials on their hardness at increased temperatures was studied.

Keywords: *resistance spot welding, resistance welding machines, electrode material, galvanized steel, service durability of electrodes, bimetal electrodes, alloy structure and hardness*

Steels with anticorrosion coating, in particular galvanized steels, are ever wider accepted in modern mechanical engineering, particularly in automotive industry and carriage engineering, as well as other industries. Resistance spot welding is the main technological process for joining these materials. Operating life of resistance welding machine electrodes in welding galvanized steels is 10–20 times lower (depending on electrode material, welding speed, etc.) compared to welding of uncoated steels. Therefore, development of new high-temperature materials on copper base with increased softening temperature and minimum adhesion of electrode material to molten zinc is an urgent task.

At present manufacturing of high-temperature copper alloys is mainly concentrated in metallurgical production, powder metallurgy, in productions with electron beam evaporation. Welding fabrication processes, namely arc surfacing, can also be used.

In metallurgical production mainly alloys of the type of chromium and chromium-zirconium bronze are manufactured, which have been the most widely accepted in different countries as material for resistance welding machine electrodes [1, 2]. Recently dispersion-strengthened composite materials (DSCM) based on copper (with additives of refractory compounds) produced by powder metallurgy method, have been ever wider accepted instead of dispersion-hardening chromium and chromium-zirconium bronzes produced by casting. Featuring a range of unique properties (high hardness, strength, electrical conductivity), which are preserved also at high temperature, they essentially increase the service durability of welding tools [3]. The most efficient method of adding oxides to the metal matrix is internal oxidation [4]. This method was realized by OMG Americas (USA) at development of Cu + Al_2O_3 DSCM under GlidCop trade name [5]. However, application of electrodes from GlidCop Al-60 material in the world practice is restrained by a quite high cost of this material, which is due to a complex technology of its manufacturing.

Recently TsNIIMT DISKOM Ltd. (Cheboksary, Russia) developed a nanocomposite material S16.102 DISKOM, which has a heterogeneous dispersion-strengthened structure and is characterized by high recrystallization temperature, high-temperature strength, electrical conductivity and service durability due to application of reaction mechanical alloying in high-energy and high-speed attritors, processes of granule metallurgy and hot pressing (extrusion) [6].

Also interesting are locally produced condensed dispersion-strengthened materials (CDSM) based on copper and molybdenum, which also have high hardness and electrical conductivity [7]. Their main advantage is high thermal stability — recrystallization temperature reaches 1000 °C [8]. They are made both with bulk distribution of molybdenum (CDSM), and with microlaminate distribution when copper and molybdenum layers alternate (CMLM).

In recent years PWI developed technologies of manufacture of bimetal electrodes for resistance spot welding by the method of nonconsumable electrode inert-gas arc surfacing using flux-cored filler wire [9].

Materials the physical properties of which are given in the Table, were selected to assess service durability of the current electrode materials made by different processes, at resistance spot welding of galvanized steel. «Cap» type electrodes were made from the above materials. Electrode with the working part from CDSM and CMLM was made by welding plates from these materials to a copper billet by percussion welding in vacuum. Procedure of accelerated testing of service durability of electrode materials in resistance spot welding of galvanized steel allowing saving of steel being welded was developed.

It consists in the following. Spot welding of low-carbon steel with anticorrosion coating applied by hot galvanizing is performed. Thickness of zinc coating in this case is 2–3 times greater than that of the coating deposited by electrochemical method. As is known

Physical properties of copper-based high-temperature materials manufactured by different processes [1–9]

Material	Hardness *HRB*	Electrical conductivity of copper, m/(Ohm·mm^2)	Recrystallization temperature, °C
Chromium bronze BrKh	55–65	80–85	475
Chromium-zirconium bronze of Cu–Cr–Zr type	70–83	75–85	550
CDSM based on copper with 2.5–12.0 wt.% Mo	50–87	82–64	> 850
Dispersion-strengthened copper produced by the method of internal oxidation GlidCop Al-60 (USA)	78	78	860
Copper-based DSCM produced by mechanical alloying	97–112	45–48	> 700
DISKOM produced by reactive mechanical alloying	89	80	850
Metal deposited with special filler wire #30 (PWI)	66–69	70–75	–

from [10], the greater the zinc coating thickness, the lower is the electrode resistance. In addition, the copper «end piece» on which the «cap» is put on, is made without a cooling channel, which also lowers its resistance in spot welding of galvanized steel. Testing was conducted in resistance spot welding machine of MT-22 model. Before welding and after the end of testing, the diameter of the electrode surface working part imprint was measured by the imprint on white paper using carbon paper (durability characteristics is the number of spots welded before increase of working surface initial diameter by 20 %). After welding every 20 spots, cast nugget diameter was measured by welding a reference spot weld on samples from the same galvanized steel 40 mm wide and tearing one plate from the other one in one direction by the method of twisting in a parallel plane. After completion of testing, graphs of the change of the cast nugget depending on the number of welded spots were plotted

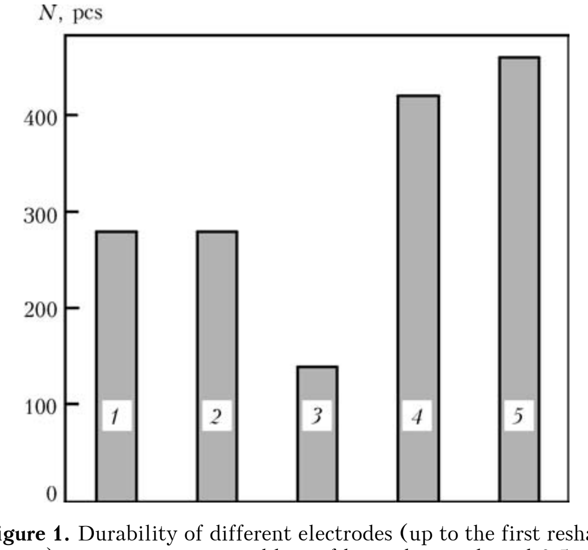

Figure 1. Durability of different electrodes (up to the first resharpening) in resistance spot welding of hot galvanized steel 0.5 mm thick (without cooling channel in the electrode); *1*, *2* — chromium-zirconium bronze manufactured in Germany and South Korea, respectively; *3* — BrKhTsr («Krasny Vyborzhets», RF); *4* — nanocomposite material S16.102 DISKOM; *5* — bimetal electrode #30 (PWI); *N* — number of spot welds

for each electrode material. In our opinion, measurement of the cast nugget diameter is a more objective criterion than measurement of the diameter of electrode working surface.

Figure 1 shows the results of comparative testing of different electrode materials for spot welding of hot galvanized steel 0.5 mm thick (coating thickness of 20–30 μm) in the following mode: I_w = 4.5–5.0 kA; t_w = 5–6 cycles; compressive force of 200 MPa; welding speed of 35 spots/min. Lowering of welding parameters compared to the standard ones is related to absence of cooling channel in the «end piece». As is seen from Figure 1, durability of electrodes from chromium-zirconium bronze (Cu–Cr–Zr) produced in South Korea and Germany is the same and is higher than that of electrodes from BrKhTsr produced by «Krasny Vyborzhets» plant (Russia). In our opinion, this is related to its higher content of zirconium (about 1 wt.%) compared to BrKhTsr (0.06 wt.% Zr). Bimetal (surfaced) electrodes demonstrated the highest durability. Durability of electrodes from nanocomposite material S16.102 DISKOM is only slightly inferior to that of surfaced electrodes.

Preliminary testing of electrodes from DSCM (mechanical alloying) showed that a considerable transfer of electrode metal to galvanized steel is observed in welding, which, apparently, is what accounts for their low resistance (100 spots).

Evaluation of service durability of bimetal electrodes the working part of which is made of CDSM — CDSM and CMLM — was performed earlier. Figure 2 shows the results of testing obtained at resistance spot welding of hot galvanized steel 0.8 mm thick using uncooled electrode. It is determined that resistance of an electrode with working part from CDSM is higher than that of electrode from CMLM.

Results of the conducted testing showed (Figure 3) that electrode material structure can considerably influence its service durability. A.A. Bochvar expressed his opinion on the advantage of the cast structure compared to deformed metal [11].

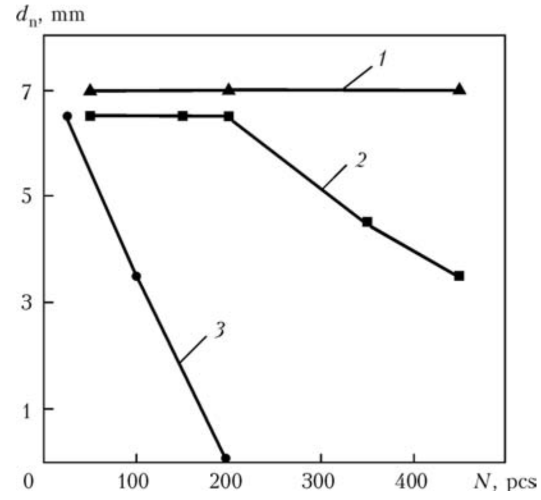

Figure 2. Dependence of spot weld nugget diameter d_n on number of welded spots N in resistance spot welding of hot galvanized steel 0.8 mm thick: *1, 2* — bimetal electrode with working part from CDSM and CMLM, respectively; *3* — electrode from chromium bronze BrKh

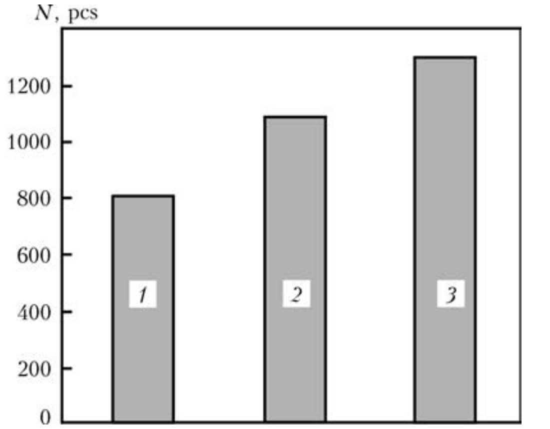

Figure 4. Durability of different electrodes (up to first resharpening) in resistance spot welding of cold galvanized steel 0.8 mm thick (with cooling channel in the electrode): *1* — Cu–Cr–Zr (Germany); *2, 3* — bimetal electrode #30 and 057, respectively (PWI)

It should be noted that testing of bimetal electrodes under the conditions of cooled electrode at resistance spot welding of cold galvanized steel 0.8 mm thick (coating thickness of 30–60 μm) showed their higher service durability (cast nugget diameter is determined after welding every 100 spots) (Figure 4). Welding was performed in the following mode: I_w = 8.8–9.5 kA; t_w = 8–9 cycles; compressive force of 280–300 MPa; welding speed of 35 spots/min.

Considering the higher service durability of bimetal electrodes, experiments were conducted on selection of an optimum alloying system and composition of deposited metal, satisfying the following requirements: high hardness at increased temperature; required electrical conductivity of bimetal electrode; cellular substructure of deposited metal; good welding-technological properties of surfacing wire.

Test flux-cored wires with different alloying system were made, which were selected on the basis of theoretical analysis of physical properties of elements. They were used for surfacing copper billets with their subsequent heat treatment. After that samples were made for metallographic investigations and hardness measurement at elevated temperature in Lozinskii microhardness meter.

Figure 5 gives the results of hardness measurements of surfaced electrodes with various microalloying ad-

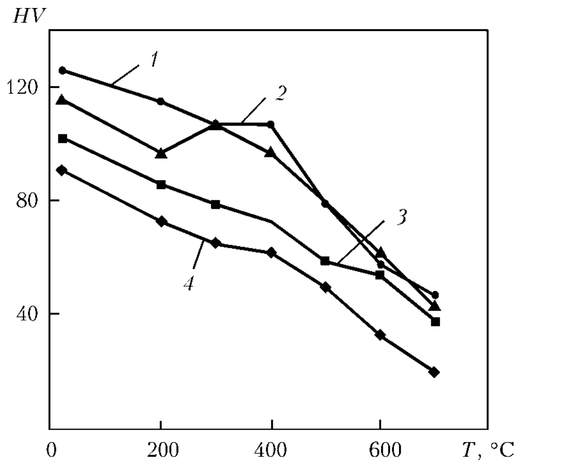

Figure 5. Dependence of hardness of test surfaced electrodes on testing temperature: *1* — #66; *2* — #72; *3* — #30; *4* — #03

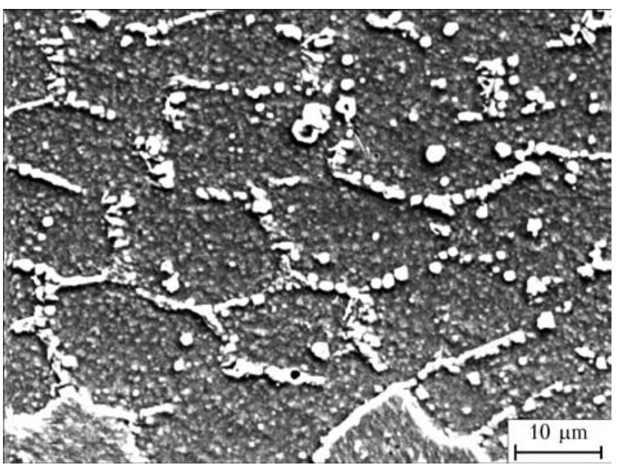

Figure 3. Microstructure of an electrode with cellular substructure of grains, the boundaries of which are decorated by strengthening phase (scanning electron microscope)

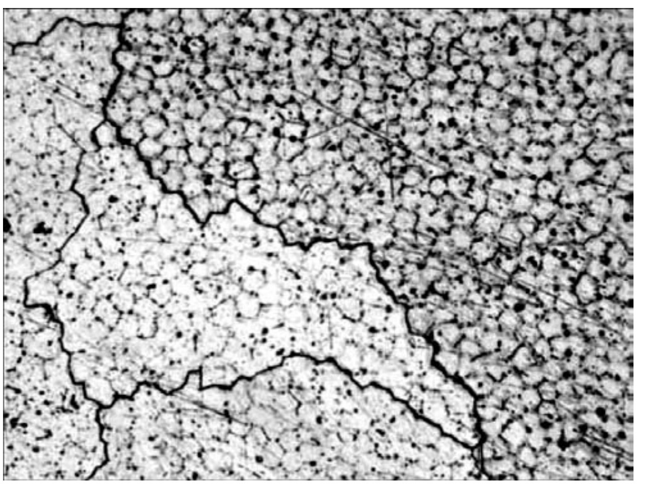

Figure 6. Microstructure (×200) of an electrode surfaced with wire #66

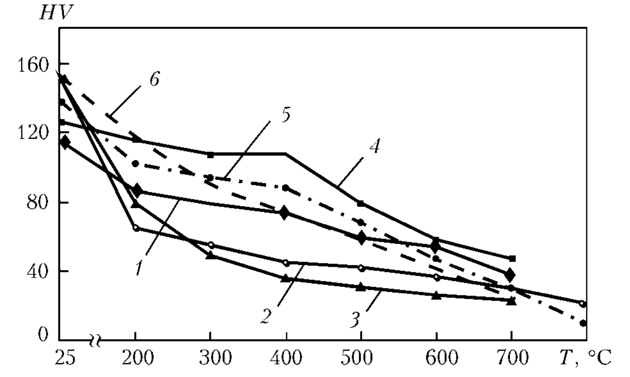

Figure 7. Dependence of hardness of electrodes from different materials on test temperature: *1* — bimetal (surfaced) #30 (PWI); *2* — GlideCop Al-60 (USA); *3* — nanocomposite material S16.102 DISKOM; *4* — bimetal (surfaced) #66 (PWI); *5* — Cu–Cr–Zr (Germany); *6* — BrKhTsr («Krasny Vyborzhets», RF)

ditives, and Figure 6 shows the cellular substructure of the electrode surfaced with wire #66.

As is seen from Figure 7, bimetal (surfaced) electrodes have higher hardness at elevated temperatures. A correlation is found between electrode hardness at elevated temperature and their service durability (see Figures 1 and 7).

To ensure efficiency and stability of the quality of bimetal electrodes it is rational to apply automatic surfacing with solid wire. Improvement of nanocomposite material composition to increase its hardness at elevated temperature is also promising. Such work is currently conducted in cooperation with TsNIIMT DISKOM.

Thus, it is established that electrodes made by arc surfacing and those from nanocomposite material have the highest service durability.

1. Nikolaev, A.K., Rozenberg, V.M. (1978) *Alloys for resistance welding electrodes*. Moscow: Metallurgiya.
2. Nikolaev, A.K., Novikov, A.N., Rozenberg, V.M. (1983) *Chromium bronzes*. Moscow: Metallurgiya.
3. Lipatov, Ya.M. (1975) Components of welding equipment of new dispersion-hardened composites. *Montazhn. i Spets. Raboty v Stroitelstve*, **4**, 11.
4. Daneliya, E.P., Rozenberg, V.M. (1979) *Internally oxidized alloys*. Moscow: Metallurgiya.
5. Shalunov, E.P., Ravitsky, G., Berent, V.Ya. (2003) Long-life electrodes for resistance welding made of copper dispersion-hardened composites: development, production, application. In: *Proc. of Int. Conf. on Electric Contacts and Electrodes* (Katsiveli, Crimea, 15–21 Sept. 2003). Kiev: IPM, 89–92.
6. Shalunov, E.P., Davydenkov, V.A. (2004) Long-life electrodes for resistance welding of copper composites. In: *Transact. of I.N. Frantsevich IPMS on Electric Contacts and Electrodes*. Kiev: IPM, 190–201.
7. *TU U 20113410.001–98*: Dispersion-hardened materials for electric contact. Specifications. Introd. 02.06.98.
8. Movchan, B.A., Osokin, V.A., Grechanyuk, N.I. et al. (1991) Structure, mechanical properties and thermal stability of condensed dispersion-hardened materials Cu–Y–Mo. Report 1. *Problemy Spets. Elektrometallurgii*, **4**, 27–32.
9. Anoshin, V.A., Ilyushenko, V.M., Podola, N.V. et al. (2003) Bimetal electrodes for resistance spot welding of steels with anticorrosive coating. In: *Abstr. of Int. Conf.* on *Current Problems of Welding and Service Life of Coatings* (Kiev, 24–27 Nov. 2003). Kiev: PWI, 6–7.
10. Yavorsky, Yu.D., Zelmanovich, V.Ya. (1966) Spot and seam resistance welding of low-carbon steels with protective coatings. *Avtomatich. Svarka*, **6**, 59–63.
11. Bochvar, A.A. (1956) *Physical metallurgy*. Moscow: Metallurgizdat.

INFLUENCE OF GETTER ADDITIVES ON HYDROGEN EMBRITTLEMENT OF WELDED JOINTS OF STRUCTURAL MATERIALS OF NPP EQUIPMENT

V.M. AZHAZHA, **S.D. LAVRINENKO, G.D. TOLSTOLUTSKAYA, N.N. PILIPENKO, Yu.P. BOBROV, A.P. SVINARENKO** and **A.N. AKSENOVA**

National Science Center «Kharkov Institute of Physics and Technology», NASU, Kharkov, Ukraine

The paper gives analysis of literature data on searching for getter materials, which can be recommended for creation of hydrogen traps by introducing them into structural materials and welded joints of NPP equipment. Hydride-forming alloys and compounds based on zirconium, titanium and vanadium are considered as the most promising ones. Rare-earth metals and their alloys, binary compounds of rare-earth metals with transition metals of VIII group are proposed as materials of getter additives to create hydrogen traps in structural materials and welded joints of NPP equipment.

Keywords: *structural materials, service life, physical simulation, weld metal, hydrogen, getter additives, nuclear-physics research*

Hydrogen is known to be one of the most harmful and hazardous impurities in metals and alloys. Practical experience and almost all experimental investigations of hydrogen influence on the processes of embrittlement, strengthening, long-term strength and thermal stability, static and cyclic fatigue, fatigue strength, fatigue resistance, creep in metals and alloys reveal its negative role in these processes. A sufficiently high content of hydrogen in structural materials under certain operation conditions can lead to significant embrittlement of these materials, and, as a result, mark-

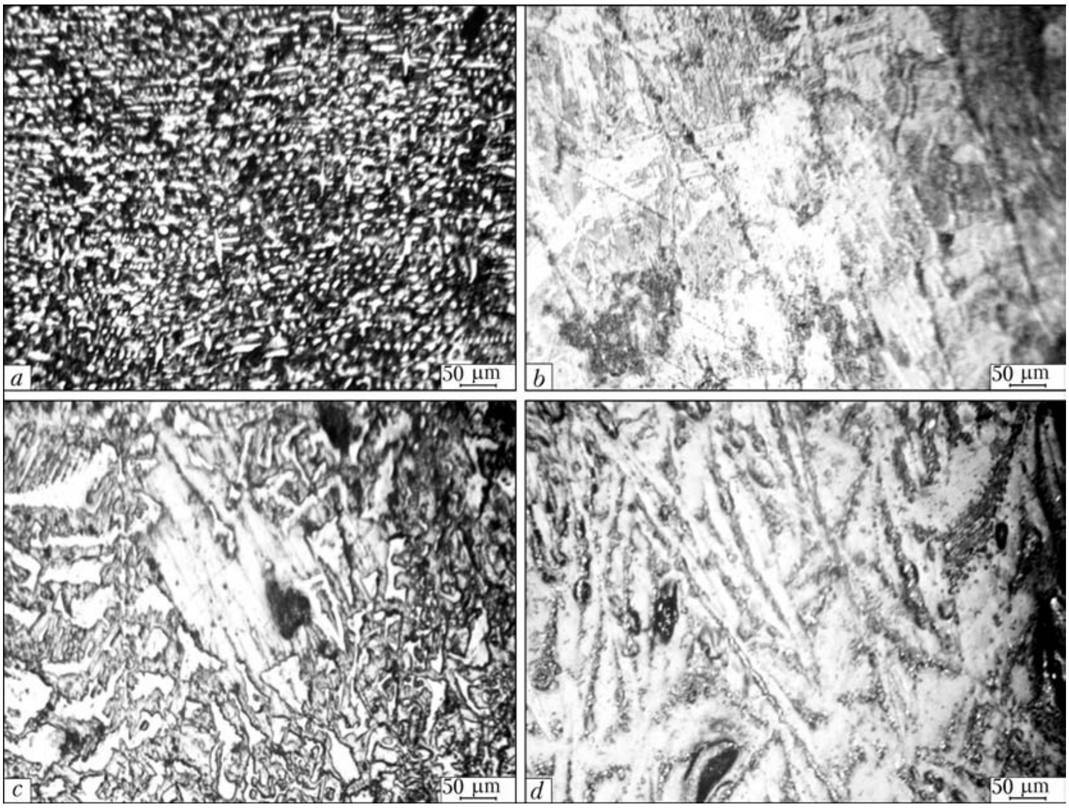

Figure 1. Microstructures of ingots of Fe–Y system alloys of different compositions: *a* — Fe90–Y10; *b* — Fe85–Y65; *c* — Fe65–Y35; *d* — Fe57–Y43

edly impair their performance, up to complete inoperability.

The weld and adjacent zone often are some of the most critical parts of the structural material. Performance degradation through embrittlement in many cases is associated with hydrogen dissolved in the weld metal. At present all the data on hydrogen behaviour in metal and alloys provide grounds for connecting the mechanisms of their hydrogen embrittlement with hydrogen interaction with their microstructural inhomogeneity: dissolved foreign atoms, vacancies, dislocations, grain and phase boundaries, phase precipitates, micro- and macropores, microcracks, inclusions of foreign particles, etc. Therefore, alongside the traditional method of reducing the probability of hydrogen embrittlement consisting in reduction of hydrogen concentration both in welding consumables and in the atmosphere, in which the welding process proceeds, other methods of embrittlement prevention through control of parameters of processes of hydrogen diffusion in the welded joint and structural material are also of interest.

Getter materials. Proceeding from the above analysis of getter materials from the viewpoint of their application as potential materials of getter additives, two series of alloys (based on Fe–Y binary and Zr–Co–Y ternary systems) were selected, which have the following initial compositions, wt.%: Fe90–Y10; Zr80.8–Co14.2–Y5; Fe85–Y15; Zr82.28–Co17.72; Fe65–Y35; Zr66.1–Co17.8–Y16.1; Fe57–Y43; Zr75.53–Co13.95–Y10.52.

Alloys of Fe–Y and Zr–Co–Y system are produced by argon-arc melting by nonconsumable (tungsten) electrode in high-purity argon atmosphere. To achieve a uniform distribution of component elements, alloy ingots were remelted several times. High-purity iron of multiple electron beam remelting, iodide zirconium, electrolytic cobalt and yttrium of 99.9 % purity were used as initial elements.

X-ray structural and metallographic analyses were applied to study the alloy phase composition and their structure. Phase composition of the produced alloys was determined by X-ray method in DRON-2M diffractometer in filtered Cu_{K_α}-radiation. Metallorgaphic investigations were conducted in MIM-8 microscope. The alloy microhardness was determined in MVT-3 microhardness meter, measurement error being ±5 %.

Prior to investigations the sample surface was ground with abrasive paper and polished with diamond paste.

For Fe–Y system alloys, 5 % solution of nitric acid in ethyl alcohol (nital) was used, and for alloys of Zr–Co–Y system, etchant of the following composition was applied: 15.4 ml HF; 17.3 ml HNO_3; 17.3 ml H_2SO_4; and 50 ml of distilled water. H_2SO_3 acid was added to the etchant for grinding the surface of samples, which was coated by passivating film during the etching process.

Mass spectrometric analysis was applied to study the gas evolution spectra [1], using MX-7203 mass-spectrometer. It is designed for hydrogen detection, as well as control of gas impurities in metals and

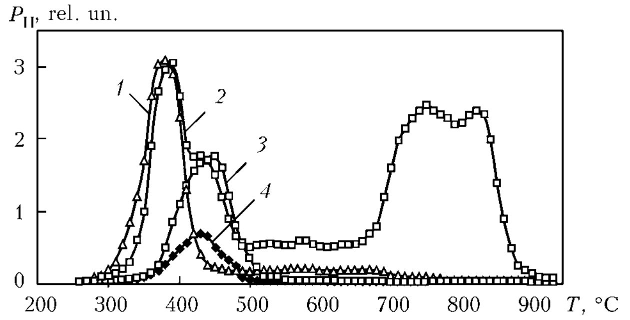

Figure 2. Variation of partial pressure of hydrogen P_H at heating in vacuum of samples of Fe–Y system alloys after hydrogen saturation at the temperature of 350 °C for 8 h: *1* — Fe85–Y15; *2* — Fe57–Y43; *3* — Fe65–Y35; *4* — Fe90–Y10

alloys, which evolve from them at heating (gases with up to 60 mass numbers are detected).

Alloy hydrogenation was conducted at the temperature of 350 °C for 8 h. Hydrogen gas evolution from the alloys before and after hydrogenation occurred at temperature rise from room temperature up to 950 °C.

According to the equilibrium diagram of Fe–Y system [2], the studied alloys are two-phase materials. Fe90–Y10 and Fe85–Y15 alloys contain α-Fe(Y) + $Fe_{17}Y_2$ phases. Assessment by the rule of segments gives their ratio as 38 and 62 % and 5 and 95 %, respectively. Alloys Fe65–Y35 and Fe57–Y43 consist of two intermetallics Fe_3Y + Fe_2Y and, according to assessment by the same rule, they have the ratio of 96 and 4 %, 14 and 86 %, respectively. Figure 1 gives microstructures of ingot surfaces of Fe–Y system alloys of the above compositions.

Quantitative ratio of phases assessed metallographically, is in agreement with earlier obtained results. Values of microhardness for alloys with increasing yttrium content are equal to 4270, 7700, 6700 and 5740 MPa, respectively.

Thermal desorption from the alloys reflects the total effect of gas evolution from phases present in them and hydrogenolysis products formed in alloy production and heating. Curves of hydrogen evolution at heating in vacuum of samples of Fe–Y system alloys are shown in Figure 2. The shape of the curves is determined, mainly, by the content of hydrogen present in the alloy phases, its redistribution in them at temperature variation, degree of hydrogen solubility and its equilibrium pressure above the alloy components.

In Fe90–Y10 and Fe85–Y15 alloys the nature of thermal desorption depends predominantly on the content of $Fe_{17}Y_2$ phase in them. Data of Figure 2 are in agreement with the data on thermal desorption of hydrogen from this phase given in [3, 4].

Curves of thermal desorption of Fe65–Y35 and Fe57–Y43 alloys, which contain Fe_3Y and Fe_2Y phases, represent the complex transformations occurring with their hydrides at temperature variation, which is not contradictory to the data of [5, 6].

Analysis of the obtained thermal desorption curves, as well as concentration of absorbed hydrogen, given in the Table, showed that Fe57–Y43 alloy, compared to other alloys of Fe–Y system, absorbs the largest amount of hydrogen and retains it up to higher temperature values (approximately 900 °C and higher).

Data of metallography and X-ray structural analysis of alloys of Zr–Co–Y system showed that Zr82.3–Co17.7 binary alloy is a single-phase alloy and consists of ZrCo intermetallic with rhombic lattice parameters a = 8.945 (Δ = 0.002); b = 10.875 (Δ =0.013); c = = 3.270 (Δ = 0.003) and elementary cell volume V = = 318,10 (Δ = 0.740), which is in good agreement with the data of [7].

Zr80.8–Co14.2–Y5 alloy consists of three phases (ZrCo, α-Zr and α-Y), having the following crystallographic parameters, respectively: a = 8.915 (Δ = = 0.250), b = 10.914 (Δ = 0.030), c = 3.298 (Δ = = 0.019) and V = 320.92 (Δ = 3.820); a = 3.238 (Δ = = 0.003), c = 5.161 (Δ = 0.001); a = 3.649 (Δ = 0.004), c = 5.752 (Δ = 0.030).

Zr75.5–Co14–Y10.5 alloy consists of the same phases as the previous alloy, and these phases have the following parameters, respectively: a = 8.932 (Δ = = 0.008), b = 10.955 (Δ = 0.400), c = 3.273 (Δ =

Hydrogen content in alloy samples before and after their saturation with hydrogen at 350 °C temperature for 8 h

Systems	Alloy	Hydrogen concentration in initial alloys		Hydrogen concentration in alloys after their hydrogen saturation at temperature of 350 °C	
		cm^3/100 g	%	cm^3/100 g	%
Fe–Y	Fe90–Y10	89	0.008	1400	0.13
	Fe85–Y15	46	0.004	3300	0.30
	Fe65–Y35	64	0.006	6700	0.60
	Fe57–Y43	138	0.012	15300	1.38
Zr–Co–Y	Zr82.3–Co17.7	81	0.007	14100	1.27
	Zr80.8–Co14.2–Y5	106	0.010	22400	2.02
	Zr75.5–Co14–Y10.5	206	0.020	22800	2.05
	Zr66.1–Co17.8–Y16.1	170	0.015	16400	1.48

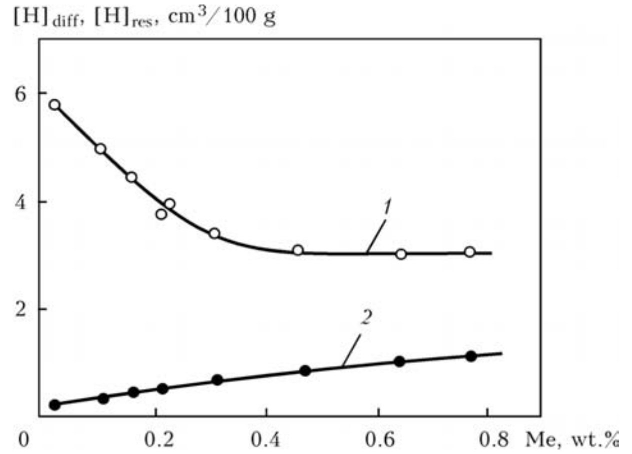

Figure 3. Influence of REE in electrode coating on concentration of diffusible (*1*) and residual (*2*) hydrogen [11]

= 0.001) and V = 320.23 (Δ = 1.560); a = 3.231 (Δ = = 0.004), c = 5.161 (Δ = 0.004); a = 3.652 (Δ = 0.005), c = 5.735 (Δ = 0.020).

In Zr66.1–Co17.8–Y16.1 alloy only Zr_3Co phase of the three metallographically detected phases was definitely identified.

Complex profiles of thermal desorption curves of Zr–Co–Y system alloys, which have been subjected to hydrogenation, are indicative of the fact that quite significant structural changes proceed in them at temperature change. Hydrogen gas evolution from these alloys occurs practically in the entire studied temperature range, and for Zr75.5–Co14–Y10.5 alloy it does not stop at maximum temperature of about 950 °C. Tabulated data show that of all the alloys of Zr–Co–Y system studied in this work, this alloy absorbs and retains the largest fraction of hydrogen.

Additives of rare-earth elements (REE) with a high affinity to gas and other interstitial elements, lead to a change in the properties of metals and alloys. Presence of an even small amount of yttrium, lanthanum, scandium, and cesium in the solid solution noticeably changes the diffusion mobility of atoms, elastic fields of dislocations and interfaces, and, therefore, the nature and kinetics of precipitates. Of special interest

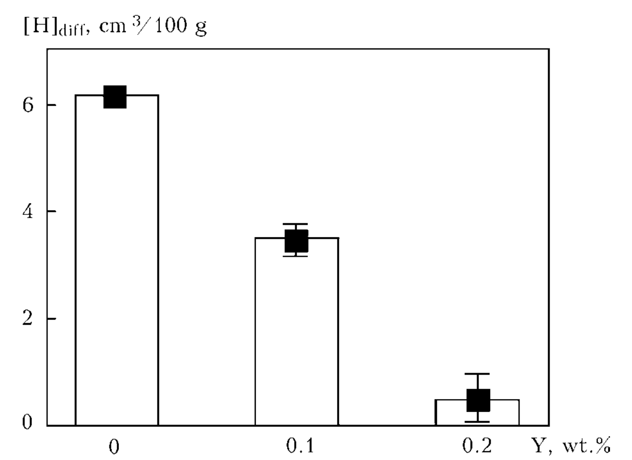

Figure 4. Influence of weight fraction of yttrium inside the powder wires (electrodes) on diffusible hydrogen concentration in the metal of weld made by welding in a mixture of gases of Ar + 0.1 % H_2 [11]

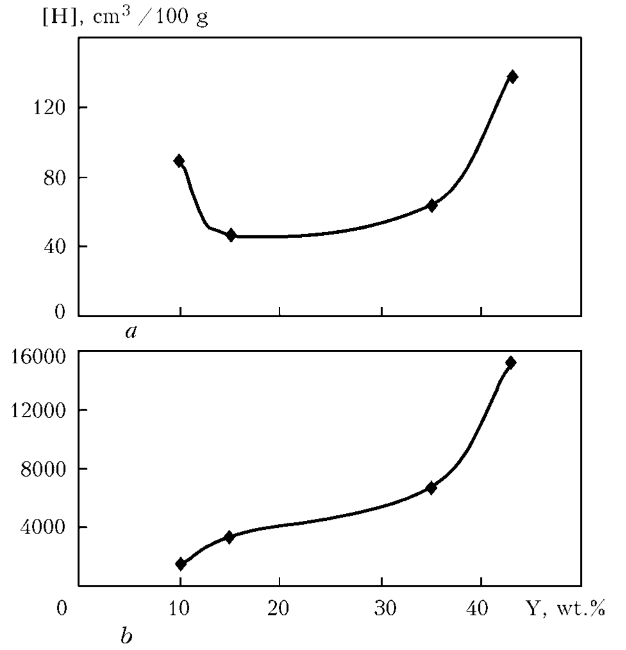

Figure 5. Concentration of hydrogen evolving from samples of alloys of Fe–Y system before (*a*) and after (*b*) their hydrogenation

is investigation of the influence of REE on evolution of structural-phase state and resistance of materials at irradiation. REE impact on radiation resistance depends on their concentration, presence of gas impurities in the solid solution and other factors. Positive influence of REE microalloying is attributable to increased density of the centers of secondary phase formation and more intensive decomposition of initial metastable solid solution [8, 9].

It should be noted that pure REE are relatively expensive. Moreover, alloying of radiation-resistant steels and alloys runs into technological difficulties associated with ensuring their uniform distribution in the solid solution, where their action on radiation

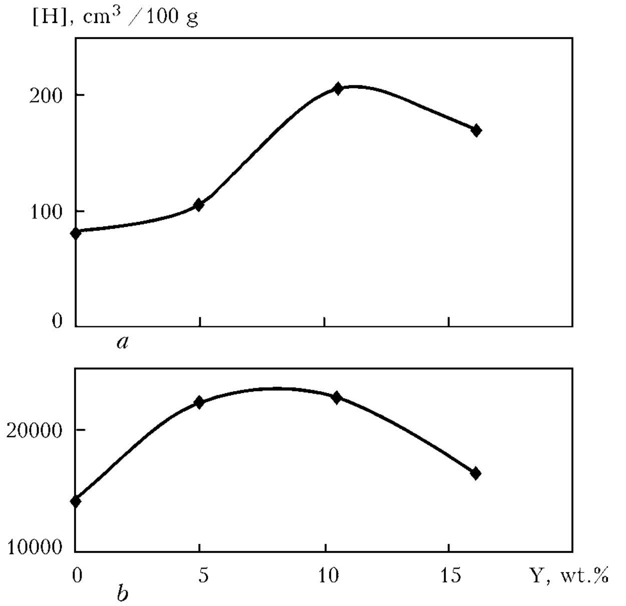

Figure 6. Concentration of hydrogen evolving from samples of alloys of Zr–Co–Y system before (*a*) and after (*b*) their hydrogenation

resistance is optimum [8, 9]. In alloy production they practically do not come to the metal because of the high reactivity of REE interaction with the slag covering the melt. Moreover, REE have a high vapour pressure [10], and scandium also has low density. Therefore, at addition in the pure form (even in the shielding atmosphere), their consumption is unreasonably high. From the view point of material saving, manufacturing of REE master alloys from their chemical compounds by metal-thermal reduction is practicable.

In the work it is shown that REE additives in the weld metal lead to reduction of the fraction of diffusible hydrogen in it (Figures 3 and 4), as they bind hydrogen, thus freeing the alloy matrix.

Change of concentration of hydrogen, which evolved from the samples of Fe–Y alloys before and after their hydrogenation, is shown in Figure 5. It is seen that increase of yttrium content in the alloy lead to an increase of absorbed hydrogen concentration, that is particularly noticeable after hydrogenation of these alloys.

Concentration of hydrogen evolving from samples of alloys of Zr–Co–Y system before and after their hydrogenation is shown in Figure 6. It is seen from the Figure that hydrogen concentration is maximum at yttrium content between 5 and 10 wt.%, and it decreases with increase of yttrium content to 15 wt.%.

Model welds with getter additives. Model samples of alloys simulating welds with special getter additives in it, capable of effective absorption, accumulation and retention of hydrogen, were made for investigations. These alloys consists of 95 wt.% Fe and 5 % of additive of Fe–Y system intermetallics. Intermetallic additives had the following compositions, wt.%: Fe90–Y10; Fe85–Y15; Fe65–Y35; Fe57–Y43.

Proceeding from metallographic analysis of sample surface, it was determined that alloys of the studied compositions consist of two phases — Fe(FeY) and FeY + Fe. Distribution of added intermetallic in iron proceeds uniformly over the entire volume. Grains of one phase take up a much larger surface of the section, and the other phase is located between the grains of the first phase in the form of thin interlayers and forms a kind of frame. Figure 7 gives the microstructures of alloy sample surface.

Microstructures of surfaces of model alloys with getter additives, containing 10 and 25 wt.% Y are similar, and microstructures of surfaces of alloys with getter additives with 35 and 43 wt.% Y are also similar, which is attributable to the difference in phase composition in the first and second case. Microhardness value in Fe(FeY) phase of these alloys (at increase of yttrium content in the getter additive) is equal to 1250, 1280, 1210 and 1270 MPa.

Curve *1* in Figure 8 is characterized by a complex profile, noticeable evolution of hydrogen starts at the temperature of approximately 300 °C and ends at 900 °C; curve *2* has a maximum at the temperature of about 600 °C, main evolution of hydrogen occurs at the temperature from 400 up to 900 °C.

Results of hydrogen thermal desorption from an alloy with getter additive containing 10 wt.% Y (see

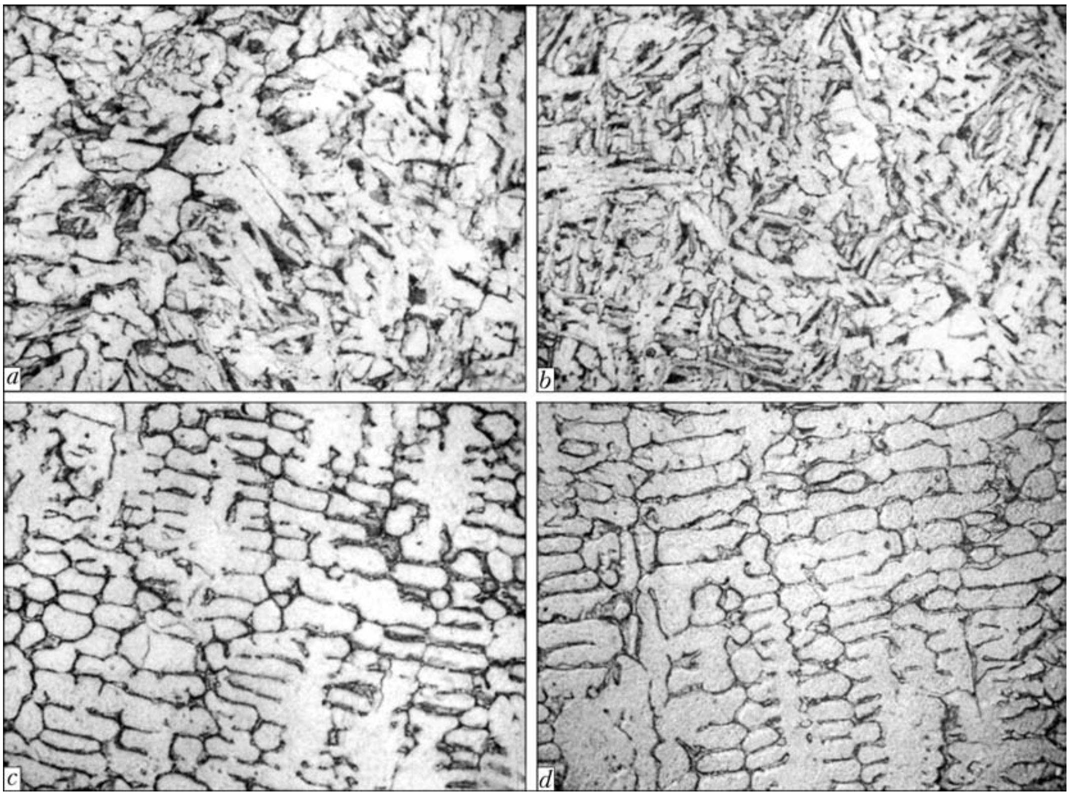

Figure 7. Microstructures (×300) of the surface of samples of alloys with getter additives containing 10 (*a*), 15 (*b*), 35 (*c*) and 43 (*d*) wt.% Y

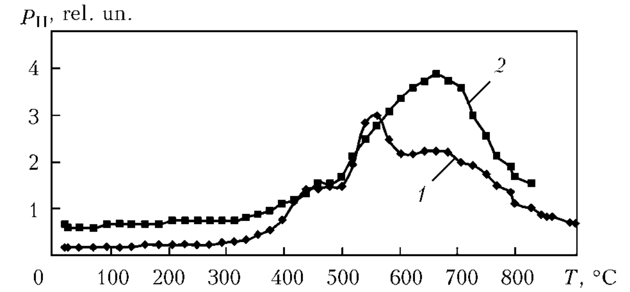

Figure 8. Change of partial pressure of hydrogen P_H at heating in vacuum of samples of an alloy with getter additive with 10 wt.% Y before (*1*) and after (*2*) hydrogenation

Figure 8), are in agreement with the data of investigation of hydrogen thermal desorption from Fe90–Y10 alloy [12], and do not disagree with the data on hydrogen thermal desorption from $Fe_{17}Y_2$ intermetallic, given in [13]. View of curve *2* and absolute value of the observed peak of hydrogen desorption, similar to our case, is influenced by the nature of hydrogen diffusion through the iron matrix. Iron content can significantly affect hydrogen diffusion and amplitude of the observed thermal desorption peaks [14].

Nuclear-physical investigation of distribution of hydrogen and its isotopes in new type of model welds. Sample saturation with deuterium was performed in Implantator unit with an oilfree pumping down system, ensuring the residual gas pressure in the target chamber on the level of $(2-3)\cdot10^{-4}$ Pa. Samples were irradiated by deuterium ions D^{2+} with energy E = 10 keV (5 keV/D^+) up to the dose of $(0.5-4.0)\cdot10^{16}$ D/cm^2.

Samples were annealed at the temperature of 300–1200 °C with direct current passage at the rate of temperature rise and drop of 7 K/s^{-1}.

After irradiation distribution of implanted particles by depth was measured through nuclear reaction $D(^3He, p)^4He$ using ^3He (E = 700 keV) beams. Measurements were performed in electrostatic accelerator ESU-2 in direct scattering geometry, ^3He ion beam hit the sample surface at an angle of 30°, and nuclear reaction products were recorded at 60° angle to the analyzed beam. Beam diameter at irradiation was 3 mm, and at analysis it was 2 mm. Division by penetration depth in direct scattering geometry was equal to 30 nm. This procedure is described in greater detail in [15].

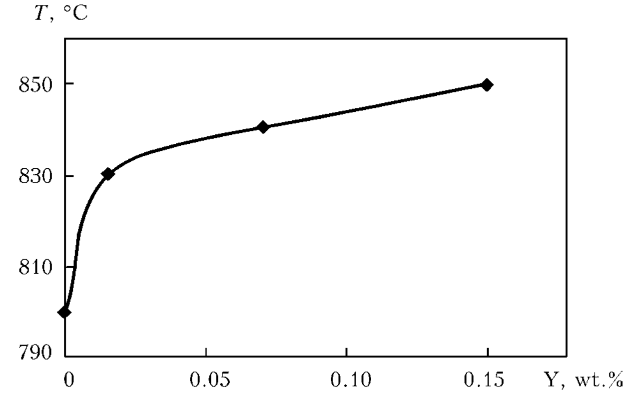

Figure 10. Temperature influence on maximum gas evolution of hydrogen from model weld metal with varying content of added yttrium

Content of deuterium, which has evolved after exposure to D^{2+} with 12 keV energy up to the dose of $5\cdot10^{16}$ D/cm^2 from samples of alloys with yttrium additives, is shown in Figure 9, from which it is seen that at increased content of yttrium added to the alloy, the content of evolving deuterium becomes higher. This is indicative of the fact that at saturation of weld metal with deuterium, it behaves as a residual element (compared to Figure 3).

Method of mass-spectrometry analysis was used to study the temperature interval of hydrogen gas evolution, depending on added yttrium content. Figure 10 shows that with increase of yttrium content in model weld metal, the temperature at which maximum evolution of hydrogen gas occurs, shifts towards high temperature region. This is indicative of the fact that at high yttrium content hydrogen is retained stronger in the model weld metal.

As is seen from Figure 11, concentration of evolved hydrogen decreases with increase of added yttrium content. This shows that absorbed hydrogen is retained by yttrium in model weld metal, i.e. is diffus-

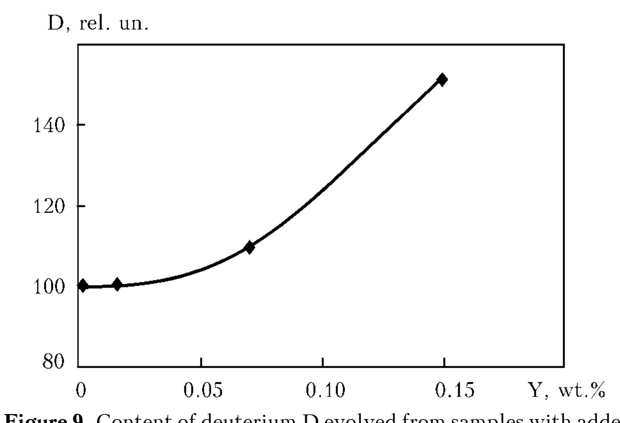

Figure 9. Content of deuterium D evolved from samples with added yttrium after exposure to ions D^{2+} with 12 keV energy up to the dose of $5\cdot10^{16}$ D/cm^2

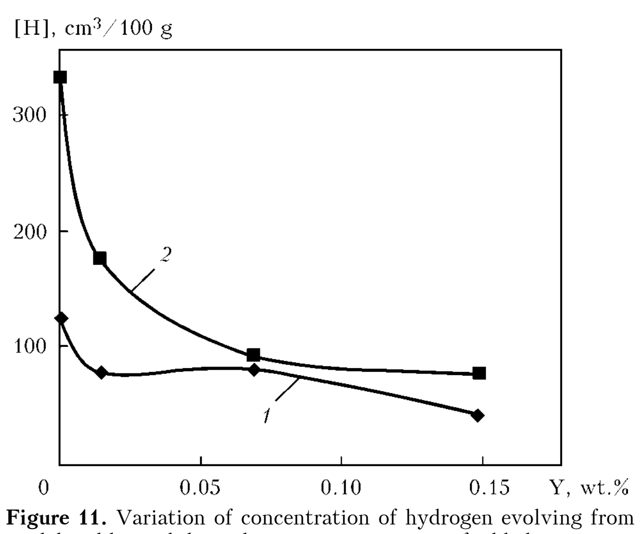

Figure 11. Variation of concentration of hydrogen evolving from model weld metal depending on concentration of added yttrium in the initial condition (*1*) and after hydrogenation (*2*)

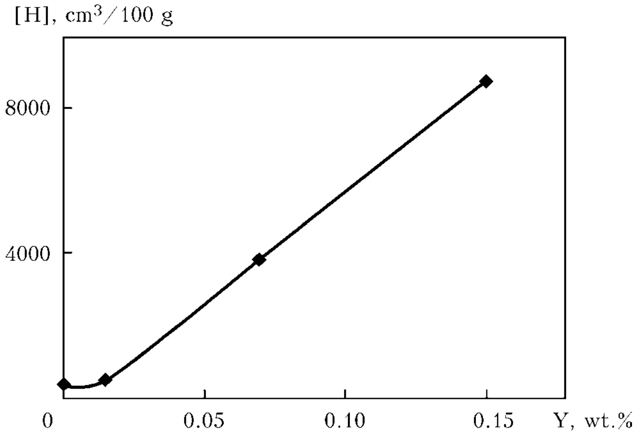

Figure 12. Change of concentration of hydrogen evolving from model weld metal depending on added yttrium content before and after hydrogenation

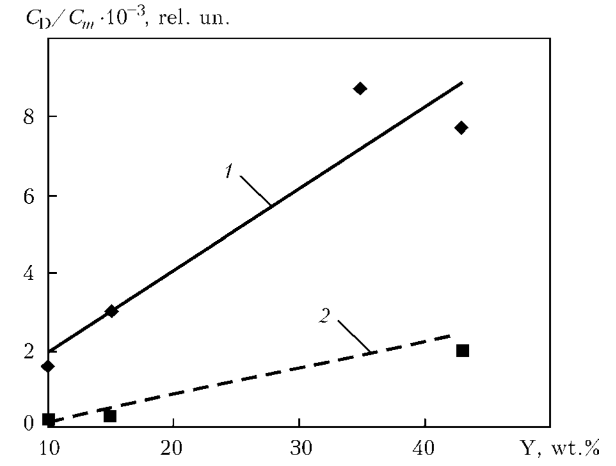

Figure 14. Influence of yttrium content in model weld metal on surface concentration (*1*) and concentration of ion-implanted deuterium at the depth of 0.5–1.8 μm (*2*) at room temperature with 6 keV energy up to the dose of $5 \cdot 10^{16}$ D/cm^2

ible. At longer time of saturation of model weld metal by hydrogen, concentration of absorbed hydrogen in yttrium rises (Figure 12).

Comparison of Figure 9 and Figure 12 may reveal the following regularity: concentration of evolved deuterium and yttrium occurs with increase of yttrium content. It is possible that there is a limit concentration of hydrogen (deuterium), starting from which the mechanism of hydrogen (deuterium) retention by yttrium changes, with hydrogen changing from diffusible to residual.

Figure 13 shows the spatial-concentrational distribution of deuterium by depth *d* of the layer, on which it is implanted (it is changed by the above procedure), in the metal of model welds with different yttrium content.

Curve of variation of deuterium content is a drooping one with about 200 nm half-width. The main part of entrapped deuterium is concentrated in this region. Part of the remaining implanted gas is uniformly distributed in the lattices to the maximum depth of

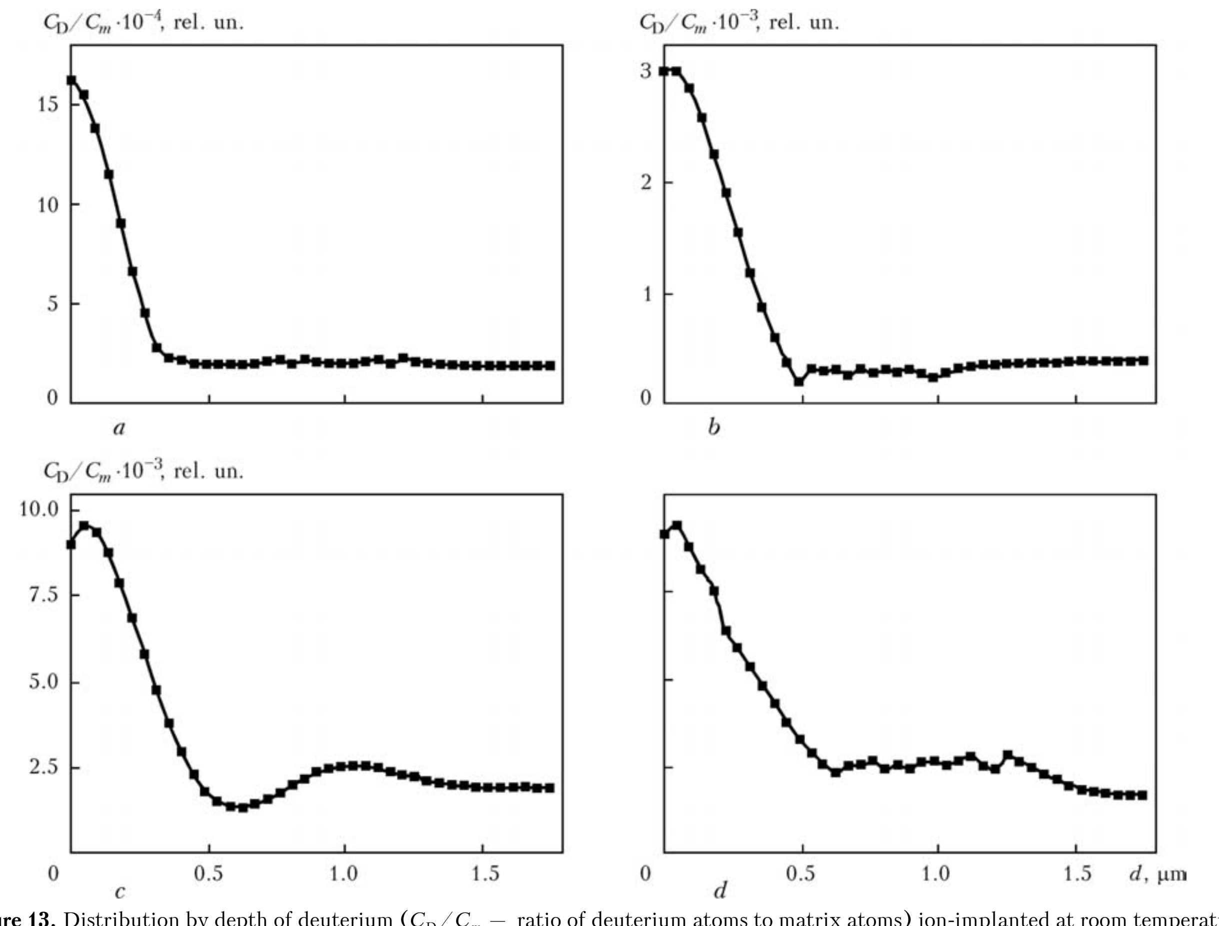

Figure 13. Distribution by depth of deuterium (C_D/C_m – ratio of deuterium atoms to matrix atoms) ion-implanted at room temperature with 6 keV energy to the dose of $5 \cdot 10^{16}$ D/cm^2 in the metal of model welds with 10 (*a*), 15 (*b*), 35 (*c*) and 43 (*d*) wt.% Y

1.8 μm, at which analysis of ^{3}He was performed in model welds at 1.4 MeV energy. Deuterium penetration to depths greatly exceeding its path length is, apparently, due to saturation of penetration layer and appearance of highly mobile gas component, capable of freely migrating to sample depth.

All the components of deuterium distribution in model weld metal (namely, its content on the surface and in the penetration layer, in the «tail» of distribution and total content of deuterium retained in the samples) increase practically linearly with increase of yttrium content in the weld metal (Figure 14). Deuterium accumulation becomes higher in samples of model welds with higher content of getter additive.

Thus, a series of alloys of Fe–Y and Zr–Co–Y system of different composition was produced. Their phase composition and thermal desorption properties were studied. It is shown that these alloys are characterized by a sufficiently high temperature of hydrogen retention and, therefore, can be considered as materials for getter additives to create hydrogen traps in structural materials and welded joints of NPP equipment, promoting an improvement of their service properties by reducing hydrogen influence.

Concentration of hydrogen evolving from getter additives of Zr–Y system rises with increase of added yttrium content.

A series of model welds of joints with different content of getter additives was produced. It is shown that concentration of hydrogen evolving from weld metal decreases with increase of yttrium content in the getter additive. This is indicative of the fact that the absorbed hydrogen is retained by yttrium in model weld metal.

Nuclear-physical investigations of distribution of hydrogen and its isotopes in the metal of new type of model welds were performed. Spatial-concentrational distribution of deuterium in model weld metal showed that content of absorbed deuterium rises with increases of yttrium content.

1. Azhazha, V.M., Bobrov, Yu.P., Bovda, A.M. et al. (2006) Examination of gas emission in vacuum heating of hydrogenated alloy Nd–Fe–B. *Voprosy Atomn. Nauki i Tekhniki. Vakuum, Pure Metals, Superconductors Series*, **1**, 156–159.
2. (1996) *Constitutional diagrams of binary metallic systems*: Refer. Book. Ed. by N.P. Lyakishev. Vol. 1. Moscow: Mashinostroenie.
3. Wirth, S., Skomski, R., Coey, J.M.D. (1998) Hydrogen in R_2Fe_{17} intermetallic compounds. In: *Structural, thermodynamics and magnetic properties: Res. Pap. Phys. Astronomy*, 55(**9**), 5700–5707.
4. Nikitin, S.A., Ovchenkov, E.A., Tereshina, I.S. et al. (1998) Synthesis of ternary hydrides and nitrides R_2Fe_{17} (R–Y, Tb, Dy, Ho, Er) and effect of interstitial elements (H_2, N_2) on magnetic anisotropy and magnetostriction. *Metally*, **2**, 111–116.
5. Kolachev, B.A., Shalin, R.E., Iliin, A.A. (1995) *Hydrogen-accumulating alloys*: Refer. Book. Moscow: Metallurgiya.
6. Leblond, T., Paul-Boncour, V., Cuevas, F. et al. (2009) Fernandez study of the multipeak deuterium thermodesorption in YFe_2D_x ($1.3 < x < 4.2$) by DSC, TD and in situ neutron diffraction. *Int. J. Hydrogen Energy*, 34, Issue 5, 11–14.
7. (1996) *Data base PCPDF*. Int. Center for Diffraction Data, 20–23.
8. Zelensky, V.F., Neklyudov, I.M. (1991) Effect of rare-earth elements on radiation resistance of materials. In: *Proc. of Int. Conf. on Radiation Materials Science* (Kharkov, Sept. 1991). Vol. 2. Kharkov, 45–57.
9. Bakaj, A.S., Gann, V.V., Zelensky, V.F. et al. (1990) Alternative polarity recombination centers of point defects. *Effects of Radiation on Materials*, **1**, 623–631.
10. Savitsky, E.M., Burkhanov, G.S. (1980) *Rare metals and alloys. Physico-chemical analysis and materials science*. Moscow: Nauka.
11. Pokhodnya, I.K., Yavdoshchin, I.R., Paltsevich, A.P. et al. (2004) *Metallurgy of arc welding. Interaction of metal with gases*. Kiev: Naukova Dumka.
12. Azhazha, V.M., Lavrinenko, S.D., Svinarenko, A.P. et al. (2009) Getter alloys for creation of hydrogen traps in structural materials and welded joints of nuclear power plant equipment. *Voprosy Atomn. Nauki i Tekhniki. Vakuum, Pure Metals, Superconductors Series*, **6**, 127–133.
13. Skomski, R. (2006) Hydrogen in R_2Fe_{17} intermetallic compounds. In: *Structural, thermodynamics and magnetic properties: Res. Pap. Phys. Astronomy*, 5700–5707.
14. Kakinichi, K., Itagaki, N., Furuya, T. et al. (2004) Role of iron for hydrogen absorption mechanism in zirconium alloys. *J. ASTM Int.*, 1(**10**), 349–365.
15. Karpov, S.A., Kopanets, I.E., Neklyudov, I.M. et al. (2004) Combination of method of nuclear reactions, thermodesorption spectrometry and double-beam radiation during investigation of helium and hydrogen behavior in structural materials. In: P*roc. of 14th Int. Meeting on Radiation Physics of Solid* (Sevastopol, 5–10 July 2004). Sevastopol, 592–596.

EFFECT OF YTTRIUM ON REDISTRIBUTION OF HYDROGEN AND STRUCTURE OF WELD METAL IN ARC WELDING OF HIGH-STRENGTH STEELS

I.K. POKHODNYA, A.P. PALTSEVICH, A.V. IGNATENKO, T.G. SOLOMIJCHUK and **V.S. SINYUK**
E.O. Paton Electric Welding Institute, NASU, Kiev, Ukraine

Transfer of yttrium into deposited high-strength low-alloy metal in welding with flux-cored wire in a shielding gas atmosphere and with covered electrodes of the basic type was investigated. Thermal desorption analysis revealed interaction of yttrium with dissolved hydrogen to form residual hydrogen depending on the concentration of yttrium. The effect of yttrium on microstructure of deposited low-alloy steel and mechanical properties of metal is shown.

Keywords: *arc welding, high-strength low-alloy steels, modification of weld metal, yttrium, redistribution of hydrogen, thermal desorption analysis of hydrogen, structure, mechanical properties*

It is a known fact [1–6] that yttrium and other rare-earth metals (REM) are used for microalloying and modification of steels and welds to improve their mechanical properties. In addition, yttrium, cerium, lanthanum, neodymium and praseodymium form compounds with hydrogen, thus decreasing the flake-sensitivity of steels [7].

Application of REMs in welding consumables to improve performance of the weld metal is described in studies [4–6]. Of special interest are the investigations aimed at decreasing the sensitivity of the welds and welded joints on high-strength low-alloy (HSLA) steels to hydrogen-induced cracking. The attempts to redistribute hydrogen absorbed by the weld pool are reported in studies [6, 8, 9]. However, the quantity of the investigations conducted is small, and their results contain a number of contradictory data concerning the effect of the REM additions on behaviour of hydrogen in the weld metal.

This study considers investigations of the effect of yttrium on the probability of redistribution of absorbed hydrogen between the diffusible and residual forms, as well as of the peculiarities of variations in structure and mechanical properties of the weld metal. Because of a high affinity of yttrium for oxygen, the effect of adding yttrium to the weld pool metal by using a flux-cored wire designed for gas-shielded welding was compared with that by using covered electrodes. The yttrium content of the weld metal was determined by using a high-sensitivity emission spectrometer with inductively coupled plasma iCAP 6000. Chemical composition of the metal was determined by using the «Spectrovak-1000» device. The content of diffusible hydrogen in the weld metal was measured, according to requirements of GOST 23338–91, by the chromatographic method using gas-analyser OB 2781P.

The content of residual hydrogen in weld metal samples was measured in the automatic mode by the thermal desorption method described in study [10] and upgraded to measure the content of residual hy-

Table 1. Chemical composition (wt.%) of deposited metal depending on yttrium content of flux-cored wire

Flux-cored wire	Yttrium content of wire	C	Si	Mn	Al	Ti	Y	Hydrogen concentration, ml/100 g	
								$[H]_{diff.\ d.m}$	$[H]_{res}$
P1 (PPAN 70)	0	0.08	0.71	1.6	<0.05	<0.08	0	$\frac{2.2–4.4}{3.5\times3}$	0.6
P2	0.3	0.08	0.74	1.7	<0.05	<0.08	0.008	$\frac{4.6–5.0}{4.7\times3}$	0.5
P3	0.8	0.09	0.90	1.8	0.11	0.064	0.013	$\frac{6.1–6.8}{6.3\times3}$	0.9
P4	1.6	0.10	0.95	1.7	0.15	0.250	0.055	$\frac{6.7–8.7}{7.7\times2}$	6.0

Note. Here and in Table 6, the numerator gives extreme values of $[H]_{diff.\ d.m}$, and the denominator — mean values over the indicated number of samples.

Table 2. Distribution of hydrogen in metal deposited with flux-cored wires in argon atmosphere

Flux-cored wire	$[H]_{diff.\ d.m}$, ml/100 g	$[H]_{res}$, ml/100 g
P1	3.8	0.2
P2	4.9	0.2
P3	4.8	1.9
P4	4.6	4.6

drogen $[H]_{res}$ and investigate thermal desorption of hydrogen from metals.

Transfer of yttrium into the weld metal and redistribution of absorbed hydrogen in welding with the 1.6 mm diameter flux-cored wire PP-AN 70 with the Fe–Y system alloy added to its core were investigated. Welding in high-purity argon was carried out at a reverse-polarity current of 220 A. Table 1 gives chemical composition of the multilayer deposited metal depending on the content of yttrium in the wire, diffusible hydrogen in the deposited metal, $[H]_{diff.\ d.m}$, and $[H]_{res}$ in the one-layer welds.

Below we give results of analysis of non-metallic inclusions in a sample made by welding with wire P4. Chemical composition of non-metallic inclusions was determined with scanning electron microscope «Jeol ISM-32CF» and dispersive energy analyser INCA Energy 350 of the «Oxford Instruments» Company (Great Britain). Non-metallic inclusions in the sample deposited with wire P4 had the following chemical composition, wt.%: 21.8 Y, 41.0 O, 13.7 Mn, 4.0 Si, 1.8 Al, 15.1 Ti, 2.6 S.

Increase in the yttrium content of the flux-cored wire core and its high deoxidising ability lead to increase in the content of silicon, aluminium and titanium in the weld metal, as well as to increase in the content of $[H]_{diff.\ d.m}$ and particularly $[H]_{res}$ in the weld metal obtained by using wires P3 and P4 (Table 1).

Supposedly, the content of hydrogen absorbed by the weld pool grows because of the presence of hydrogen in the Fe–Y system alloy and its hydration in manufacture and storage of the wires.

The content of diffusible hydrogen $[H]_{diff}$ was measured in samples of the weld pool metal taken

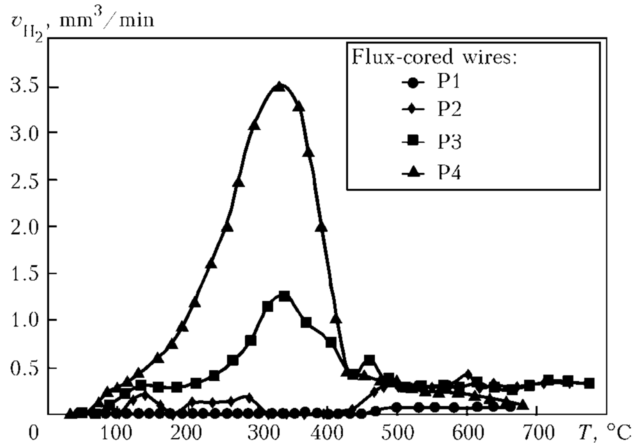

Figure 1. Spectrum of thermal desorption of residual hydrogen from samples taken into quartz ampoule (average sample heating rate — about 7 deg/min)

with a quartz tube in deposition of the fourth layer (Table 2), and thermal desorption analysis of $[H]_{res}$ was carried out to study in more detail the probability of redistribution of absorbed hydrogen depending on the yttrium content of the metal. The samples were cooled in water every 1–2 s and stored in liquid nitrogen before analysis.

The high content of $[H]_{res}$ takes place at an yttrium content of 0.013 to 0.053 wt.%, resulting in a peak of residual hydrogen (Figure 1) with a maximal temperature of 340–350 °C.

It is a known fact [11] that decomposition of yttrium hydride $YH_{1.6}$ during heating occurs in two stages — at temperatures of 360–410 and 1100–1300 °C. Yttrium monohydride transforms into yttrium metal at the second stage during heating. At an yttrium content of 0.013 wt.% or more, it is contained in non-metallic inclusions and iron solution in the weld [12], this leading to formation of the bond of dissolved hydrogen and yttrium.

Experiments on welding with basic electrodes were carried out by adding FeY (Y = 26 wt.%) or AlNiY (Y = 13.3 wt.%) into the electrode coverings.

Tables 3 and 4 give chemical compositions of the multilayer metal deposited with the experimental electrodes at a reverse polarity direct current of 160–170 A. Increasing the content of FeY and AlNiY in a covering causes a small increase in the yttrium content of the deposited metal with both series of electrodes,

Table 3. Chemical composition (wt.%) of metal deposited with electrodes containing FeY in their coverings

Electrode index	Y content of covering	C	Si	Mn	S	P	Cr	Ni	Mo	V	Al	Ti	Y
IP 1	0	0.043	0.274	0.98	0.007	0.015	0.88	2.36	0.45	0.18	0.007	0.005	–
IP 2	0.026	0.041	0.276	0.99	0.006	0.014	0.86	2.35	0.45	0.18	0.006	0.006	0.0001
IP 3	0.052	0.044	0.256	0.99	0.007	0.016	1.02	2.37	0.46	0.18	0.006	0.006	0.0001
IP 4	0.078	0.044	0.281	1.02	0.006	0.015	0.77	2.35	0.47	0.18	0.006	0.007	0.0001
IP 5	0.156	0.044	0.252	1.00	0.005	0.015	0.94	2.53	0.53	0.18	0.007	0.007	0.0002
IP 6	0.260	0.048	0.280	1.02	0.006	0.015	0.85	2.38	0.44	0.17	0.006	0.007	0.0006

Table 4. Chemical composition (wt.%) of metal deposited with electrodes containing AlNiY in their coverings

Electrode index	Y content of covering	C	Si	Mn	S	P	Cr	Ni	Mo	V	Al	Ti	Y
IP 7	0	0.035	0.278	0.95	0.005	0.012	0.83	2.14	0.45	0.21	0.007	0.005	–
IP 8	0.043	0.035	0.320	1.00	0.006	0.014	0.87	2.33	0.46	0.21	0.008	0.007	0.0001
IP 9	0.128	0.048	0.381	1.08	0.006	0.013	0.88	2.32	0.47	0.16	0.009	0.009	0.0001
IP 10	0.212	0.042	0.466	1.18	0.007	0.014	0.88	2.39	0.48	0.16	0.011	0.008	0.0001
IP 11	0.320	0.046	0.571	1.25	0.007	0.015	0.93	2.45	0.51	0.23	0.015	0.009	0.0002

Table 5. Chemical composition (wt.%) of metal deposited with electrodes containing FeY + AMP in their coverings

Electrode index	AMP and Y content of covering	C	Si	Mn	S	P	Cr	Mo	V	Al	Ti	Y
IP 12	–	0.079	0.278	1.20	0.015	0.021	0.94	0.45	0.21	0.007	0.016	–
IP 13	1.5 AMP	0.081	0.347	1.30	0.015	0.024	0.98	0.44	0.23	0.009	0.017	–
IP 14	0.56 Y 1.5 AMP	0.090	0.376	1.29	0.013	0.021	0.94	0.44	0.23	0.009	0.017	0.0006
IP 15	3.0 AMP	0.087	0.490	1.42	0.013	0.022	0.98	0.45	0.24	0.013	0.022	–
IP 16	0.56 Y 3.0 AMP	0.097	0.460	1.41	0.013	0.025	0.99	0.46	0.23	0.013	0.025	0.0010

the content of $[H]_{res}$ remaining almost unchanged (Figure 2).

The probability of increase in transfer of yttrium into the weld metal by adding strong deoxidisers, i.e. aluminium and magnesium, into the coverings was evaluated in a series of experiments on welding by using electrodes with Fe–Y + AMP added into their coverings.

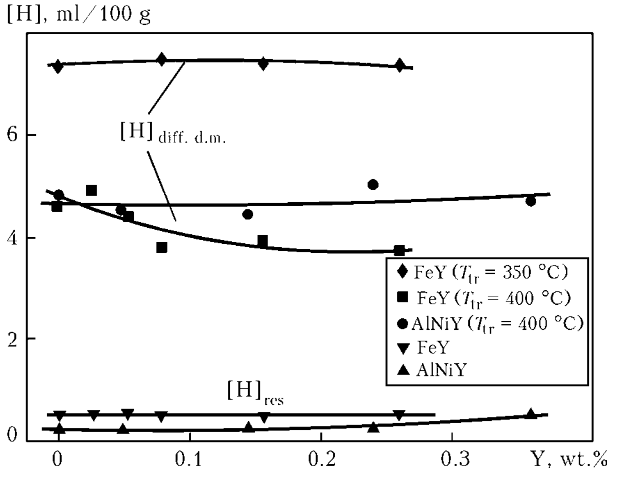

Figure 2. Contents of $[H]_{diff.\,d.m}$ and $[H]_{res}$ versus content of yttrium in electrode covering

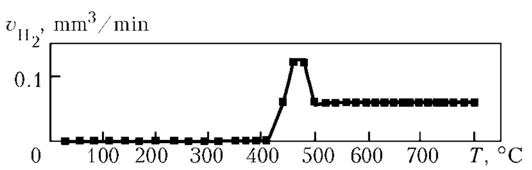

Figure 3. Spectrum of thermal desorption of residual hydrogen from deposited metal of one-layer weld made with electrode IP 16

Table 5 gives chemical composition of the multilayer metal deposited at a reverse polarity direct current of 160–170 A, and Table 6 — results of measurements of the $[H]_{diff.\,d.m}$ and $[H]_{res}$ contents.

Adding the aluminium-magnesium powder (AMP) into the electrode coverings leads to a substantial increase in the contents of silicon, manganese, aluminium, titanium and yttrium (Table 5). The content of $[H]_{res}$ remains almost unchanged (Table 6), and there is no peak of hydrogen in a 340 °C temperature range in the thermal desorption spectrum (Figure 3).

Adding yttrium together with AMP to the electrode coverings allows increasing the yttrium content of the weld metal to 0.001 wt.%. However, no redistribution of hydrogen was observed in this case.

Table 6. Content of hydrogen in weld metal obtained with electrodes containing FeY + AMP in their coverings

Electrode index	$[H]_{diff.\,d.m}$, ml/100 g	$[H]_{res}$ in heating to 800 °C, ml/100 g
IP 12 (basic)	$\frac{3.8–4.1}{3.9\times3}$	0.5
IP 13 (1.5 wt.% AMP)	$\frac{3.9–4.2}{4.0\times3}$	0.5
IP 14 (0.56 wt.% Y, 1.5 wt.% AMP)	4.9×3	0.7
IP 15 (3 wt.% AMP)	$\frac{5.0–5.2}{5.1\times3}$	0.3
IP 14 (0.56 wt.% Y, 3 wt.% AMP)	$\frac{5.5–5.7}{5.6\times3}$	0.5

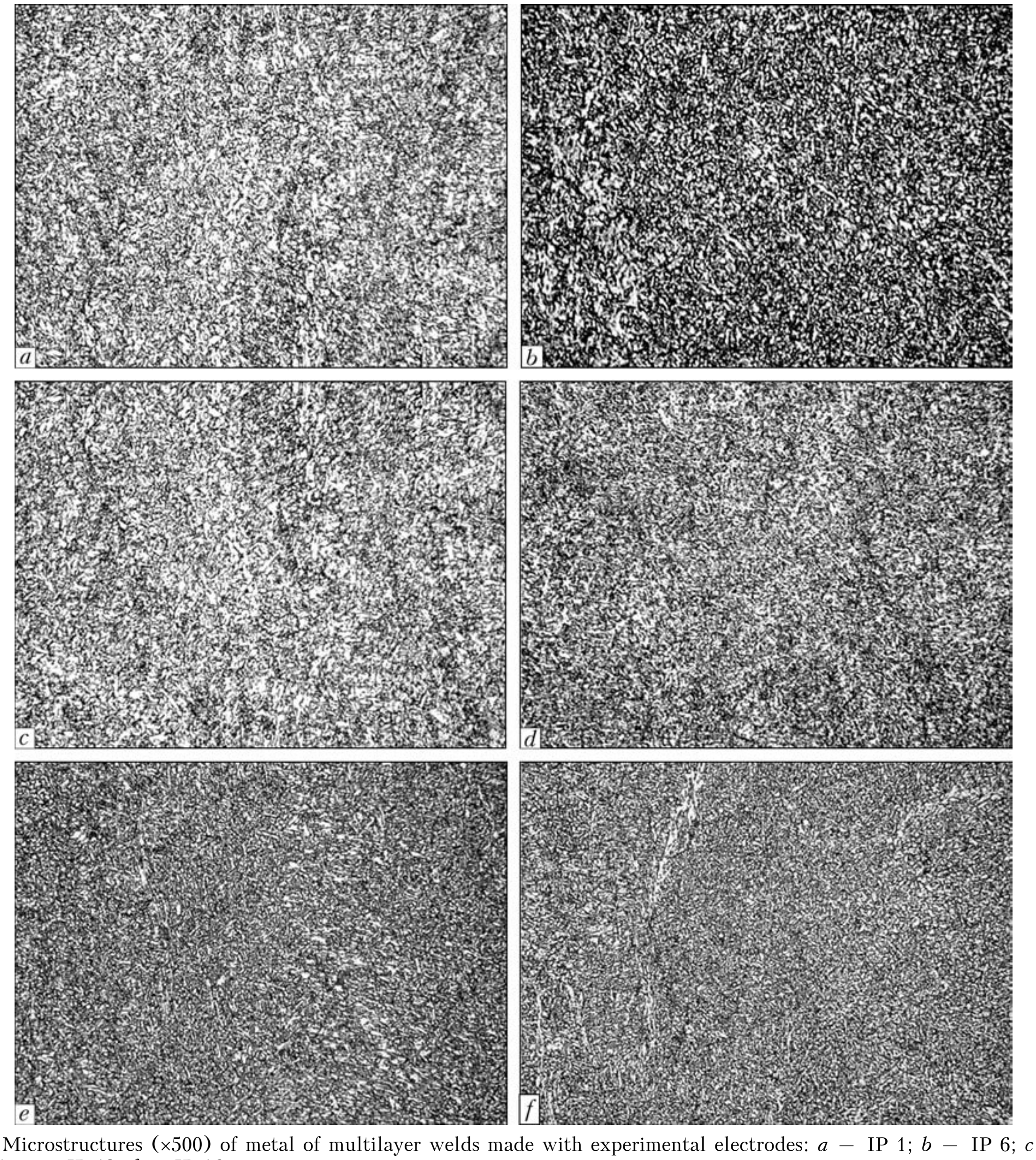

Figure 4. Microstructures (×500) of metal of multilayer welds made with experimental electrodes: *a* — IP 1; *b* — IP 6; *c* — IP 7; *d* — IP 11; *e* — IP 12; *f* — IP 16

The effect of yttrium on the metal structure and content of non-metallic inclusions was investigated on samples of the ten-layer welds made under the following conditions: I_w = 160–165 A (direct current of reverse polarity), U_a = 24–26 V, v_w = 8–9 m/h, experimental electrodes.

Microstructures of the multilayer weld metals were examined with microscope «Neophot-32». Photos of the microstructures shown in Figure 4 were obtained with camera «Olympus».

Microstructures of the samples from the upper layer of the deposited metal are approximately identical. They are of the bainitic type with fine precipitates of polygonal ferrite along the cast crystalline grain boundaries. Heat treated regions of the samples have structure of the mostly bainitic type without polygonal ferrite.

The fine-grained structure of all the samples is caused by alloying the weld metal with chromium, nickel and aluminium [13], and decrease in its dispersion degree is determined by adding yttrium.

It was established that adding FeY and AlNiY to the electrode coverings leads to decrease in the volume content of non-metallic inclusions. Chemical compositions of non-metallic inclusions in metal of the weld samples with the maximal yttrium content are given in Table 7. Inclusions are mostly silicon and manganese oxides with a low content of sulphur. The aluminium and titanium content was increased, and yttrium was detected in some inclusions at the highest FeY + AMP content of the electrode coverings.

Table 7. Chemical composition (wt.%) of non-metallic inclusions

Electrode index	O	Si	Mn	Al	Ti	S	Y
IP 6	38	13.6	43	0.5	2.8	2.1	–
IP 11	38	13.2	39	3.7	4.0	2.1	–

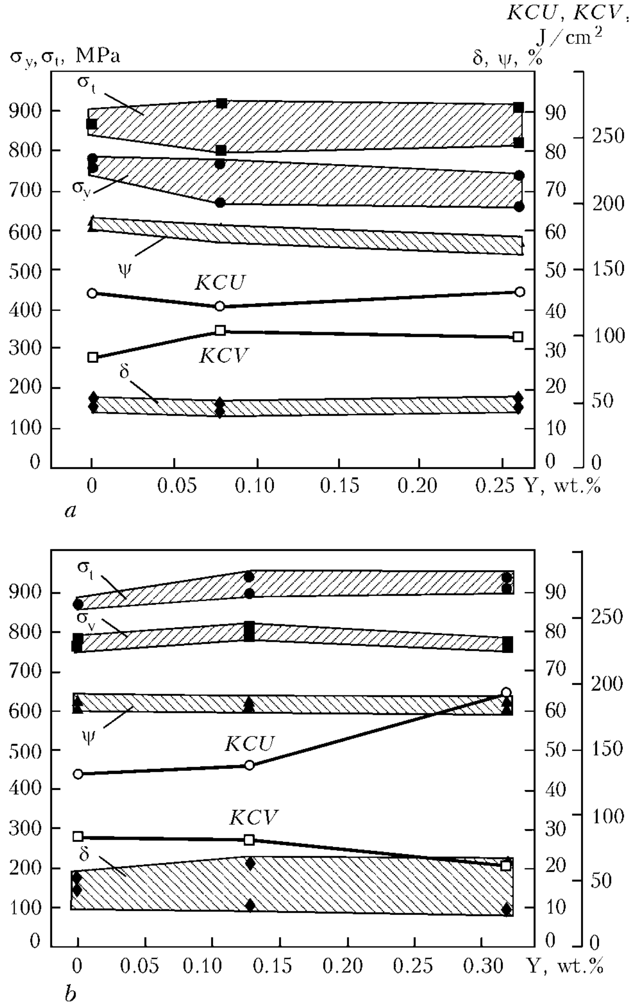

Figure 5. Effect of yttrium on mechanical properties of weld metal: *a* — electrodes with FeY in their coverings (series IP 1– IP 6); *b* — electrodes with AlNiY in their coverings (series IP 7– IP 11)

Bead on plate (steel VST3sp (killed) acc. to GOST 9466–750) welding was carried out under the following conditions to determine the effect of yttrium on mechanical properties of the deposited metal: I_w = = 160–165 A (direct current of reverse polarity), U_a = = 24–26 V, v_w = 8 m/h. Results of the mechanical tests conducted at 20 °C are shown in Figure 5.

The high values of strength and ductility of the deposited metal are preserved at 20 °C owing to alloying (see Tables 3 and 4) and fine-grained structure.

CONCLUSIONS

1. Welding with flux-cored wires in argon atmosphere provides a marked transfer of yttrium into the deposited metal and its interaction with hydrogen.

2. Thermal desorption analysis revealed formation of residual hydrogen with a maximal removal temperature of 340–350 °C at Y ≥ 0.013 %.

3. Welding with basic electrodes containing up to 0.35 wt.% Y in their coverings failed to provide the yttrium content of the deposited metal necessary for redistribution of hydrogen because of a high oxidation potential of the coverings.

4. Adding yttrium leads to decrease in the dispersion degree of structure of the deposited metal and volume content of non-metallic inclusions. Strength and ductility of the deposited metal remain at a constant level.

1. Kreshchanovsky, N.S., Sidorenko, M.F. (1970) *Modification of steel*. Moscow: Metallurgiya.
2. Braun, M.P. (1982) *Microalloying of steel*. Kiev: Naukova Dumka.
3. Goldshtejn, Ya.E., Mizin, V.G. (1986) *Modification and microalloying of cast iron and steel*. Moscow: Metallurgiya.
4. Efimenko, N.G. (2003) Integrated evaluation of effect of yttrium on properties of steel welds. *The Paton Welding J.*, **8**, 23–26.
5. Efimenko, N.G. (1980) Application of rare-earth metals in welding electrode coverings. *Svarochn. Proizvodstvo*, **7**, 28–29.
6. Musiyachenko, V.F., Melnik, I.S., Movchan, M.B. et al. (1987) Effect of modification of non-metallic inclusions with rare-earth metals on structure and properties of weld metal in welding of high-strength steels. *Avtomatich. Svarka*, **6**, 1–6.
7. Goldshtejn, Ya.E., Zeldovich, V.I., Kejs, N.V. et al. (1962) Effect of treatment of molten chrome-nickel steel with cerium on character of its crystallisation. *Steel*, **3**, 258–261.
8. Naoyukis, S. (1980) The prevention of weld cracking by addition of special elements. *IIW Doc. II-A-513–80*.
9. Lensing, C.A., Park, Y.D., Maroeff, I.S. et al. (2004) Yttrium hydrogen trapping to manage hydrogen in HSLA steel welds. *Welding J.*, **9**, 254–266.
10. Paltsevich, A.P. (1999) Chromatographic method for determination of the content of hydrogen in components of electrode coverings. *Avtomatich. Svarka*, **6**, 45–48.
11. Kost, M.E. (1962) About yttrium hydride. *Doklady AN SSSR*, 143(**1**), 119–121.
12. Terekhova, V.F., Savitsky, E.M. (1967) *Yttrium*. Moscow: Nauka.
13. Grabin, V.F. (1982) *Physical metallurgy of fusion welding*. Kiev: Naukova Dumka.

DEVELOPMENT OF ZIRCONIUM- AND STAINLESS STEEL-BASED COMPOSITES FOR MANUFACTURE OF ADAPTERS TO NPP STRUCTURES

I.M. NEKLYUDOV, B.V. BORTS, A.T. LOPATA, N.D. RYBALCHENKO, V.I. SYTIN and **V.A. ALEKSANDROV**
National Science Center «Kharkov Institute of Physics and Technology», NASU, Kharkov, Ukraine

The paper describes the developed composite materials produced with application of solid-phase welding. Zr1Nb–08Kh18N10T composites with different interlayers were manufactured in the vacuum rolling mill. Their physico-mechanical properties were studied after rolling, heat treatment, corrosion testing and electron bombardment. Zr1Nb–08Kh18N10T composite with nickel interlayer was selected as the most promising for further investigations.

Keywords: *vacuum rolling, layered composites, zirconium, stainless steel, adapters, microstructure, strength, heat treatment, corrosion, barrier interlayers, adapter elements*

The joints from dissimilar metals and alloys, which are different in composition and physico-mechanical properties, are used in assembly units of the structures in many branches of industry, including nuclear-power engineering. Mechanical, thread-brazing methods or fusion welding are used for making such joints.

The fuel elements (FE) of series of reactors have permanent joints from zirconium to 08Kh18N10T stainless steel. Obtaining of high strength and safe joints from these metals using fusion welding is not possible since they are metallurgically incompatible. Brittle intermetallic phases appear at that on the boundaries of components of composites and can grow up to critical sizes under the action of significant heat flows that leads to a formation of macro and microcracks in the joint zone and then to complete loss of a structure integrity.

We developed and manufactured the adapters from zirconium alloy Zr1Nb and stainless steel 08Kh18N10T [1–3] using solid-phase welding with the aim to increase a life time and safe operation of aggregates and separate assembly units of the structure of NPP reactors. Safety and life time of composite products can be provided through an introduction of barrier and damping interlayers on the boundaries of the main components in composition of layered composites.

The present paper studied physico-mechanical properties of composite materials Zr1Nb with 08Kh18N10T through single interlayers of nickel or niobium as well as double interlayers of niobium or vanadium from the side of zirconium and copper or nickel from the side of stainless steel (SS) depending on time and temperature of annealing, corrosive environment as well as under conditions of electron bombardment.

Solid-phase welding of 08Kh18N10T type SS with Zr1Nb alloy was performed on Duo-170 vacuum rolling mill of a design of the NSC «Kharkov Institute of Physics and Technology» after modernization of a range of assembly units [4].

Metallographic investigations were carried out on optical microscope GX-51 of «Olympus» company with IA-32 picture analyzer. Microhardness of composite components were measured on the LECO LM-700AT digital micro hardness gage.

Mechanical properties of the composites were studied on cylinder samples cut out from composites along the whole thickness perpendicular to the boundaries of layers joining. Diameter of test portion of the samples made 4 mm and its length was 20 mm. The tests were performed on a tensile-testing machine at temperature of 20 °C with transverse speed of a moving holder of 2 mm/min. Test procedure corresponded to GOST 1497–84. The flat samples of 35 × 8 × 1 mm size were used during tests of bombarded samples to layers separation.

Corrosion tests were carried out by means of autoclaving method at a temperature and pressure, simulating working parameters, in liquid medium corresponding in composition to real conditions in the reactor [5]. Water, cleaned by means of double distillation, close in composition to working fluid of a primary coolant circuit of a can of reactor FEs of NPP was used in autoclave testing. The temperature made 350 °C and water pressure was 16.5 MPa. The microsections for investigation of corrosion process in time were polished and studied in a course of 50, 100, 500 and 1000 h after the tests without preliminary etching of composites' structure with the aim to trace surface changes of their components after corrosion. The bombardment of composites was carried out with 10 MeV energy electrons of $(3.3–330)\cdot 10^{20}$ el/m^2 dose on an accelerator KUT-1 of a design of the NSC «Kharkov Institute of Physics and Technology».

Analysis of the data of study [6] about a nature of materials joining in solid phase as well as the factors having influence on adhesive strength of layers in composite materials gives the basis to state that the mechanical properties of permanent joints are determined by initial properties of composite components as well as significantly depend on technological parameters, i.e. residual gas pressure in a chamber at heating and rolling, temperature, reduction of cross-sectional area of package, deformation rate. Besides, a level of structural and mechanical inhomogeniety and peculiarities of stress-strain state of the material near the boundaries of joining of composite components have an influence on adhesion strength.

We did not succeed in a selection of any barrier intermediate interlayer, except double Nb–Cu, which forms a series of continuous solid solutions with zirconium and SS, in studying constitutional diagrams of binary alloys [7, 8]. All other metals used as an interlayer between zirconium and SS form intermetallic compounds at different temperature of heating. This factor limits a selection of maximum temperature of hot vacuum rolling by values of temperature at which formation of brittle intermetallic phases on the boundaries of joining of composite components took place. It follows from the analysis given above that the double interlayers Nb–Cu and V–Ni and single interlayers of niobium and nickel were selected as the most perspective.

Width of the package made 65–70 mm and its length was 150–200 mm, thickness of zirconium and steel 08Kh18N10T made 15–20 mm (for each package), thickness of intermediate interlayers in the initial condition was 1.5–2.0 mm.

The following parameters of the rolling process were selected as the most optimum conditions for obtaining Zr1Nb–08Kh18N10T composites based on experimental data: residual pressure in furnace chamber of $(1-5)\cdot 10^{-3}$ Pa; reduction of cross-sectional area of (30 ± 2) %; furnace temperature of (900 ± 50) °C.

The microstructure of composite materials immediately after hot vacuum rolling and heat treatment of different duration at temperature of 350–500 °C was studied with the help of metallographic analysis. The changes on the boundaries of composite components were investigated depending on influence of increased temperature taking into account standard temperature of the reactor core and its possible short-time change, provided by technological incidents in reactor work.

The analysis of structure of composites was carried out on templates cut out along the thickness normal to the boundaries of layers joining. Mass transfer from one metal into other on the boundaries of composite components with interlayers was studied by a method of micro X-ray spectrum analysis in parallel with the metallographic analysis.

Analysis of diffusion changes on the boundaries of joining of layers after heat treatment showed the presence of the following factors:

• absence of visible transient zones on the boundaries of joining in Zr1–Nb–Cu–08Kh18N10T composite after all modes of heat treatment;

• presence of a thin (2–3 μm) transient layer with increased microhardness in separate places on V–Ni boundary in Zr1Nb–V–Ni–08Kh18N10T composites after annealing at 500 °C during 10 h. Approximate chemical composition of this layer — 13 wt.% V and 87 wt.% Ni — was determined by micro X-ray spectrum analysis. An increase of holding time up to 50 h resulted in formation of solid V–Ni intermetallic layer of up to 5 μm thickness. Appearance of the brittle intermetallic phase reduces the strength of joining of layers and provides failure of the composite along the joining boundary;

• thin transient zone of 2–3 μm width, which at continuous annealing does not have significant increase, was found on Zr–Nb boundary in Zr1Nb–Nb–08Kh18N10T composite after annealing at 500 °C during 10, 30 and 50 h;

• there were no intermetallic phases in Zr1Nb–Ni–08Kh18N10T composite on the boundaries of their components after annealing at 500 °C during 10 h. Transient zones from the side of nickel of up to 4 μm and from the side of zirconium of up to 15 μm, which belong to solid solution type, appear after annealing during 50 h and holding.

One of the most important problems occurring during development of new materials is their corrosion resistance in operating environment. A method of autoclaving under temperature and pressure, simulating conditions of operation of the materials in reactors [5], is used for evaluation of the quality of elements of structures from zirconium alloys during manufacture under industrial conditions.

It is quite difficult to use traditional methods for determination of the level of corrosion resistance of metals and alloys on weight increments of the samples per unit of area in a course of specified testing time for layered composites. Materials included in content of composites (three or four) differ by various oxidation resistance in corrosive medium. It is virtually impossible to determine contribution of each of them into general weight increment of the samples. Therefore, the following factors are the criterion for evaluation of corrosion properties of composites in autoclaving:

• state of the surface of microsection (homogeneity, density and color of films);

• presence or absence of the defects in the form of cracks, corrosion, accumulation of products of corrosion on the boundaries of joining of composite components;

• mechanical properties (tearing strength of layers) of the samples after different time of holding in the autoclave under working conditions.

As can be seen from Figure 1, *a, b*, there is a transient zone of width up to 3 μm on the boundary between zirconium and nickel on the surface of Zr1Nb–Ni–08Kh18N10T before and after corrosion treatment. Its width increases up to 5–7 μm after corrosion tests

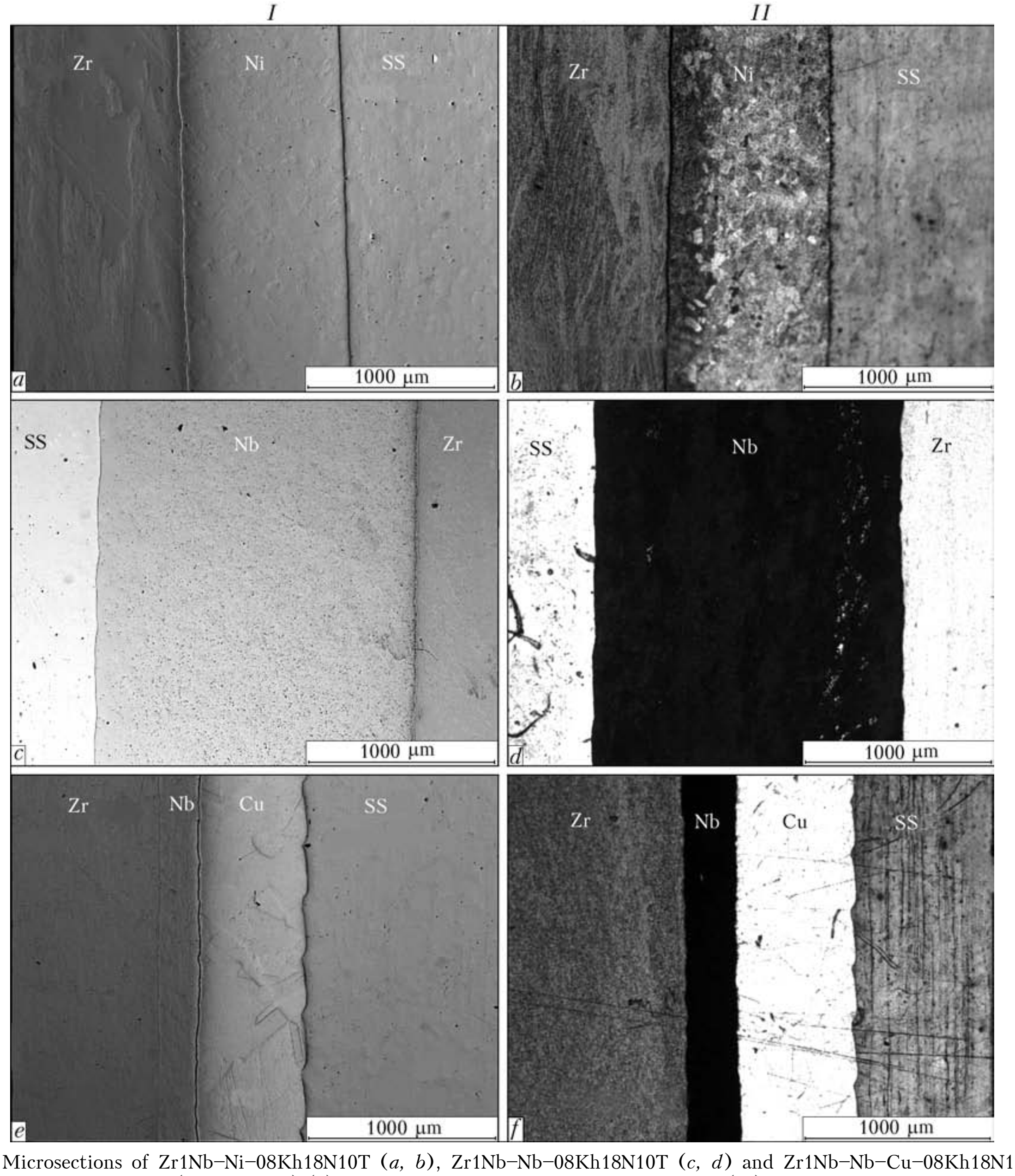

Figure 1. Microsections of Zr1Nb–Ni–08Kh18N10T (*a, b*), Zr1Nb–Nb–08Kh18N10T (*c, d*) and Zr1Nb–Nb–Cu–08Kh18N10T (*e, f*) composites in the initial state (after rolling) (*I*) and after corrosion treatment during 100 h (*II*)

during 1000 h. With increase of the time of corrosion tests insignificant pitting corrosion appears on nickel surface, and grain structure is formed in nickel and zirconium. There are no significant changes on the surface of SS except for light oxidation of the areas situated around precipitates of residual ferrite and carbides, giving these areas bluish color.

In the initial state of composite Zr1Nb–Nb–08Kh18N10T no intermediate transient zones on the boundary between composite components were found before and after corrosion treatment (Figure 1, *c, d*). Gray dense oxide film occurs on the surface of niobium interlayer after 50 h of corrosion tests and light areas appear in separate places, apparently, not yet covered by oxide layer. More dark areas appear on gray oxide film and it takes spotted nature after 100 h of tests. The main composite components did not suffer from significant changes except the appearance of thin oxide layers as in other compositions. The niobium interlayer gets significant thinning due to surface corrosion after 500 h of tests, it becomes loose, delamination in its surface sections from a free surface contacting with liquid corrosion medium, takes place. A stair of height up to 30–40 μm forms between zirconium and niobium due to difference in the rate of corrosion between these metals. A character of observed changes is kept after 1000 h of tests, the stair between zirconium and niobium increases up to 70 μm. The surface of niobium remains spotted with light and dark grey areas that can be an effect of formation of two or three types of oxides — NbO, NbO_2 and Nb_2O_5.

An appearance of intermediate zones on the boundaries of the components was not determined in Zr1Nb–Nb–Cu–08Kh18N10T composite (Figure 1, *e,*

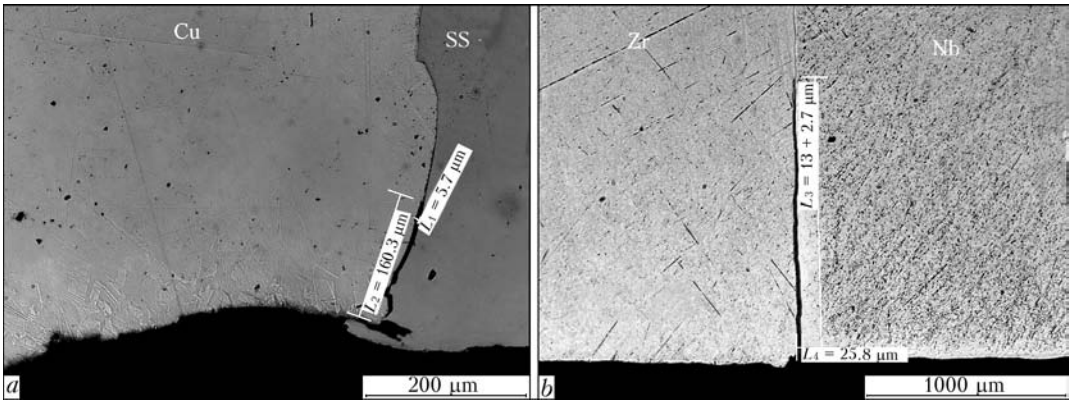

Figure 2. Microstructures with delamination after corrosion tests during 1000 h of composites Zr1Nb–Nb–Cu–08Kh18N10T on Cu–SS boundary (L_1 — delamination width, L_2 — its length) (*a*) and Zr1Nb–Nb–08Kh18N10T on Zr–Nb boundary (L_3 — delamination length, L_4 — its width) (*b*)

f) in the initial state (after rolling) and after corrosion tests. Structure is revealed in copper interlayer after 500 and 1000 h of corrosion tests. Copper surface remains light without significant oxidation marks after 1000 h and the pits of etching of dislocation structure were determined inside the copper coarse grains. The changes of the surface of niobium interlayer after corrosion tests are similar to that of composite Zr1Nb–Nb–08Kh18N10T.

For more detailed study of the changes in the state of boundaries of composites after corrosion tests the microsections were remanufactured from surface of which a layer damaged by corrosion was removed. At that, a layer of 5–7 μm thickness was determined in composition Zr1Nb–Nb–08Kh18N10T on Zr–Nb boundary after 500 h of corrosion tests and after 1000 h its thickness increased up to 11–12 μm. Discontinuities in the form of narrow crack are formed in the separate places with free surface of the sample on Zr–Nb boundary.

Very thin delaminations of a length from several micrometers up to 350 μm were formed in Zr1Nb–Nb–Cu–08Kh18N10T composite on the boundary of copper with steel after 500 and 1000 h of corrosion tests from both sides of free surfaces of microsections. The delaminations over 1000 μm length and up to 25 μm width were formed on Zr–Nb boundary in Zr1Nb–Nb–08Kh18N10T composite after 1000 h of tests. Found delaminations on Cu–SS and Zr–Nb boundaries (Figure 2), obviously, are the result of formation of galvanic couples from materials having different electrode potentials (Zr–Nb and Cu–SS) [9].

Mechanical tests of samples of the composites in the initial state (after rolling) and after corrosion treatment were carried out at temperature of 20 °C. As can be seen from Figure 3, all compositions in the initial state are characterized by significantly high strength properties. The greatest values of tensile strength (445–465 MPa) take place in composite Zr1Nb–Ni–08Kh18N10T. Failure of the samples occur along the intermediate interlayers.

Significant reduction in strength of the composites is observed after corrosion treatment. Thus, a tensile strength in composite Zr1Nb–Nb–08Kh18N10T after 1000 h of tests reduces from 340–350 (in the initial state) down to 100–110 MPa (after corrosion treatment) and from 390–410 down to 145–155 MPa, respectively, in composite Zr1Nb–Nb–Cu–08Kh18N10T. The data of metallographic analysis of fault samples indicate that the discontinuities in the form of cracks on the boundaries of interlayers with zirconium and steel are formed in the process of autoclaving as a result of electrochemical corrosion and stresses on the boundaries of composite components due to different coefficients of linear thermal expansion. The delamination occurs along perimeter of samples in the places of contact with corrosion medium that results in significant reduction of joints strength and premature failure of the composites.

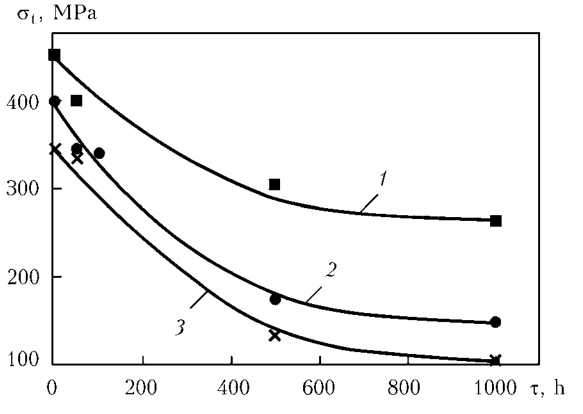

Figure 3. Dependence of tensile strength σ_t of Zr1Nb–Ni–08Kh18N10T (*1*), Zr1Nb–Nb–Cu–08Kh18N10T (*2*) and Zr1Nb–Nb–08Kh18N10T (*3*) composites on time τ of corrosion tests

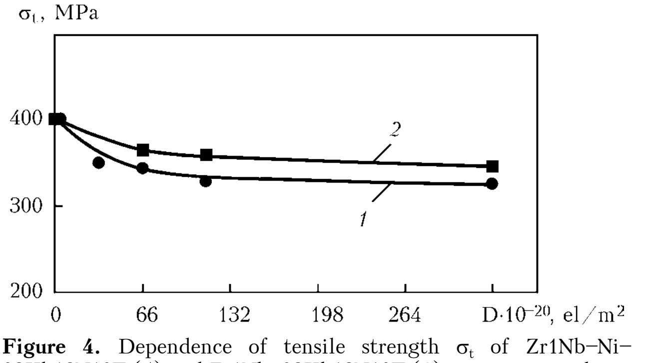

Figure 4. Dependence of tensile strength σ_t of Zr1Nb–Ni–08Kh18N10T (*1*) and Zr1Nb–08Kh18N10T (*2*) composites on bombardment dose D

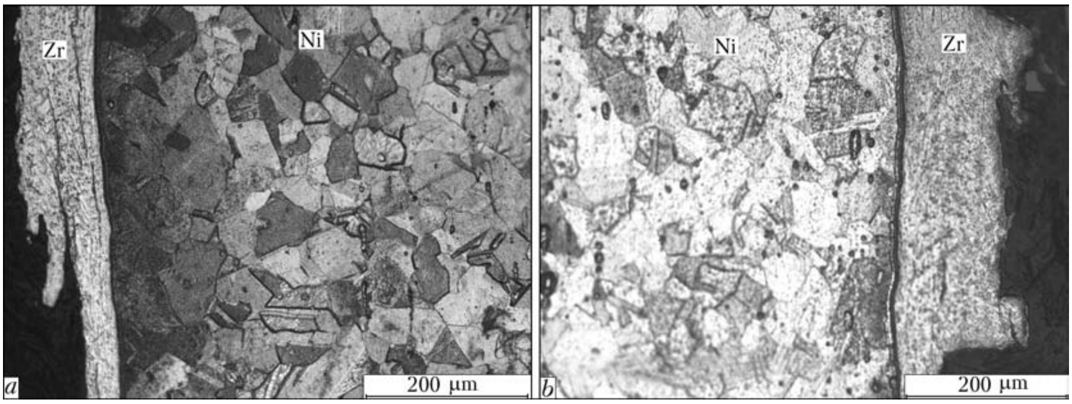

Figure 5. Microstructure of Zr1Nb–Ni–08Kh18N10T composite without (*a*) and after (*b*) bombardment by electrons of 10 MeV energy at D = $110 \cdot 10^{20}$ el/m^2

Reduction of strength of Zr1Nb–Ni–08Kh18N10T composite after corrosion tests during 500 and 1000 h is related, apparently, with an increase of width of transient zone (possibly, Zr_2Ni) on the boundary of zirconium with nickel. There were no defects in the form of porosities and delaminations on the boundaries of contact of composite components.

Composite Zr1Nb–Ni–08Kh18N10T was selected as the most perspective for further investigations of radiation resistance based on carried out analysis of studied composites and composite Zr1Nb with steel 08Kh18N10T without interlayer was takes for comparison.

Bombardment of the composites was carried out on the accelerator KUT-1 by electrons of 10MeV energy with bombardment dose which made (3.3–330)$\cdot 10^{20}$ el/m^2. The influence of bombardment on mechanical properties of studied composites was evaluated after short-time tests at temperature of 20 °C with respect to maximum tearing strength of flat samples (Figure 4).

Investigation results showed that the tearing strength of layers for both composites reduces insignificantly and after dose of bombardment of $66 \cdot 10^{20}$ el/m^2 virtually does not change up to maximum dose $330 \cdot 10^{20}$ el/m^2. Maximum reduction in strength for both composites makes 15 %.

The character of composite failure is different depending on presence or absence of nickel interlayer. Thus, the failure in composite Zr1Nb–08Kh18N10T always occurs on the boundary of zirconium with steel and it takes place along zirconium component of the composite close to boundary with nickel (Figure 5) in the case of presence of nickel interlayer.

CONCLUSIONS

1. Physico-mechanical properties of composites Zr1Nb–Nb–08Kh18N10T, Zr1Nb–Ni–08Kh18N10T, Zr1Nb–Nb–Cu–08Kh18N10T and Zr1Nb–V–Ni–08Kh18N10T in the initial state (after rolling) as well as after temperature and corrosion tests were investigated. Composite Zr1Nb–Ni–08Kh18N10T has the highest value of strength after rolling (445–465 MPa).

2. Investigations of changes in the states of surface and strength of developed composites in corrosion medium, which simulates working conditions in WWER-1000 type reactors, were carried out. It is determined that the corrosion treatment results in significant reduction of strength of solid state joint of the composites being studied. The highest strength values (255–280 MPa) after 1000 h of corrosion tests were determined in composite Zr1Nb–Ni–08Kh18N10T.

3. Study of the influence of electron bombardment up to dose of $330 \cdot 10^{20}$ el/m^2 on strength properties of composite Zr1Nb–08Kh18N10T with and without nickel interlayer showed that the maximum reduction of tearing strength of layers for both composites makes up to 15 %.

4. Composite material Zr–SS with interlayer from nickel, which is differ by good corrosion resistance and preserves significantly high strength after influence of aggressive medium and bombardment, is the most perspective based on results of carried out tests for application as adapter elements for dissimilar metal joints in reactor structures.

1. Neklyudov, I.M., Borts, B.V., Vasekha, I.I. et al. *Method of solid phase welding of metal plates*. Pat. 80204 Ukraine. Int. Cl. B 23 K 20/00. Publ. 25.06.2007.
2. Borts, B.V., Neklyudov, I.M., Lopata, A.T. et al. (2005) Study of welding process of multilayer structures from crystals of various chemical composition by means of vacuum hot rolling. *Voprosy Atomn. Nauki i Tekhniki. Physics of radiation damages and radiation materials science Series*, 88(**5**), 156–158.
3. Neklyudov, I.M., Borts, B.V., Lopata, A.T. et al. (2007) Production of zirconium–steel layered composites by solid phase welding. *Fizika i Khimiya Obrab. Materialov*, **1**, 5–9.
4. Amonenko, V.M., Tron, A.S., Mukhin, V.V. et al. (1960) Vacuum rolling mill. *Steel*, **10**, 920–922.
5. Petelgusov, I.A. (1999) *Serviceability of fuel elements of nuclear power reactors of WWER, PWR and BWR type: Review*. Kharkov: NNTs KhFTI.
6. Krupin, A.V. (1974) *Vacuum rolling of metals*. Moscow: Metallurgiya.
7. Hansen, M., Anderko, K. (1962) *Structure and properties of binary alloys*. Pts 1, 2. Kiev: Metallurgizdat.
8. Heis, E.T., Robertson, A.H., Paashe, O.G. (1955) Constitutional diagrams of zirconium–nickel system. In: *Zirconium*. Pt 2. Moscow: Inostr. Literatura.
9. Antropov, L.I. (1975) *Theoretical electrochemistry*. Moscow: Vysshaya Shkola.

INSTRUMENTS FOR ACOUSTIC EMISSION CONTROL AND DIAGNOSTICS OF WELDED STRUCTURES

A.Ya. NEDOSEKA, S.A. NEDOSEKA, A.A. GRUZD, M.A. OVSIENKO, M.A. YAREMENKO and **L.F. KHARCHENKO**
E.O. Paton Electric Welding Institute, NASU, Kiev, Ukraine

The paper presents materials of testing and investigation of performance of instrumentation for acoustic emission and diagnostics of the new generation, as well as the results of introduction of updated software for the above instrumentation, which offers new technological capabilities for its practical application.

Keywords: *welded structures, diagnostics, acoustic emission control, instruments, material strength*

Experience of expert examination of higher risk facilities is mainly based on modern achievements in the fields of development of theory and efficient methods and instrumentation for control and technical diagnostics. This directly concerns the technologies of diagnostics based on acoustic emission method, the effectiveness of which is confirmed by their wide application in the most critical facilities. PWI conducts a number of developments on technical diagnostics in such high priority directions as software and instrumentation realizing the control technology and including the programs of acquisition, processing and compression of input information, algorithms of destructive process identification based on mathematical statistics, theory of probability, prediction and decision theory; certification of the developed procedures and control equipment; training personnel performing work on control of the condition of structure material, etc.

Four channel acoustic emission (AE) instrument GALS1 upgraded and tested under different operation conditions together with SPC «Prompribor» and laboratory sample of AED instrument for new generation diagnostic systems EMA-3.5 developed together with Hungarian Company «Videoton», were selected as objects of investigation (Figure 1) [1]. Tested instruments are new generation developments in the field of AE technology and have new technological capabilities, namely high resolution, real-time processing of AE signal shape, as well as a large number of adjustment parameters, allowing filtration of false AE signals and efficient processing of the useful ones.

Basic software of EMA-3.5 system was upgraded for new AE systems allowing for the data communication protocols developed by manufacturers. Algorithms of data saving on a hard disc in unchanged format in keeping with the new data communication protocols were realized. Instrument operation under the laboratory conditions and in PWI industrial testing facility was tested. Stability of instrument operation was checked, as well as their acoustic and other indices, and possibility of AE signal location at different configuration of location arrays (location array means a group of AE transducers, which process the data simultaneously, in particular, in order to determine AE source coordinates).

In this study the influence of error of measurement of the time of AE signal arrival to the transducer on their localization using AE diagnostic system EMA-3 was established and obtained data will be taken into account at certification of new and currently developed AE diagnostic systems, as well as preparation of procedural and normative documents.

The effectiveness of the methods of AE source coordinate determination, also under the conditions of simulation of various sources in the industrial testing facility and during actual mechanical testing was con-

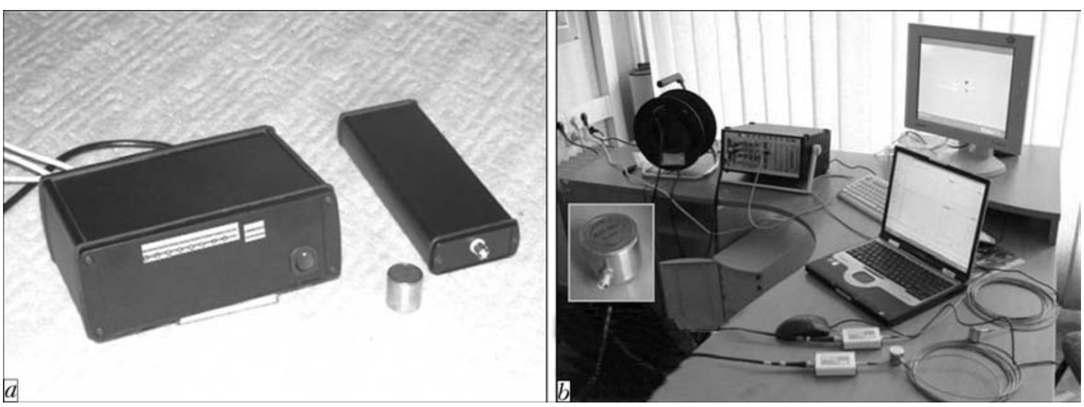

Figure 1. Appearance of GALS1 (*a*) and EMA-3.5 (*b*) instruments

firmed, using GALS1, AED instruments and EMA-3 software.

Signals were simulated using transducer-simulators and at breaking of a pencil lead. The quadrant was divided by a net, in the nodes of which AE sources were simulated (Figure 2). As is seen from the Figure, there are certain deviations in location of AE signals, coming from concrete points. Visually determined deviations are minor, real value of the error does not exceed 3 % of the distance between AE transducers. A conclusion can be made that for a reliable adjustment of AE instrumentation it is necessary to apply common simulation means, for instance, electronic simulator with adjustable signal parameters or breaking of a pencil lead.

To assess the errors of determination of AE source coordinates, a special schematic (Figure 3) was developed, according to which the zones of the object of control with the same level of coordinate calculation error, are represented by the same colour. Error of determination of AE source coordinates is calculated for several different methods, in particular, for accurate and approximate mathematical formulas and directed search method (a variant of Monte-Carlo method).

Testing of AE instruments was performed during testing of samples for static cutting and control of some industrial facilities. In addition, the instruments were tested for serviceability in long-term operation mode. Testing showed satisfactory operation of AE instruments. Obtained results are indicative of a real possibility of bringing the instruments to a level allowing performance of their metrological certification, and recommending them for introduction.

EMA type software was developed so as to ensure hardware independence. This means that with the same or similar basic principles of organization of AE instrumentation from various manufacturers, a uniform system of data acquisition, their preprocessing and high-level analysis algorithms can be achieved, allowing an automated decision to be taken as regards the condition of control objects.

Considering the incompatibility of the types of data obtained from different instrumentation, a special mechanism of matching these data on a high level, using so-called polymorphous classes, is introduced into EMA-3.5 software.

A modification of EMA-3.5 instrument was applied at testing by internal pressure of three pipes from steel 20 of 600 mm diameter with 10 mm wall thickness. A hydraulic pump was used as the loading system, water being the working medium. During loading of the control object, a stop and unloading were performed, and then it was loaded up to fracture.

The objective of the research was to demonstrate the effectiveness of application of AE means to determine fracture site coordinates. EMA-3.5 diagnostic system was used in the same mode as EMA-3. AE signals were recorded during loading, and data on pressure variation were entered into the logbook and after testing they were entered into EMA-3.5 system.

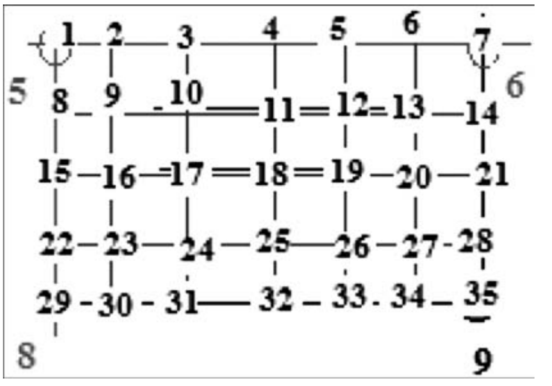

Figure 2. Coordinates of AE sources at simulation

Testing of pipe 1 was conducted at an extremely rapid pressure rise (test duration was 206 s) directly up to fracture without intermediate stops. Fracture occurred at the pressure of 13.8 MPa. EMA-3.5 system showed preliminary coordinates of fracture site at about 2.6 m distance from transducer 1.

Testing of pipe 2 was conducted in three stages: pressure rise up to 100 MPa; unloading and pressure rise up to 110 MPa; unloading and pressure rise up to fracture (fracture ran at the pressure of 14.2 MPa). EMA-3.5 system gave preliminary indication of fracture site coordinates. A feature of testing consisted in that the crack was of a rather large size outlined by AE clusters.

Testing of pipe 3 was also conducted in three stages: pressure rise up to 10 MPa; unloading and pressure rise up to 110 MPa; unloading and pressure rise up to fracture (fracture occurred at the pressure of 12.5 MPa). EMA-3.5 system gave preliminary indication of fracture site coordinates in the pipe central part, between transducers 3 and 4.

Let us give as an example of successful application of developed AE systems in industry, the results of testing by AE method the drums of BKZ 75/39 boilers, conducted together with specialists of technical diagnostics laboratory of «Nikolaev Alumina Plant» Ltd. using EMA-3.5 system [2].

Testing was conducted in keeping with DSTU 4227–2003 «Guidelines on conducting acoustic emis-

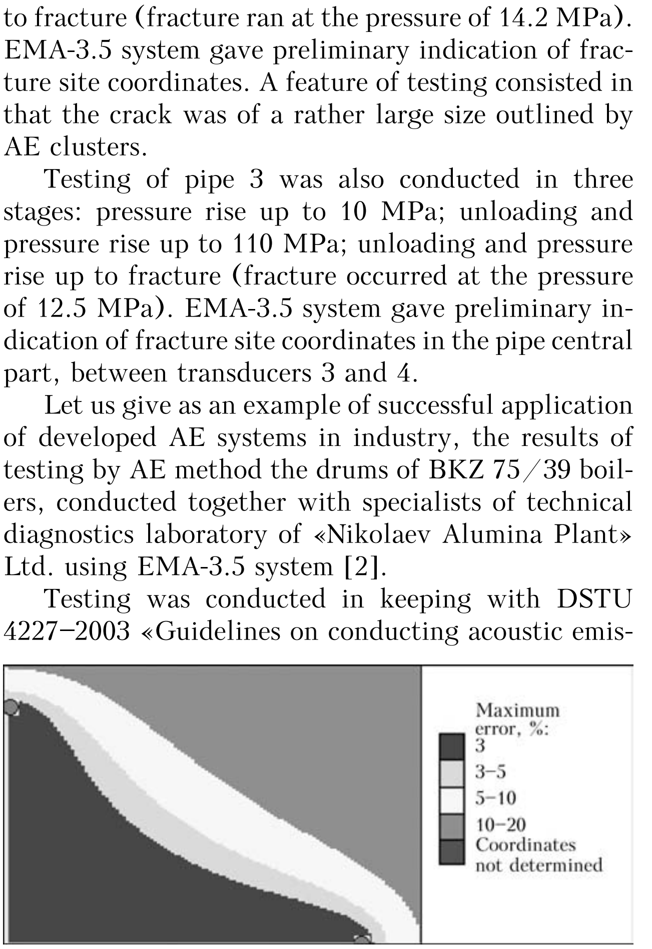

Figure 3. Example of application of schematic of representation of error of calculation of AE source coordinates (location by an accurate formula; error of calculation of AE source coordinates within a flat zone outlined by transducers is not more than 3 % of array base)

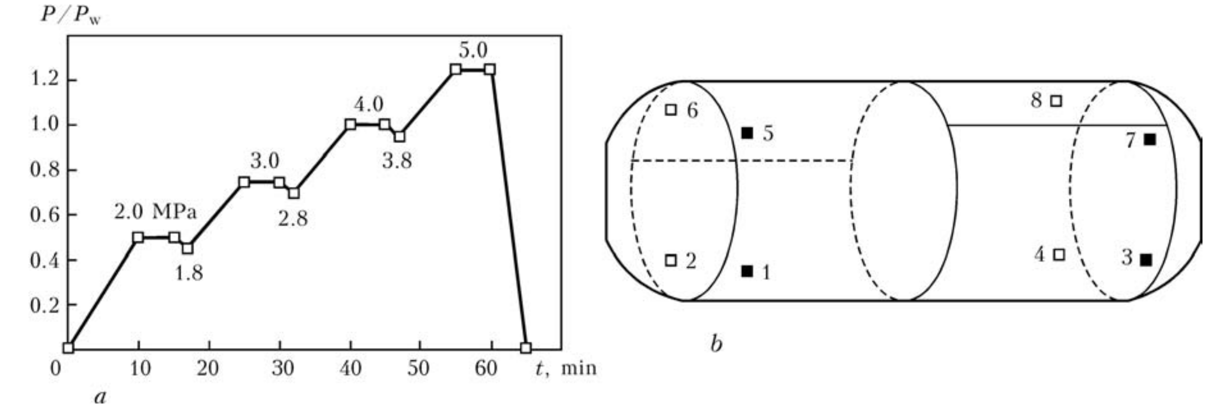

Figure 4. Graph of the program of loading (a) and arrangement of transducers of AE measuring instrument on the surface of drum of BK3 boiler: 1–8 — transducer numbers; ■, □ — visible and invisible points of AE sensor mounting; t — testing time

sion diagnostics of higher risk objects». «Technological map of AE monitoring of drum of BKZ 75/39 boiler» was made before the start of testing.

During testing internal pressure P in boiler drums was raised up to 1.25 of working pressure, namely from 0 up to 5 MPa with five minute soaking at the load of 0.4, 0.6, 0.8 and 1.0 of the maximum one and its lowering by 0.2 MPa after soaking.

AE parameters were recorded during testing. Then values of breaking load for drums of BKZ 75/39 boilers were calculated in the mode of computer rerun of testing.

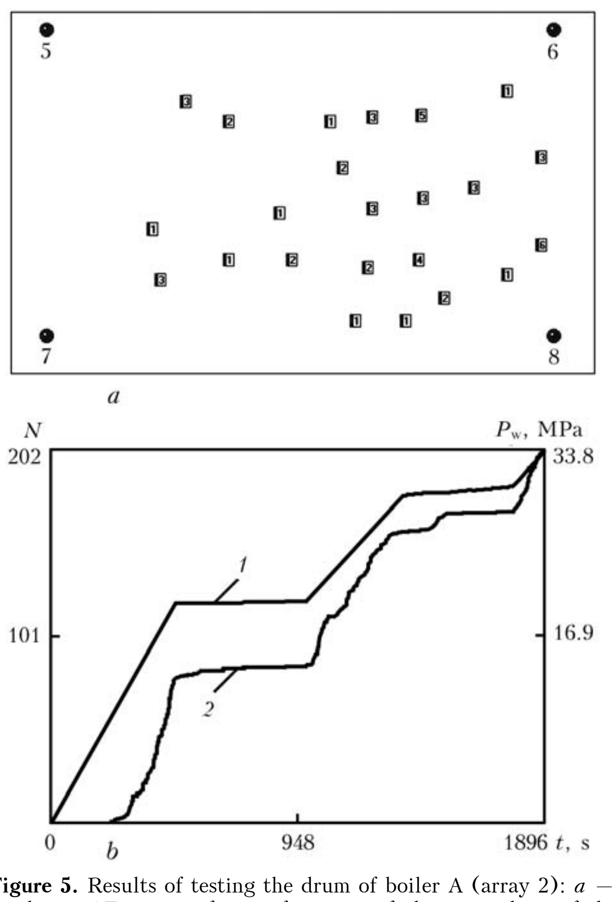

Figure 5. Results of testing the drum of boiler A (array 2): a — localizing AE events after performance of cluster analysis of the data (□ — clusters with indication of the number of AE events; ● — location of transducers 5–8); b — curves of load P_w (*1*) and accumulation of AE events N (*2*) during testing

Assessment results were the basis for issuing recommendations on subsequent operation of control objects, and treatment of boilers marked A and B. Drums of boilers from steel 20k have the operating life period of 25 years, and are operating at working pressure P_w = 3.9 MPa. Operating medium (steam) temperature was equal to 450 °C.

By the data of operating enterprise, AE testing was preceded by nondestructive testing of boiler drum walls, including thickness measurement and ultrasonic testing (UT), which did not reveal any defects.

Testing of the drum of boiler A showed that at loading and soaking (Figure 5, *a*) numerous AE signals were recorded practically over the entire surface being controlled, both for the measuring location array 1 (from transducers 1–4) and for measuring location array 2 (from transducers 5–8).

Main sections of concentration of numerous AE signals are located in the central right part of the drum (Figure 4, *b*) controlled by array 2 (transducers 5–8). Figure 5 gives the data provided by EMA-3.5 program on initial test results (by AE data and load values).

Processing and cluster analysis of test results given in Figure 4, revealed the presence of hazardous defects in the material of the object of control, which, however, do not create any emergency situation during monitoring. Data of cluster analysis graphically presented in the program, are indicative not only of the presence of a large number of dispersed damage, but also of absence of defects propagating in a critical manner.

Graphs of EMA-3 program (Figure 5) are indicative of the change of number N of AE events and P_w, depending on the time from the start of the test up to its completion. As is seen from the Figure, testing included two soaking periods with subsequent pressure rise.

A sufficiently high noise level was recorded, which rises together with the load, which is indicative of the presence of dispersed damage in the boiler drum material [3].

Considering the detected sites of acoustic activity [4], the possibility of boiler drum material damage as a result not of disturbance of the condition of strength, but formation of local cracks should be considered.

During testing of the drum of boiler B the total number of AE events was recorded, which is much smaller than during testing of the drum of boiler A. An important essential difference of this test is the fact that the noise level remains unchanged practically during the entire loading time. On the whole, the material of the drum of boiler B is less damaged than the drum of boiler A. In the last two soaking periods, AE signals are absent at all, unlike the results of testing the drum of boiler A.

In terms of strength characteristics, the material satisfies the applied service requirements. However, presence of AE sources scattered over the surface material, requires allowing for the possibility of gradual damage of boiler drum material as a result of defect localization and microcrack formation.

Proceeding from test results, the following recommendations were issued for further operation of the drum of boiler A:

• perform additional UT of the surface of drum of boiler A in the sites of initiation of acoustic activity, using cluster data;

• take the decision on the modes and terms of further operation of drum of boiler A after performing additional UT.

Technical diagnostics laboratory of «Nikolaev Alumina Plant» performed UT, which revealed in the wall of boiler A defects of the type of cavities and mcirocracks, corresponding by their location to clusters 2 and 3 of array 1 and clusters 3, 7, 10, 12 of array 2. Laboratory staff performed evaluation of criticality of the defects, in keeping with factory standards. Detected defects by their characteristics were regarded as admissible for this type of products under normal operation conditions. A decision was taken to perform object control by AE method with the frequency of once every 6 months.

As regards further operation of the drum of boiler B, the following recommendations were issued:

• repeat AE monitoring of the surface of drum of boiler B and additional monitoring of the surface of drum of boiler B after 6 months;

• take the decision on the modes and terms of further operation of the drum of boiler B after repeated AE monitoring.

In keeping with the above recommendations, technical diagnostics laboratory of «Nikolaev Alumina Plant» performed repeated control of drum of boiler B, and after 6 months — another additional control. Considering a similar situation at testing and no deterioration of its condition after 6 months, the laboratory took a decision on extension of operation of drum of boiler B in the working mode and performing AE monitoring every 6 months.

Thus, after performance of control not requiring dismantling or other serious expenditure, the term of operation of drums of boilers A and B was extended. Control covered 100 % of materials of drum surface and took about 2 h together with mounting of the measuring instrument and system deployment. As a result of testing all the information required for taking the decision on boiler condition was obtained, which provides grounds for stating serious advantages of this procedure of AE control of industrial facilities.

CONCLUSIONS

1. Retrofitting of the developed instrumentation for AE control was performed. Changes in data communications protocol were made, and program interfaces for data storage and transfer were developed. Data processing capabilities were expanded, and first of all, frequency analysis and filtration.

2. Analysis of different methods of calculation of AE source coordinates was performed. Level of error at application of the above methods was assessed. Method of direct search was selected, which gives the smallest error. A method to evaluate the error of calculation of AE source coordinates using a colour scheme was developed.

3. AE instruments were tested during control of some real industrial facilities, their performance was verified in long-term operation mode. It is determined that the instruments can be applied in the future as mobile AE systems with a small number of channels.

1. Nedoseka, S.A., Nedoseka, A.Ya. (2005) Diagnostic systems of EMA family. Main principles and specifics of architecture (Review). *Tekhn. Diagnostika i Nerazrush. Kontrol*, **3**, 20–26.
2. *DSTU 4223–2003*: Boilers, pressure vessels and pipelines. Technical diagnostics. General requirements. Valid from 12.01.2003.
3. Nedoseka, A.Ya. (2001) On evaluation of state of material of welded structures. In: *Proc. of Plenary Papers of 2nd Int. Symp. on Welding and Related Technologies: World Experience and Achievements* (Minsk, 28 March 2001). Minsk, 33–39.
4. Nedoseka, A.Ya., Yaremenko, M.A., Ovsienko, M.A. et al. (2006) Determination of coordinates of propagating defects on cylindrical surfaces. *Ibid*., 11–13.

INTERNATIONAL CONFERENCE «TITANIUM-2010 IN CIS»

Traditional annual International Conference «Titanium in CIS», organised by Inter-State Association «Titan», was held on 16–19 May 2010 in Ekaterinburg (Russia). Over 230 people from Russia, Ukraine, Kazakhstan, Tadjikistan, China, Germany, France, Italy, Japan, Luxemburg, Poland and other industrialised countries attended the Conference. Scientists and specialists in the field of titanium from leading R&D organisations and industrial enterprises of Russia and Ukraine (Federal State Unitary Enterprise CRISM «Prometey», Federal State Unitary Enterprise «All-Russian Institute of Aviation Materials», Open Joint Stock Company «All-Russian Institute of Light Alloys», USTU UPI — «Ural State Technical University — B.N. Eltsin Ural Polytechnic Institute», MATI — K.E. Tsiolkovsky Russian State Technological University, Institute for Metals Superplasticity Problems of the Russian Academy of Sciences, Institute of Structural Macrokinetics and Materials Science of the Russian Academy of Sciences, Open Joint Stock Company «Corporation «VSMPO-AVISMA», Federal State Unitary Enterprise «Giredmet», Open Joint Stock Company «Uralredmet», Joint Stock Company «Sukhoi Design Bureau», Open Joint Stock Company «Elektromekhanika», Open Joint Stock Company «Kaluga Turbine Factory», E.O. Paton Electric Welding Institute of the National Academy of Sciences of Ukraine, G.V. Kurdyumov Institute for Metal Physics of the National Academy of Sciences of Ukraine, I.M. Frantsevich Institute for Problems of Materials Science of the National Academy of Sciences of Ukraine, Donetsk O.O. Galkin Institute of Physics and Engineering of the National Academy of Sciences of Ukraine, State Research and Design Institute of Titanium, Antonov Aeronautical Scientific-Technical Complex, etc.). Totally, over 90 papers were presented at sessions «Raw Materials. Metallurgy» and «Metal Science and Technologies of Titanium Alloys». In addition, the Conference included sessions of the «Current Peculiarities of the World Titanium Market» Discussion Club and «Melting of Titanium» Thematic Workshop.

The plenary session of the Conference was held in Verkhnyaya Salda (Sverdlovsk Region). Then participants of the Conference visited production shops of Corporation VSMPO-AVISMA, which is one of the world-leading manufacturers of the entire range of critical-application titanium semi-finished products (forgings, tubes, rods, plates, etc.), covering 100 % of the demand of defence and aircraft engineering enterprises of Russia and Ukraine for titanium components, and about half of the demand of foreign civil aircraft manufacturers for titanium semi-finished products.

M.V. Voevodin, Director General of VSMPO-AVISMA, noted in his presentation that despite the world

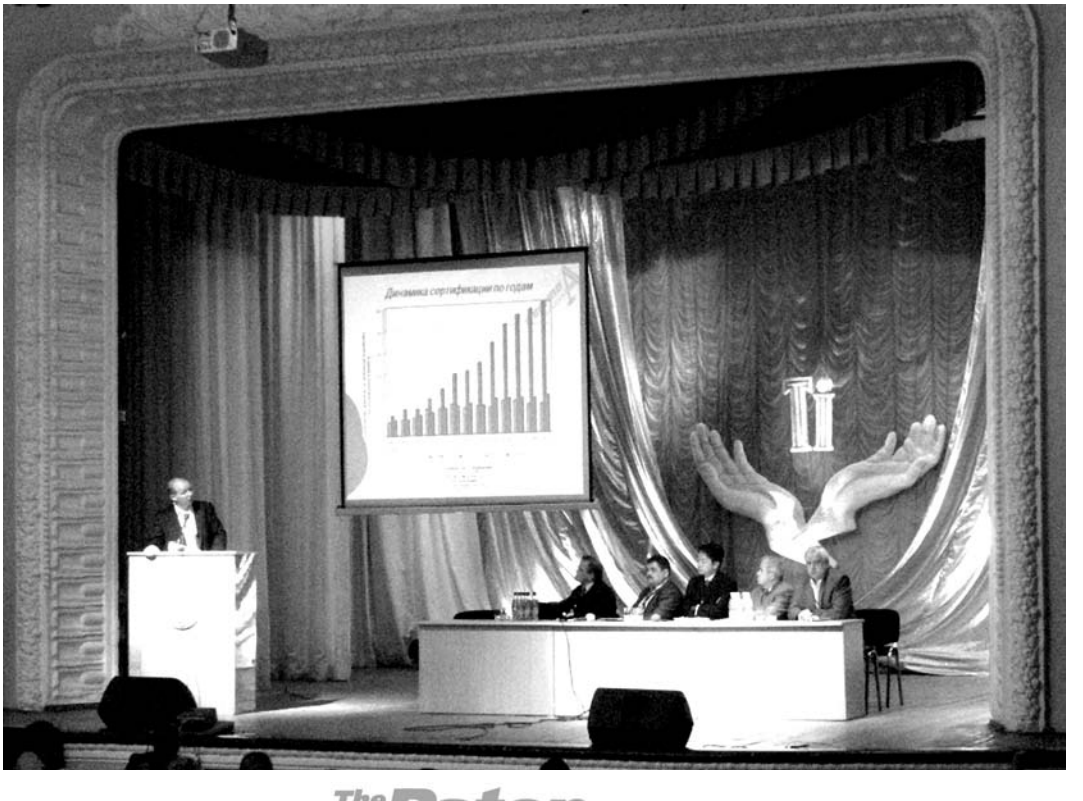

economic crisis the Company continues its upgrading program towards increasing the titanium output and proportion of high-processing products. For example, cooperation between the joint venture companies and «Boeing» has been started in 2010 in the field of machining of titanium alloy forgings for gas-turbine engine disks and airliner landing gears. Titanium sponge production capacities should amount to 44,000 t per year.

Specialists of CRISM «Prometey», one of the world-leading centres in the field of development of titanium alloys and technologies for their welding, melting, heat and deformation treatment, presented a large number of papers. Out of a wide variety of welding technologies, the focus at the Conference was on argon arc and electron beam welding of thick-walled titanium alloy structures. Scientists from USTU UPI and MATI, involved in intensive R&D efforts in the field of titanium and titanium-base alloys materials science, including for application of titanium in medicine, took an active part in the work of the Conference.

Institutions of the National Academy of Sciences of Ukraine, including the E.O. Paton Electric Welding Institute, presented their scientific-and-technical developments. They were described in papers dedicated to magnetically controlled arc narrow-gap and vertical-plane TIG welding of titanium alloys in argon atmosphere, electron beam melting of large ingots of titanium-base refractory alloys, electroslag melting and welding of titanium with controlled hydrodynamic processes, and investigation of floating zone recrystallisation of titanium aluminide.

Specialists of the G.V. Kurdyumov Institute for Metal Physics considered physical, technological and economic aspects of manufacture of parts from titanium alloys by the powder metallurgy methods. Representatives of the Donetsk O.O. Galkin Institute of Physics and Engineering presented their developments in the field of production of nanostructured titanium billets by screw extrusion methods.

Presentations at a session of the «Current Peculiarities of the World Titanium Market» Discussion Club were made by A.V. Aleksandrov (CJSC «Inter-State Association «Titan»), A.N. Stroshkov (VSMPO-AVISMA), Turgyn Rahman (Advanced Materials Japan Corp.), Steven Hancock (TiRus International SA, Switzerland), T. Nishimura (NTC Corporation for Titanium, Japan) and many other specialists operating in the titanium market. Almost all speakers noted growth of the volumes of orders for titanium products in 2010 both in civil and military aircraft engineering, and in civil industrial sectors, although the production level of 2008 has not been achieved so far.

New technological processes for production of pure titanium have not yet exceeded the bounds of laboratory studies. Hence, the key method for production of titanium is still the expensive Kroll process. In this connection, at present one might not expect any substantial reduction in costs of manufacture of titanium. This is confirmed by the fact that in the crisis year of 2009 the up-to-date factories manufacturing titanium sponge, which were constructed in China, could not reduce the costs of their products below the average world level. Therefore, the world titanium market is characterized by a high competition, where the decisive factors of success are a high quality of products and their low manufacturing costs, which can be achieved through applying new advanced technologies.

Analysis of different technologies for melting of titanium at the «Melting of Titanium» Thematic Workshop allowed a conclusion that the vacuum-arc remelting technology remains to be the key method for production of ingots of titanium-base alloys, whereas the electron beam melting technology has been finding an increasingly wider application for melting of ingots and slabs of unalloyed titanium. This is proved by the fact that new electron beam furnaces for melting of titanium have been launched in the last three years in the USA (TIMET), Germany (ThyssenKrupp), China (Bao Ti Group) and Ukraine (Zoporozhie Titanium-Magnesium Integrated Plant), and several new units have been constructed in these countries.

In conclusion, we would like to note a high level of the Conference and express gratitude to its organisers represented by the «Inter-State Association «Titan» and its chairman A.V. Aleksandrov.

Prof. S.V. Akhonin, PWI

S.I. KUCHUK-YATSENKO IS 80

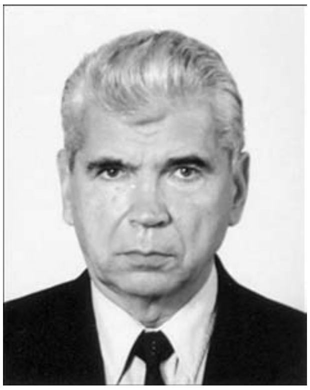

August 2, 2010 marked 80th birthday anniversary of Sergey I. Kuchuk-Yatsenko, First Deputy Director of the E.O. Paton Electric Welding Institute of the NAS of Ukraine, academician of the NAS of Ukraine.

After graduating from the Kiev Polytechnic Institute, S.I. Kuchuk-Yatsenko was placed on a job at the E.O. Paton Electric Welding Institute, where he has successfully worked his way from young specialist-engineer to professor, Doctor of Science in Engineering, head of one of leading departments, First Deputy Director of the Institute on research, academician of the National Academy of Sciences of Ukraine. In 1960 S.I. Kuchuk-Yatsenko defended the thesis of Candidate and in 1972 — thesis of Doctor of Science. In 1978 he was elected the Corresponding Member, and in 1987 he became the Full Member of the National Academy of Sciences of Ukraine.

Research performed by S.I. Kuchuk-Yatsenko is related to investigation of physico-metallurgical processes in solid-phase welding of different materials. In particular, he obtained new data on peculiarities of producing joints with formation of a thin layer of the melt on contacting surfaces of the parts being welded, its behaviour under the impact of electrodynamic forces and features of its interaction with the gas medium in the contact zone. It was shown for the first time that condition of the melt in the period preceding deformation of the parts being welded, has a dominating influence on formation of metal bonds between the contacting surfaces and development of chemical inhomogeneity in the contact zone. Influence of oxide structures in the melt on joint quality was studied in detail and ways of optimization of oxidation processes in the mentioned welding period were determined.

Alongside the above-mentioned investigations, S.I. Kuchuk-Yatsenko has for many years conducted purposeful study of fast processes of heating and breaking up of unit contacts at high energy concentrations. He established a number of new regularities characterizing energy indices of the process of contact melting of metals, determined the methods of automatic control of the main parameters of the process to obtain more favourable conditions of heating and deformation of parts being welded.

A practical result of the above-mentioned fundamental investigations is development by S. Kuchuk-Yatsenko of new processes of continuous, impulse and pulsed flash-butt welding patented in leading countries of the world. On their basis S. Kuchuk-Yatsenko together with a team of staff members developed technologies of welding various products, control systems and new samples of welding equipment, having no analogs in the world practice. Equipment has a high efficiency, minimum consumed power and weight, provides a stable and high quality of the joints. These advantages are the most significant in welding parts of a complex configuration with large cross-sections. Over the recent years, he has been studying resistance welding of parts from difficult-to-weld alloys, composite materials using activating coatings and special interlayers of a composite structure, including those consisting from multilayered nanostructured materials. This allowed development of new technologies of joining high-temperature materials based on nickel and titanium intermetallics, as well as tool alloys. Scientific and engineering activity of S. Kuchuk-Yatsenko is characterized by an integrated approach to solving the posed problems. Fundamental research performed by him, is accompanied by development of original technologies of welding, automatic and over the recent years, computerized control of the welding process and development of modern welding equipment.

Organization of industrial production of the developed new welding equipment and its mass introduction into industry are performed with his direct participation. Some of the most important stages of S. Kuchuk-Yatsenko's activity are described below. S. Kuchuk-Yatsenko has been working on rail welding for more than fifty years. Technologies and equipment for rail welding developed with his active involvement and guidance allowed for the first time in the world practice application of highly efficient flash-butt welding in the field, this greatly promoting transfer of the railways to continuously by welded rail tracks. With active participation of S. Kuchuk-Yatsenko batch production of such equipment was organized in the Kakhovka Plant of Electric Welding Equipment, which beginning from 1970s became world exporter of such equipment. Over the past years, more than ten generations of rail-welding machines were developed, which are used in CIS and many countries of the world. S. Kuchuk-Yatsenko actively participates in improvement of this equipment and technology of welding, thus allowing its high competitiveness to be maintained. Over the recent years new generations of welding machines have been developed, allowing welding rails of infinite length at repair of continuously welded rail tracks with simultaneous stabilization of their stressed state. In 1966 S.I. Kuchuk-Yatsenko with a team of authors was awarded the Lenin Prize for development and introduction of a machine for butt welding of rails in repair and construction of continuously welded rail tracks. He was awarded the title of «Honorary Railway Worker of the USSR».

Developments of S.I. Kuchuk-Yatsenko and his associates have been also applied with success in mechanical engineering plants in manufacture of circular billets, shafts and blanks from dissimilar materials. Particularly effective was application of multiposition resistance welding, allowing welding large-sized parts in several locations simultaneously (engine cases, radiators of powerful transformers). Introduction of one machine in the line for production of cases of blocks of powerful diesel engines at Kolomna Diesel Locomotive Plant allowed increasing labour efficiency 70 times and making 380 welders available for other jobs. Considerable effect was also achieved as a result of multiposition welding in Zaporozhie Transformer Plant in manufacture of transformer radiators. In 1976 S.I. Kuchuk-Yatsenko as part of a team of authors was awarded the State Prize of the Ukr. SSR for development and introduction into industry of a new technology and highly-efficient assembly-welding systems for batch production of large-sized structures from modules.

For the first time in the world practice, S.I. Kuchuk-Yatsenko with a group of associates developed an original technology of flash-butt welding of items of a complex shape and large cross-section from aluminium-base high-strength alloys, providing joints of practically equivalent strength with that of the base metal. It was the basis for developing and mastering production of unique equipment which is used in manufacturing of space systems in the plants of Ukraine and RF. In 1986 S.I. Kuchuk-Yatsenko as a member of a team of authors was awarded the USSR State Prize for development of the technology and equipment for flash-butt welding of structures from high-strength aluminium alloys.

S.I. Kuchuk-Yatsenko made a considerable contribution into development of technology and equipment for flash-butt welding of various-purpose pipelines. Technologies, control systems and equipment for flash-butt welding of pipes of 60 to 1400 mm diameter were developed and its wide-scale introduction in pipeline construction in ex-USSR territory was performed with his active participation. Flash-butt welding was used to weld more than 70,000 km of various pipelines, including 4,000 km. of the most powerful pipelines in Extreme North regions. Application of flash-butt welding allowed increasing labour efficiency and ensuring pipeline reliability. This work was also awarded the Lenin Prize in 1989.

Work on development of technologies of pressure welding of position butts of various-purpose pipes is going on under his leadership and with his direct participation. Technologies and equipment for pressure welding with heating by a magnetically impelled arc of pipes of up to 300 mm diameter with 5–15 mm wall thickness were developed for the first time in the world, the equipment featuring a high efficiency at minimum energy content of the process.

S.I. Kuchuk-Yatsenko takes an active part in all the stages of the above-mentioned activities. In 1998 he received the title of «Honoured Scientist and Engineer of Ukraine», in 2000 he was awarded the Evgeny Paton Prize for scientific work «Solid-Phase Welding». S.I. Kuchuk-Yatsenko is the author of 640 scientific publications, including 9 monographs, 350 author's certificates. He was granted more than 300 Ukrainian and foreign patents, many of which were purchased by license agreements by foreign companies.

At present academician S.I. Kuchuk-Yatsenko continues actively working on urgent problems in the field of welding, development of advanced technologies of joining difficult-to-weld materials. He is head of one of the leading scientific departments of PWI. S.I. Kuchuk-Yatsenko has had fruitful co-operation for many years with Kakhovka Plant of Electric Welding Equipment — one of the leading enterprises-manufacturers of welding equipment in Ukraine. He is actively involved in organization of batch production of flash-butt welding machines for welding railway rails and pipes.

S.I. Kuchuk-Yatsenko is Deputy Director of PWI Scientific Council, Deputy Editor-in-Chief of «Avtomaticheskaya Svarka» journal, Member of Interestate Scientific Council on Welding and Allied Technologies. He prepared more than ten Candidates and Doctors of Science in Engineering. He was elected the first President of the Society of Welders of Ukraine, he is member of the Society Board, member of the Society of Welders of USA and Great Britain.

The scientists' contribution was awarded two orders of the Labour Red Banner, Order of Merit, Order of Prince Yaroslav the Wise and medals.

GUANG XIAO IS 75

Guang Xiao was born on July 2, 1935 in the city of Tiayun (China) in the family of engineer-architect. In 1952–1953 he took the preliminary course, and in 1953–1959 he studied at N.E. Bauman MSTU, from which he graduated with honours. Having started to work at Beijing RIAT, he was soon offered a post-graduate course (1959–1963).

Under the guidance of G.A. Nikolaev, Guang Xiao prepared Candidate's thesis at N.E. Bauman MSTU on the subject of «Argon-arc welding of aluminium decking of prefabricated transportable bridges» (1963).

Coming back to China, Guang Xiao continued working at Beijing RIAT. Here he led a group of welding engineers with great energy and enthusiasm, solving a number of urgent practical issues arising in fabrication of aircraft structures, and wrote production instructions and norms.

At the end of 1960s–beginning of 1970s Guang Xiao was the leading specialist and he is involved in development of research and introduction of new welding processes, technologies and equipment for manufacturing structures of local aircraft, aircraft jet engine cases and components, in particular such as pulsed consumable and nonconsumable electrode argon-arc welding, flash-butt welding, electron beam welding, plasma and diffusion welding, brazing, etc. For his contribution to development of welding equipment in aircraft construction Guang Xiao was awarded a State Prize and Award at the Chinese Congress of Science in 1978.

Later Guang Xiao performed fundamental studies on kinetics of elasto-plastic displacements of metal occurring directly during welding using moire method. He managed to obtain a quantitative distribution of actual elastic-plastic welding strains in welded joint section, depending on technological parameters of welding. This fundamental work allowed Guang Xiao substantiating the possibility of development of «strainfree welding» process. This method was recognized in the world welding community as «deformationfree welding for joining thin materials».

Starting from 1984, Guang Xiao combines his job with giving a course on welding mechanics at the Beijing University of Aviation and Aeronautics, organizes China's first International Conference on Welding in the city of Han-Zhou devoted to application of fracture mechanics for studying welding problems. State Key Laboratory of Beam Treatment of Materials is organized by his initiative and with his direct participation.

In 1987 by the invitation of the Royal Society, London, Guang Xiao fulfilled a one year research program of co-operation with The Welding Institute, where he successfully improved the technique of deformationfree welding.

Guang Xiao is a fervent supporter of establishment and strengthening of creative connections and business contact between scientists and specialists of various countries, he is developing co-operation between Beijing RIAT and foreign organizations and universities. He initiated wider avenues of co-operation and specialist exchange between PWI and Chinese organizations, including Beijing RIAT. He is a member of the international editorial board of «Avtomaticheskaya Svarka» journal.

By the initiative of Guang Xiao the Chinese Center of Friction Stir Welding was organized at Beijing RIAT in 2002. And this advanced welding process was quickly accepted in various industries of the country, and due to that it became the subject of research performed by many specialists.

In 1994 Guang Xiao was elected a member of the Chinese Academy of Engineering (CAE). During 2000–2002 he was the Head of Department of «Carrier Engineering and Means» at CAE Presidium, and in 2000 he became Presidium Member.

Guang Xiao has paid and is now paying a lot of attention to training young scientists. Tens of theses of Candidate and Doctor of Science were defended under his guidance.

Guang Xiao was awarded numerous scientific awards and honorary diploma, including the title of «Advanced worker in science and technology of China», Gold Medal of Aviation of China, awards granted by IIW and Chinese Society of Welders for his achievements in science and technology, Brooker (TWI medal), HLHL prize and award for contribution to science and technology, etc.